Evaluating the role of local climate change on reduced freshwater availability at the Peace-Athabasca Delta using paleolimnology

by

Kathleen Claire Brown

A thesis

presented to the University of Waterloo

in fulfillment of the

thesis requirement for the degree of

Master of Science

in

Biology

Waterloo, Ontario, Canada, 2022

Author's Declaration

I hereby declare that I am the sole author of this thesis. This is a true copy of the thesis, including any required final revisions, as accepted by my examiners.

I understand that my thesis may be made electronically available to the public.

Abstract

Abundant small, shallow lakes across northern freshwater landscapes are particularly sensitive to alteration of hydrological processes, which makes them vulnerable to multiple potential stressors. At the Peace-Athabasca Delta (PAD; Treaty 8; northeastern Alberta), a Ramsar Wetland of International Importance, lake drying and associated ecological consequences present a critical water security concern due to potential stressors such as climate change and upstream industrial projects. Hydrometric, paleolimnological, and other studies have identified multiple mechanisms that have contributed to lake drying to varying degrees during the past century including upstream river regulation, climate driven changes in flood frequency and magnitude, geomorphic change in distributary flow, and contraction of Lake Athabasca from low lying areas of the PAD. The many mechanisms at play within the delta have made it challenging to distinguish the relative role of local hydroclimatic processes and conditions (i.e., catchment runoff, precipitation, evaporation, relative humidity) on lake drying at the PAD. This study focuses on identifying intervals when local hydroclimate has increased evaporation of lakes during the past ~400 years using paleolimnological analysis at four hydrologically isolated lakes adjacent to the PAD. Then, to determine the relative role of local hydroclimate in lake drying at the PAD, paleohydrological records from the study lakes were compared to paleohydrological data and contemporary hydrological monitoring records from perched basins within the PAD that exhibit recent drying. Specific intervals of interest include previously identified episodes of drying in the PAD during the Little Ice Age (LIA; 1600-1900 CE) and during the twentieth (1900-2000 CE) and twenty-first (2000-2019 CE) centuries. Lake water oxygen isotope composition was reconstructed from cellulose oxygen isotope composition (cellulose-inferred $\delta^{18}O_{lw}$). Stratigraphic intervals of cellulose-inferred $\delta^{18}O_{lw}$ values > 1 standard deviation above the lake-specific long-term mean were considered intervals more strongly influenced by evaporation. These 'intervals of ^{18}O enrichment' were identified at two or more study lakes during the early LIA, late LIA, and since ca. 1995 and correspond to reconstructions of low relative humidity from tree ring records. Results identify that local hydroclimate contributed, in part, to lake drying in the PAD during the early LIA but was offset by increased influence of river floodwaters during the late LIA. During the twentieth century, local hydroclimate appears to have played little to no role in drying trends at lakes in the PAD, whereas a significant trend in

cellulose-inferred $\delta^{18}O_{lw}$ values at one study lake during the past two decades suggests local hydroclimate may have contributed marginally to very recent lake drying trends. Importantly, twentieth century PAD lake drying does not appear to be influenced markedly by local hydroclimate; rather, increased evaporation at PAD lakes has been driven primarily by reduced frequency and magnitude of flooding. This research informs ongoing policy and conservation decisions by discerning the influence of local hydroclimate on lake-level drawdown within the PAD.

Acknowledgements

Brent and Roland, thank you for this amazing project, the many opportunities to mentor students in the lab and lead in various ways, and giving me this space to grow as a scientist and person. Brent especially, thank you for investing so many hours teaching me and discussing ideas.

Thank you, Heidi and Rebecca for inspiring curiosity and wonder in every conversation we have.

Thank you, Robert and Barbara Grandjambe for welcoming me into your home and teaching me so much about the land and how the delta is, has been, and has changed.

Jen, thank you for your invaluable, sustained guidance and friendship. Thank you, Johan for sharing your enthusiasm for science and for dating these cores. James, thank you for your mentorship and teaching me how fun every day can be.

Thank you to all my friends in the Wolfe/Hall lab, especially those who helped with field work. Amanda, thank you for your easy-going nature and support in the lab. Thank you to our helicopter pilot Mitch who can hold ‘er steady no matter the weather. Amy, Ethan, Sean, and Tiffany, thank you for all your hard work through your undergraduate theses!

Laura, screaming at ravens, endless walks, dreaming together, thank you for making every moment we spend together special. Mia, I’m so glad we got to do this in step with each other, thank you for your friendship, and sharing a sense of calm amidst a storm. Katie T., thank you for your endless compassion.

Rachel, you are a joy, thank you for encouraging me to put my computer away and do something fun. Jenny, thank you for your perspective and friendship. Wynona and Steph, thank you for your understanding ears and kind words. Erica and Cat, thank you for your goofy energy and antics.

Sarah, Yara, Kyle – thank you for holding my hand through the hardest moments.

Mom and Dad, I love you so much.

Dedication

For Oscar and Peggy.

Table of Contents

Author's Declaration ii

Abstract iii

Acknowledgements v

Dedication vi

List of Tables ix

List of Figures x

Chapter 1. Introduction 1

1.1 Security of water supply at northern freshwater landscapes 1

1.2 Peace-Athabasca Delta 2

1.3 Paleohydrological research in the Peace-Athabasca Delta 5

1.4 Objectives 6

Chapter 2. Methods 8

2.1 Study area 8

2.1.1 Meteorological record 8

2.1.2 Lakes selected for paleohydrological reconstructions 9

2.2 Field methods 11

2.3 Laboratory methods 12

2.3.1 Loss-on-ignition analysis 12

2.3.2 Radiometric dating 13

2.3.3 Analysis of cellulose oxygen isotope composition and organic carbon and nitrogen elemental and isotope composition 14

2.3.4 Lake water isotope composition 16

2.4 Numerical and statistical analyses 16

2.4.1 Designation of intervals of ^{18}O enrichment and trend tests 16

2.4.2 Evaporation-to-inflow ratio calculations 17

Chapter 3. Results and Discussion 19

3.1 Radiometric dating 19

3.2 Assessment of organic matter source 22

3.3 Reconciling relations between measured $\delta^{18}O_{lw}$ and cellulose-inferred $\delta^{18}O_{lw}$ 23

3.4 Evaluating paleohydrological responses of the study lakes to local hydroclimate since ca. 1600 29
3.4.1 Paleohydrological responses of the study lakes to local hydroclimate during the Little Ice Age 29
3.4.2 Paleohydrological responses of the study lakes to local hydroclimate during the twentieth and twenty-first centuries 31
3.4.3 Reconciling paleohydrological records at the study lakes 32
3.5 Discerning the relative role of local hydroclimate on episodes of drying at lakes in the Peace-Athabasca Delta 35
Chapter 4. Conclusions and Recommendations 39
4.1 Key findings 39
4.3 Recommendations 42
References 44
Appendix A: Water isotope and limnological data 52
Appendix B: Compiled chronology data 53
Appendix C: Compiled loss-on-ignition data 68
Appendix D: Compiled carbon and nitrogen elemental and isotope data 106
Appendix E: Compiled cellulose oxygen isotope data 122
Appendix F: Stratigraphic records of carbon and nitrogen elemental and isotope data 137
and cellulose oxygen isotope data 137
Appendix G: Statistical analyses 138

List of Tables

Table 2.1. Locations and sediment core information for the four study lakes..... 10

Table 2.2. Paleolimnological analyses performed on each core. Two cores from each lake were used for the multiple paleolimnological analyses because the volume of sediment in each interval was too low for all analyses to be performed on a single core. A filled cell with an X denotes which core was used for each analysis. 13

Table 3.1. Summary statistics of organic matter content, C:N and $\delta^{13}C_{org}$ from the non-dated sediment cores at study lakes. 22

Table 3.2. Range and difference between cellulose-inferred $\delta^{18}O$ in upper strata of the sediment core and 2019 measured lake water $\delta^{18}O$ values at the four study lakes. 26

Table 3.3. Range of evaporation-to-inflow (E/I) ratios estimated for AC1, AC3, AC5, and PC4 during intervals of ^{18}O enrichment identified at two or more study lakes during the early LIA, late LIA, and ca. 1995 to 2019. Corresponding ranges of E/I ratios are also reported for PAD 5 and PAD 12. For PAD 5 and PAD 12, the early LIA was considered as ca. 1620 to ca. 1730 and the late LIA was considered as ca. 1820 to ca. 1870 (see Figure 3.5). E/I ratios above 0.50, where evaporation has more influence on lake water balance than inflow, are bolded. Early LIA, Late LIA, 1995 to 2000, and 1995 to 2019 E/I ratios are based on cellulose-inferred $\delta^{18}O_{lw}$ records and 2001 to 2019 E/I ratios are based on measured $\delta^{18}O_{lw}$. 38

List of Figures

Figure 1.1. Location of the Peace-Athabasca Delta (PAD) in northern Alberta, Canada. The bottom panel shows locations of the study lakes (AC1, AC3, AC5, PC4; purple dots), which are within 10 km of the PAD boundary. Also shown are the locations of paleohydrological reconstructions from key lakes within the PAD (PAD 5, PAD 12, and PAD 15; grey dots; Wolfe *et al.,* 2008a). Maps were made from open government sources (Department of Natural Resources and Government of Alberta). 4

Figure 1.2. Paleoenvironmental reconstructions of lake water oxygen isotope composition at an upland lake in the PAD (PAD 5; Wolfe *et al.*, 2008a), flood frequency and magnitude from z-scored measurements of magnetic susceptibility at an oxbow lake in the PAD near the Peace River (PAD 15; Wolfe *et al.*, 2008a), and decadal relative humidity at an upstream location near the Athabasca River headwaters (Edwards *et al.*, 2008) and annual relative humidity within the PAD (Bailey, 2008) from annual isotope measurements of tree-ring records. Long-term trends are displayed by running means at PAD 5 (10-point), PAD 15 (5-point; blue: high flood frequency and magnitude, yellow: low flood frequency and magnitude), Athabasca River headwaters (5-point), and PAD (20-point). Note x-axis is reversed for PAD 15, the Athabasca River headwaters tree-ring record, and the PAD tree-ring record to align with direction of drying in the PAD 5 cellulose oxygen isotope record. The vertical dashed line in the PAD 5 record is the contemporary value for the isotope composition of a terminal lake at hydrologic and isotopic steady state (δ_{SSL}; Remmer *et al.*, 2020a). Values to the right are interpreted to represent intervals of lake-level drawdown. Lower z-score values for relative humidity represents lower relative humidity. Dashed vertical lines identify zero of z-scored data. The Little Ice Age (LIA; ~1600-1900 CE) is distinguished by light grey shading. 7

Figure 2.1. Adjusted and homogenized annual meteorological data at Fort Chipewyan (stations: 3072659 and 3072658) since 1883. An increasing temporal trend in mean annual air temperature (left panel) was identified by linear regression (accompanying grey bands denote the 95% confidence interval of the trend line). Zero degrees Celsius is also identified (dashed line). Total annual precipitation at Fort Chipewyan (right panel; blue) was supplemented with data from the Fort Smith station (grey; station: 2202200) since data available were sparse and total annual snow is distinguished at both stations (white vertical bars). Adjusted and homogenized climate data were obtained from the Environment and Climate Change Canada (GoC, 2021, November 18). Relative humidity data were not available. 9

Figure 2.2. Photos of the four study lakes located adjacent to the Peace-Athabasca Delta: lake AC1 (September 13, 2019), lake AC3 (September 13, 2019), lake AC5 (July 15, 2019), and lake PC4 (May 14, 2019; Photos: K.C. Brown). 11

Figure 3.1. Graphs showing stratigraphic profiles of radioisotope activities, age-depth relations and organic matter content in cores from the study lakes AC1-C3, AC3-C1, AC5-C1, and PC4-C3. Activity profiles (left panel) are displayed for measured ^{226}Ra (white), ^{137}Cs (grey), and ^{210}Pb (black). CRS age model (middle panel; black) and linear extrapolation (grey) are displayed along with the depth of peak ^{137}Cs (green star) plotted at the CRS-defined date of 1963. Cross-matched radiometrically dated (right panel; black) and non-dated cores (grey; AC1-C2, AC3-C2, AC5-C2, and PC4-C2) are displayed by depth. 21

Figure 3.2. Mean $\delta^{13}C_{org}$ values and carbon-to-nitrogen ratios (C:N) from sediment cores at the study lakes (AC1: white, AC3: dark grey, AC5: grey, PC4: black) are displayed relative to ranges for algae, C3 land plants, and C4 land plants (shaded areas) reported by Meyers & Teranes (2001, p. 243). Horizontal and vertical bars around the mean values represent the range of values at each lake. 23

Figure 3.3. Panels AC1, AC3, AC5, and PC4 project stratigraphic profiles of cellulose-inferred lake water $\delta^{18}O$ since 1999 (light green) onto lake-specific evaporation lines defined by the May 2019 lake water isotope data and the 2015-2019 isotope framework developed by Remmer *et al.* (2020a) for the PAD. Included are the Local Meteoric Water Line (LMWL; solid black) and Local Evaporation Line (LEL; dashed light grey). Note that the range of cellulose-inferred $\delta^{18}O_{lw}$ values for the post-1999 stratigraphic records are lower than the measured lake water $\delta^{18}O$ values from 2019 for AC1, AC3, and PC4, likely a consequence of snowmelt bypass in 2019. Bottom panels include meteorological data where 2019 (dark blue) is compared to 1981-2010 climate normal (green). See text for explanation of labels. 27

Figure 3.4. Photos of the Peace-Athabasca Delta (March 30 and 31, 2019): lakes were ice-covered and there was little to no snow accumulation across the surrounding catchments, suggesting snowmelt occurred before ice-off in 2019 (Photos: A. Ghosh). 28

Figure 3.5. Tree-ring isotope-based reconstructions of a) relative humidity (Edwards *et al.*, 2008; Bailey, 2008) are displayed along with cellulose-inferred lake water $\delta^{18}O$ reconstructions for b-e) the study lakes and f-g) two perched lakes in the PAD near the Peace River (PAD 5, PAD 12; Wolfe *et al.*, 2008a). a) Long-term trends of relative humidity reconstructed from measurements of carbon and oxygen isotope composition of tree-rings at the headwaters of the Athabasca River by Edwards *et al.* (2008; dark purple) and within the Peace-Athabasca Delta by Bailey (2008; teal) are displayed using running means (5-point and 20-point, respectively). The dashed vertical line identifies the zero of z-scored data based on the full 1000-year record from Edwards *et al.* (2008). Note, the x-axis is reversed such that lower relative humidity is to the right. b-e) Cellulose-inferred lake water $\delta^{18}O$ records for the study lakes, including three-point running means (black line). Values greater than one standard deviation above the long-term mean were considered high (yellow circles) and are differentiated from the rest of the record (dark blue circles). Additionally, values exceeding lake water oxygen isotope composition (measured $\delta^{18}O_{lw}$) of samples collected in 2019 (> -10.0‰) are identified (bold outline). 'Intervals of ^{18}O enrichment', where high values were persistent, are identified at each study lake and are identified by the grey bars. A dotted vertical line identifies the 1600 to present average cellulose-inferred $\delta^{18}O_{lw}$ for each record. The end of the Little Ice Age (LIA; ~1600-1900 CE) is distinguished by a horizontal dashed line at 1900. The vertical dotted line identifies the 1600 to present average cellulose-inferred $\delta^{18}O_{lw}$. 34

Figure 3.6. Average open-water season measured $\delta^{18}O$ for PAD 5 and PAD 12 (two lakes in the PAD near the Peace River) and cellulose-inferred $\delta^{18}O$ from the study lake AC5 for 2000-2019. A significant positive trend was identified at AC5 (Mann Kendall U test; AC5) since 2000 and a linear trendline visually displays this finding. Dashed line identifies the theoretical oxygen isotope composition of a terminal basin in steady state (δ_{SSL}) based on the 2000-2019 average lake water $\delta^{18}O$ value of PAD 18, a terminal lake considered to be in hydrological steady state (Yi *et al.*, 2008). 38

Chapter 1. Introduction

1.1 Security of water supply at northern freshwater landscapes

Northern water-rich landscapes provide important habitat for wildlife, including migratory birds and species at risk, but their aquatic ecosystems may be subject to marked water level drawdown and terrestrialization due to reduction of water supply caused by climate change and other stressors (Carroll *et al.*, 2011; Wrona *et al.*, 2016). Consequences of climate change across the North are especially concerning for small, shallow lakes which are sensitive to changes in the rates of supply and loss of water (Smol & Douglas, 2007; Carroll *et al.*, 2011). As climate change continues to drive rising temperatures across western North America with marginal change in precipitation (Debeer *et al.*, 2016; Zhang *et al.*, 2019), and duration of ice-free season increases (Cutforth *et al.*, 2004), reduced freshwater delivered by river floodwaters could lead to a water security crisis for floodplain landscapes (Schindler & Donahue, 2006; Wrona *et al.*, 2016). Furthermore, multiple upstream anthropogenic stressors such as river regulation, water extraction for industrial activities, consumptive water usage by urban populations, and increased agricultural water use have complicating negative implications for water delivery to downstream ecosystems (Peters *et al.*, 2006; Schindler & Donahue, 2006; Rasouli *et al.*, 2013).

Understanding the many hydrological drivers of change to floodplain landscapes is integral since the consequences of declining freshwater availability includes restricted land user access to lakes and channels, and displacement of species reliant on inland wetlands (e.g., fish, migratory birds, muskrat; Wrona *et al.*, 2016). However, hydrometric and meteorological records are typically short and sparse, and they are prone to intervals of missing or inconsistent data collection (Zhang *et al.*, 2019). Thus, other sources of long-term data that characterize responses of freshwater ecosystems to climatic change are important for understanding implications for wildlife habitat

and ecosystem function (Smol *et al.*, 2005; Smol & Douglas, 2007). Paleolimnological assessment provides a robust approach to investigate lake responses to climate change especially in remote, northern environments where meteorological and other observational records are limited in space and time (Smol *et al.*, 2005; Smol & Douglas, 2007; Watson & Medeiros, 2021).

1.2 Peace-Athabasca Delta

Concern over freshwater security is a central theme at the Peace-Athabasca Delta (PAD; Figure 1.1), a dynamic floodplain in northeastern Alberta where the Peace and Athabasca rivers provide important sources of water (Timoney, 2013). The PAD is a Ramsar Wetland of International Importance and 80% of it is protected within Wood Buffalo National Park, which is recognized internationally for its "Outstanding Universal Value" as a UNESCO World Heritage Site (Timoney, 2002; WHC/IUCN, 2017). Its many rivers, channels, shallow lakes, and wetlands provide ideal habitat for waterfowl, muskrat, and numerous other wildlife species (Timoney, 2013). This landscape is within Treaty 8 and is the traditional territory of Mikisew Cree First Nation, Athabasca Chipewyan First Nation, and Métis Nation of Alberta (Bill *et al.*, 1996; Timoney, 2002; Straka *et al.*, 2018). Local Knowledge Holders and scientific researchers have raised concerns of declining water availability and associated cascading negative effects to aquatic ecosystem function, wildlife populations, and navigation routes (Prowse & Conly, 2002; Wolfe *et al.*, 2008; MCFN, 2014; Remmer *et al.*, 2018; Straka *et al.*, 2018). Water security concerns at the PAD were raised in a petition to UNESCO by Mikisew Cree First Nation to declare WBNP as "World Heritage in Danger" (MCFN, 2014). In response, recommendations were made (WHC/IUCN, 2017) and an Action Plan was developed (WBNP, 2019). Successful implementation of the Action Plan requires comprehensive knowledge of drivers of hydrological change so that remedial interventions are strategic, appropriate, and effective (Romero-Lankao *et*

al., 2014; WBNP, 2019). However, there is ongoing debate over the relative roles of climate change and the regulation of Peace River flow by the W.A.C. Bennett Dam since 1968 on observed drying of the delta's perched basins in recent decades (Beltaos, 2018; Timoney *et al.*, 2018; Wolfe *et al.*, 2020). Although there is widespread acceptance that regulation of Peace River flow has led to drawdown of perched basins at the PAD, long-term perspectives of hydrological change derived from lake sediment records have suggested lake drying began several decades before construction of the dam and that climate change is the overwhelming cause (Wolfe *et al.*, 2012; 2020).

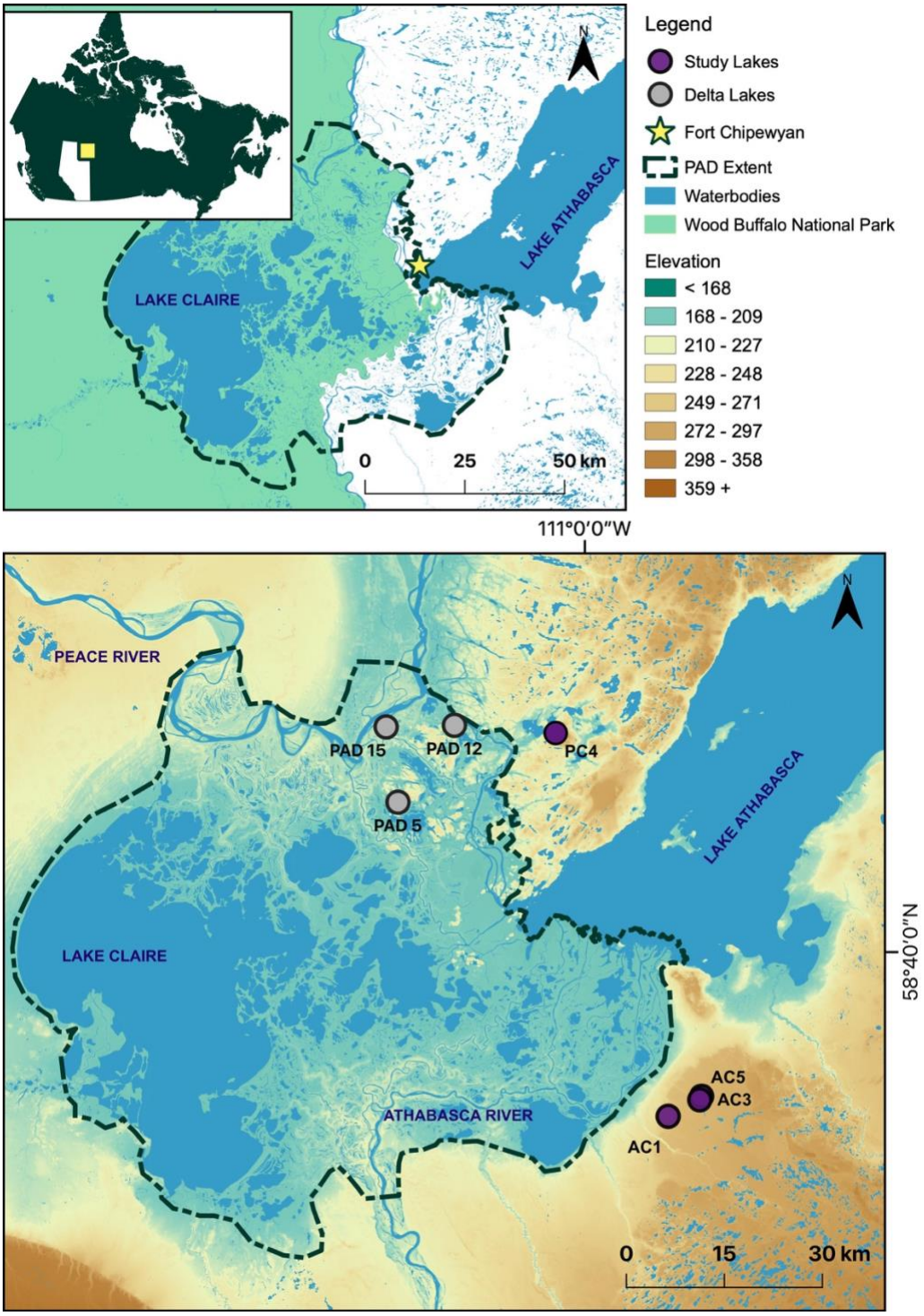

Figure 1.1. Location of the Peace-Athabasca Delta (PAD) in northern Alberta, Canada. The bottom panel shows locations of the study lakes (AC1, AC3, AC5, PC4; purple dots), which are within 10 km of the PAD boundary. Also shown are the locations of paleohydrological reconstructions from key lakes within the PAD (PAD 5, PAD 12, and PAD 15; grey dots; Wolfe *et al.*, 2008a). Maps were made from open government sources (Department of Natural Resources and Government of Alberta).

1.3 Paleohydrological research in the Peace-Athabasca Delta

Key among the paleolimnological reconstructions at the PAD are records of past variation in hydrological conditions at an upland lake in the northern Peace sector of the delta (PAD 5; Figure 1.2; Wolfe *et al.*, 2005; 2008a). Measurement of cellulose oxygen isotope composition used to reconstruct lake water oxygen isotope composition provided evidence of episodic drying during the past 400 years. An episode of extreme lake drying occurred during the early Little Ice Age (LIA; 1600s) when the lake may have periodically desiccated (Wolfe *et al.*, 2005; 2008a). At this time, paleolimnological records from an oxbow lake (PAD 15) indicate that flood frequency and magnitude declined substantially, and regional paleoclimate reconstructions indicate low relative humidity (Wolfe *et al.*, 2006; Edwards *et al.*, 2008; Figure 1.2). Thus, both low flood frequency and low relative humidity may have contributed to the extreme lake drying at PAD 5 during the 1600s. Following a trend to increasing relative humidity during the latter part of the LIA (~1700-1900), another interval of lake drying occurred during the 20th century (Wolfe *et al.*, 2005; 2008a). At this time, flood frequency and magnitude declined (Wolfe *et al.*, 2005; 2006; 2008a) and coincided with a period of low relative humidity in the PAD (Bailey, 2008), which corresponds with increased influence of evaporation at PAD 5 (Figure 1.2). Lake-level drawdown has been observed at PAD 5 since the early 2000s and measurements of water isotope composition indicate that water balance has been dominated by evaporation (Remmer *et al.*, 2018; 2020a). Similarly in recent decades at PAD 12, a historically flood-prone lake, water isotope composition indicates that water balance has become increasingly dominated by evaporation, as has also been documented at many other lakes in the delta (Wolfe *et al.*, 2008a; Remmer *et al.*, 2018; 2020a). Other causes of drying in the PAD during the twentieth and twenty-first centuries, inferred from paleohydrological records and other sources, include

recession of Lake Athabasca from lowland areas (Johnston *et al.*, 2010; Sinnatamby *et al.*, 2010) and geomorphic change that altered distributary flow of the Athabasca River (Wolfe *et al.*, 2008b; Kay *et al.*, 2019). Although multiple causes of drying have been identified in the paleohydrological records, the role of local hydroclimate processes and conditions (i.e., catchment runoff, precipitation, evaporation, relative humidity) remains unknown during episodes of drying at PAD 5 and in recent lake drying across large portions of the delta. Knowledge of the contribution of local hydroclimate to hydrological change across the PAD is important to discern the roles of multiple potential stressors on recent drying, and to inform effective ecosystem management and climate change adaptation planning (Romero-Lankao *et al.*, 2014; WBNP, 2019).

1.4 Objectives

The role of local hydroclimate on lake drying in the PAD has proven difficult to distinguish amongst several other processes (i.e., river flood regimes, variation in open-drainage water levels, geomorphic processes) that have potential to strongly influence lake water balance within this dynamic deltaic landscape. To characterize the role of local hydroclimate on episodes of drying of perched basins in the PAD, when lakes were strongly influenced by evaporation (i.e., early LIA, twentieth century, early twenty-first century), paleohydrological techniques are employed at headwater lakes adjacent to the PAD which are removed from the influence of river flood regimes and deltaic processes. By reconstructing lake water oxygen isotope composition at these sites, temporal variation in lake water balance caused by local climatic variation is assessed. Specifically, hydrological response due to local hydroclimate at study lakes is determined during the LIA (Objective 1), twentieth century (Objective 2), and the first two decades of the twenty-first century (Objective 3).

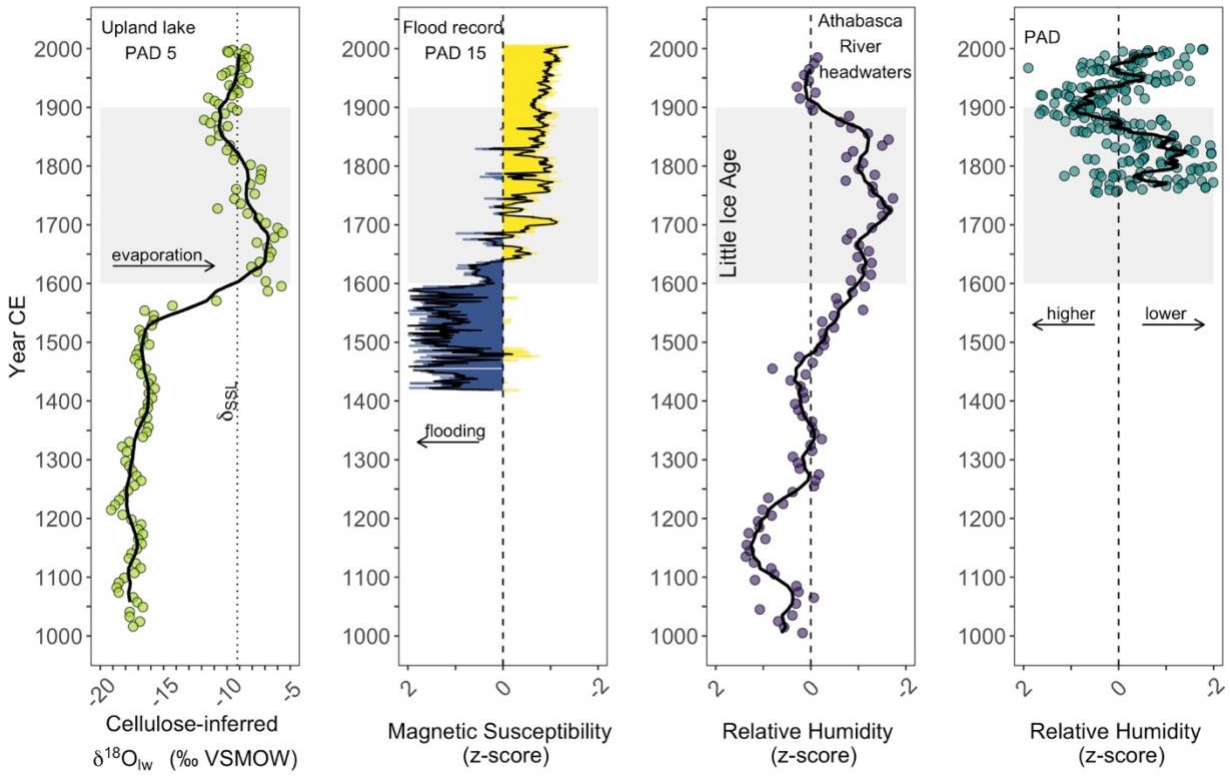

Figure 1.2. Paleoenvironmental reconstructions of lake water oxygen isotope composition at an upland lake in the PAD (PAD 5; Wolfe *et al.*, 2008a), flood frequency and magnitude from z-scored measurements of magnetic susceptibility at an oxbow lake in the PAD near the Peace River (PAD 15; Wolfe *et al.*, 2008a), and decadal relative humidity at an upstream location near the Athabasca River headwaters (Edwards *et al.*, 2008) and annual relative humidity within the PAD (Bailey, 2008) from annual isotope measurements of tree-ring records. Long-term trends are displayed by running means at PAD 5 (10-point), PAD 15 (5-point; blue: high flood frequency and magnitude, yellow: low flood frequency and magnitude), Athabasca River headwaters (5-point), and PAD (20-point). Note x-axis is reversed for PAD 15, the Athabasca River headwaters tree-ring record, and the PAD tree-ring record to align with direction of drying in the PAD 5 cellulose oxygen isotope record. The vertical dashed line in the PAD 5 record is the contemporary value for the isotope composition of a terminal lake at hydrologic and isotopic steady state (δ_{SSL}; Remmer *et al.*, 2020a). Values to the right are interpreted to represent intervals of lake-level drawdown. Lower z-score values for relative humidity represents lower relative humidity. Dashed vertical lines identify zero of z-scored data. The Little Ice Age (LIA; ~1600-1900 CE) is distinguished by light grey shading.

Chapter 2. Methods

2.1 Study area

2.1.1 Meteorological record

Meteorological records from stations near the PAD (Fort Chipewyan, AB and Fort Smith, NWT) are consistent with regional trends (Zhang *et al.*, 2019) and indicate mean annual air temperature has increased since ca. 1880 (adjusted $R^2 = 0.237$; linear regression, $F = 29.63$, $p = 4.40 \times 10^{-7}$, d.f. = 1, 91), with a small increase in total annual precipitation since ca. 1950 (Figure 2.1). Mean annual temperature has exceeded 0 °C in six years since 1987, whereas only one year exceeded this value between 1883 and 1987. Total annual precipitation at Fort Chipewyan ($\bar{x}$ = 397.38 mm, σ^2 = 83.17 mm) and Fort Smith ($\bar{x}$ = 408.83 mm, σ^2 = 88.22 mm) were comparable and have shifted to higher values since the 1950s, while total snow accumulation has remained stable (F.C.: $\bar{x}$ = 144.89, F.S.: $\bar{x}$ = 158.46 mm), suggesting increased precipitation has been driven by greater rainfall. Although data on frost-free days were too sparse to explore at the Fort Chipewyan station, increasing temperature and higher precipitation in recent decades may indicate a lengthening of the ice-free season consistent with observations across the Prairies (Cutforth *et al.*, 2004).

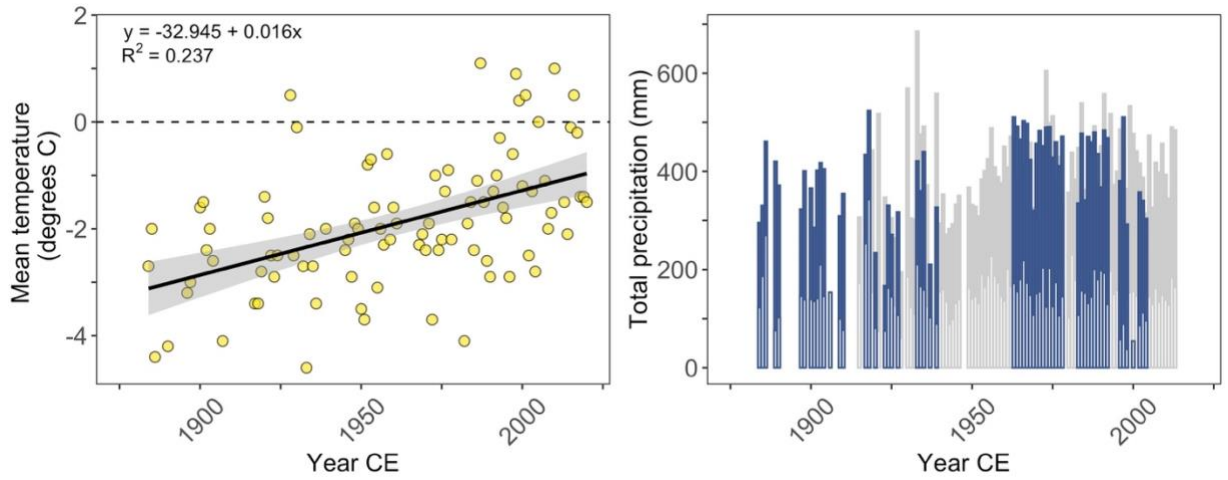

Figure 2.1. Adjusted and homogenized annual meteorological data at Fort Chipewyan (stations: 3072659 and 3072658) since 1883. An increasing temporal trend in mean annual air temperature (left panel) was identified by linear regression (accompanying grey bands denote the 95% confidence interval of the trend line). Zero degrees Celsius is also identified (dashed line). Total annual precipitation at Fort Chipewyan (right panel; blue) was supplemented with data from the Fort Smith station (grey; station: 2202200) since data available were sparse and total annual snow is distinguished at both stations (white vertical bars). Adjusted and homogenized climate data were obtained from the Environment and Climate Change Canada (GoC, 2021, November 18). Relative humidity data were not available.

2.1.2 Lakes selected for paleohydrological reconstructions

Shallow lakes (<6 m) located adjacent to and outside of the PAD were selected for this study (Figure 1.1, 2.2). The lakes lacked identifiable inflow or outflow channels. Since they can be assumed to be directly affected by precipitation, runoff, and evaporation, climate is expected to be the primary driver of hydrological change at the study lakes. Four lakes were selected for paleohydrological reconstructions: three (AC1, AC3, AC5) adjacent to the southern Athabasca sector of the PAD within eolian sand deposits, and one (PC4) adjacent to the northern Peace sector of the PAD within a bedrock basin composed primarily of granite (Table 2.1, Figure 2.2). Located 5 km southeast of the PAD, AC1 (58.414694, -110.764306; 2.4 m deep) is situated in a flat landscape where there is an absence of trees and growth of low-lying vegetation along a small eastern bay (Figure 1.1, 2.1, 2.2). This suggests that water-level has varied over time and declined

in recent years, as water once filled this area. Located approximately 5 km to the northeast of AC1 are lakes AC3 (58.437056, -110.681528; 5.2 m deep) and AC5 (58.441667, -110.676389; 4.2 m deep). These lakes are adjacent to one another with slight embankments along their eastern shores compared to the flat surrounding landscape and tree growth on the outskirts of exposed sandy shoreline, which may indicate recent variation in lake water-level, especially at AC5. Located approximately 8 km northeast of the PAD is PC4 (58.941833, -111.06025; 5.7 m deep), a lake within a basin of granitic bedrock and a catchment of greater relief than other lakes near the Athabasca sector and coniferous tree cover is comparatively sparse. There is no visual evidence of a connected wetland, although lake-wetland connectivity is common in the area, nor is there evidence of recent water-level change (i.e., no exposed shoreline or low-lying vegetation).

Table 2.1. Locations and sediment core information for the four study lakes.

	AC1	AC3	AC5	PC4
Latitude	58.414694	58.437056	58.441667	58.941833
Longitude	-110.764306	-110.681528	-110.676389	-111.06025
Depth (m)	2.4	5.2	4.2	5.7
Date of collection	May 15, 2019	July 12, 2019	July 15, 2019	May 14, 2019
Dated core (cm)	73.5 (C3)	91.5 (C1)	83.0 (C1)	94.5 (C3)
Undated core (cm)	61.0 (C2)	91.0 (C2)	83.5 (C2)	88.0 (C2)
Archive Core (cm)	48.0 (C1)	89.5 (C3)	75.0 (C3)	36.0 (C1)

Figure 2.2. Photos of the four study lakes located adjacent to the Peace-Athabasca Delta: lake AC1 (September 13, 2019), lake AC3 (September 13, 2019), lake AC5 (July 15, 2019), and lake PC4 (May 14, 2019; Photos: K.C. Brown).

2.2 Field methods

Lake sediment cores were retrieved in May (AC1, PC4) and July (AC3, AC5) of 2019 from a central deep-water region of each lake using a modified Glew hammer-driven gravity corer fitted with PVC core tubes (86 mm ID; Telford *et al.*, 2021) deployed off the pontoon of a helicopter. At each lake, three sediment cores were collected ranging in length from 36.0 to 94.5 cm (Table 2.1). After transport to the field base in Fort Chipewyan, Alberta, cores were described and sectioned at 0.5-cm intervals into Whirl-Pak® bags (Telford *et al.*, 2021). Cores were designated

for radiometric dating, for other paleolimnological analyses or archived based on length (Table 2.1). Samples were refrigerated (2-4°C) until analyses were performed at University of Waterloo and Wilfrid Laurier University. In May, July, and September 2019, water was collected from the four study lakes at 0.5 m below the water surface and stored in tightly capped 30 ml high-density polyethylene bottles before measurement of hydrogen and oxygen isotope composition at the University of Waterloo – Environmental Isotope Laboratory (UW-EIL).

2.3 Laboratory methods

2.3.1 Loss-on-ignition analysis

Loss-on-ignition (LOI) analysis was performed on the two longest cores from each lake to assess stratigraphic variation in sediment composition and align stratigraphic samples between dated and non-dated sediment cores collected from the same lake (Table 2.2; AC1-C2, AC1-C3, AC3-C1, AC3-C2, AC5-C1, AC5-C2, PC4-C2 and PC4-C3). Sequential heating of sub-samples from each 0.5-cm interval of sediment at three temperatures was used to determine the water, organic matter, mineral matter, and carbonate content (Heiri *et al*., 2001). For each interval, 0.5 ±0.05 g of well-mixed wet sediment was sub-sampled into dry pre-weighed crucibles. Samples were first heated at 90°C for 24 hours and placed in a desiccator for 2 hours to cool without absorbing ambient moisture before re-weighing to determine the water content. Samples were then heated at 550°C for 2 hours and placed in a desiccator for 2 hours to cool without absorbing ambient moisture before re-weighing to determine organic matter content. Finally, samples were heated to 950°C for 2 hours and placed in a desiccator for 2 hours to cool without absorbing ambient moisture before re-weighing to determine the carbonate content (LOI 1000*1.36; Heiri *et al*., 2001). The remaining material ((100 % – organic matter %) – carbonate %) was characterized as carbonate-free mineral matter.

Table 2.2. Paleolimnological analyses performed on each core. Two cores from each lake were used for the multiple paleolimnological analyses because the volume of sediment in each interval was too low for all analyses to be performed on a single core. A filled cell with an X denotes which core was used for each analysis.

	AC1		AC3		AC5		PC4	
	C2	C3	C1	C2	C1	C2	C2	C3
LOI	X	X	X	X	X	X	X	X
Radiometric dating		X	X		X			X
C/N and Cellulose	X			X		X	X	

2.3.2 Radiometric dating

Gamma-ray spectrometry was used to measure ^{210}Pb and ^{226}Ra activities (via daughter isotopes ^{214}Bi and ^{214}Pb) and establish sediment core chronologies, and a peak in ^{137}Cs activity was used as an independent chronological marker to assess accuracy of the age-depth relations based on ^{210}Pb dating (Appleby and Oldfield, 1978; Appleby, 2001). However, ^{137}Cs may be mobile in organic-rich sediment and may not precisely mark peak fallout in 1963 (Appleby, 2001). Well mixed subsamples of sediment from one core at each lake were combined from two adjacent 0.5-cm intervals to yield 1.0-cm thick samples that were used for the radiometric dating analysis, except for core C3 from AC1 which was analysed at 0.5-cm intervals (Table 2.2). Consecutive 0.5- or 1.0-cm intervals through the upper 20.0 cm of each core and every second cm from 21.0-42.0 cm were freeze-dried using a SP Scientific VirTis BenchTop freeze-dryer and packed to 3.5 cm into polystyrene tubes (Sarstedt 55.523; 8ml round base tube). Additional samples between 21.0-42.0 cm were prepared in the same manner, as needed. Samples were sealed with a silicon septum and 1 cc epoxy and then set aside for at least 21 days to allow ^{222}Rn to equilibrate with ^{226}Ra prior to analysis at the University of Waterloo WATER Lab using an Ortec co-axial HPGe Digital Gamma Ray Spectrometer with Maestro 32 software. Chronologies were estimated using

the Constant Rate of Supply (CRS) model, which assumes constant flux of ^{210}Pb to sediment but allows sedimentation rates to vary (Appleby and Oldfield, 1978; Appleby, 2001; Sanchez-Cabeza and Ruiz-Fernandez, 2012). Below the stratigraphic horizon where unsupported ^{210}Pb activity approached zero (i.e., were equivalent to supported or background ^{210}Pb activity; Binford, 1990; Appleby, 2001, equation 34), the chronology was linearly extrapolated based on average dry-sediment accumulation rate. For each lake, the CRS age model developed using the radiometrically dated sediment core was applied to the second core by comparing and aligning stratigraphic variations in organic matter content and applying a depth-correction factor. A graphical 'cross-matching' approach was used to account for variation in sedimentation across the lakebed, which may result from slight differences in slope between adjacent coring locations and the angle at which the core tube entered the lake sediment (Thompson *et al.*, 2012).

2.3.3 Analysis of cellulose oxygen isotope composition and organic carbon and nitrogen elemental and isotope composition

Temporal change in lake water oxygen isotope composition was reconstructed using measurements of cellulose oxygen isotope composition (Table 2.1; Wolfe *et al.*, 2001). Aquatic plants and algae incorporate the oxygen isotope composition of lake water predictably (rather than available forms of atmospheric oxygen incorporated by terrestrial plants) and is independent of plant species or temperature (fractionation factor: 1.028 ±0.0015; Wolfe *et al.*, 2001; Savage *et al.*, 2021). Carbon-to-nitrogen ratios (C:N ratio) and $\delta^{13}C_{org}$ were assessed to confirm lake sediment organic matter was primarily aquatic in origin. Lake algae and surface sediment C:N ratios values are low (typically <10) whereas values for terrestrial organic material are much higher (typically >20; Meyers & Lallier-Vergès, 1999; Meyers & Teranes, 2001).

Sediment sub-samples from each 0.5-cm interval were treated with 10% HCl (by volume) to remove inorganic carbon (carbonates), freeze-dried using a SP Scientific VirTis BenchTop freeze-dryer, dry sieved (250 mm) to remove coarse (potentially terrestrial) material, weighed, and submitted for analysis of organic carbon and nitrogen elemental and isotope composition at the UW-EIL. Results are reported as organic %C (%C_{org}) and %N, from which C:N ratios were calculated, in addition to $\delta^{13}C_{org}$ (‰ VPDB ±0.2‰), and $\delta^{15}N$ (‰ AIR ±0.3‰) where $\delta_{Sample} = [(R_{sample}/R_{standard}) -1] \times 10^3$ and R represents the sample and standard ratio $^{13}C/^{12}C$ or $^{15}N/^{14}N$, respectively (Appendix D and F).

Samples of the acid-washed fine fraction were then treated with a solvent extraction (2:1, benzene:ethanol) to remove lipids, resins, and tannins; a bleach solution (glacial acetic acid and sodium chlorite) to remove lignin; an alkaline hydrolysis solution (17% sodium hydroxide) to remove xylan, mannan, and non-glucan polysaccharides; and an oxyhydroxide leaching solution (sodium dithionite, tri-ammonium citrate, and hydroxylamine hydrochloride) to remove iron and manganese oxyhydroxides (Wolfe *et al.*, 2001). Samples were then freeze dried, which separated material by weight leaving organic remains (i.e., cellulose) atop the remaining fine grained minerogenic material. Thus, heavy-liquid density separation (Wolfe *et al.*, 2007) was considered unnecessary. Cellulose was carefully removed from minerogenic residue, weighed, and submitted for oxygen isotope analysis at the UW-EIL. Results are reported as $\delta^{18}O$ (‰ VSMOW ±0.3‰), where $\delta_{Sample} = [(R_{sample}/R_{standard}) -1] \times 10^3$ and R represents the sample and standard $^{18}O/^{16}O$ ratio. Cellulose-inferred lake water oxygen isotope composition (cellulose-inferred $\delta^{18}O_{lw}$) was reconstructed using a cellulose-water oxygen isotope fractionation factor of 1.028 ±0.0015 (Wolfe *et al.*, 2001; Savage *et al.*, 2021).

2.3.4 Lake water isotope composition

Lake water samples collected in 2019 were measured using off-axis integrated cavity output spectroscopy (O-AICOS) at the UW-EIL. Results were normalized to VSMOW-SLAP (Coplen, 1996) and reported as $\delta^{18}O$ (‰ VSMOW ±0.2‰) and $\delta^{2}H$ (‰ VSMOW ±0.8‰), where $\delta_{Sample} = [(R_{sample}/R_{standard}) -1] \times 10^{3}$ and R represents the sample and standard ratio of $^{18}O/^{16}O$ or $^{2}H/^{1}H$. Results were compared to the uppermost stratigraphic records of cellulose-inferred $\delta^{18}O_{lw}$ in $\delta^{18}O$-$\delta^{2}H$ space, using the 2015-2019 framework developed by Remmer *et al.* (2020a) for the PAD, to inform interpretation of the cellulose-inferred lake water oxygen isotope reconstructions. Additional calculations were performed using the May 2019 values to estimate the isotope composition of source water (δ_I) and lake-specific water vapour (δ_E) using the coupled-isotope tracer approach (Yi *et al.*, 2008).

2.4 Numerical and statistical analyses

2.4.1 Designation of intervals of ^{18}O enrichment and trend tests

To determine stratigraphic intervals when evaporative influence was relatively high at the study lakes, cellulose-inferred $\delta^{18}O_{lw}$ values more than one standard deviation above the lake-specific long-term mean were identified. Where there were multiple adjacent measurements > 1 standard deviation above the lake-specific long-term mean, intervals of ^{18}O enrichment were established. Intervals of local hydroclimate driven evaporative influence were considered to be when at least two study lakes had temporally overlapping intervals of ^{18}O enrichment.

Mann-Kendall U rank trend tests were performed for each lake to evaluate hydrological responses to local hydroclimate during twentieth century drying trends in cellulose-inferred $\delta^{18}O_{lw}$ and to evaluate temporal trends during the first two decades of the twenty-first century.

Cellulose-inferred $\delta^{18}O_{lw}$ records at the study lakes, as well as estimated evaporation-to-inflow ratios for intervals of ^{18}O enrichment, following approaches used in Wolfe *et al.* (2005), were then compared to equivalent records (and recent water isotope monitoring data) at PAD 5 and PAD 12. Numerical and statistical analyses were performed using R version 3.6.2 and R Studio version 1.2.1335 (R Core Team, 2019; R Studio Team, 2019). Key R packages included Kendall and tidyverse (McLeod, 2011; Wickham *et al.*, 2019).

2.4.2 Evaporation-to-inflow ratio calculations

To further explore the role of local hydroclimate on episodes of drying in the PAD, stratigraphic intervals of ^{18}O enrichment at the study lakes were characterized by estimating the associated ranges of evaporation-to-inflow ratios. Since the study lakes are hydrologically isolated, it is assumed that they are 1) terminal basins (no surface outflow) receiving no surface inflow from another body of water which has undergone evaporation, 2) controlled primarily by hydroclimatic processes and conditions (i.e., catchment runoff, precipitation, evaporation, relative humidity), and 3) cellulose-inferred $\delta^{18}O_{lw}$ records reflect water balance under steady state conditions. Given these assumptions, an isotope-mass balance equation, defined as and used by Wolfe *et al*. (2005):

$$\frac{E}{I} = \frac{1 - h + 10^{-3}\varepsilon_k}{h - 10^{-3}\varepsilon} \times \frac{\delta_I - \delta_L}{\delta_E - \delta_L}$$

was applied using parameters from the 2015-2019 water isotope framework developed for the PAD by Remmer *et al.* (2020a), where h is relative humidity, ε is the isotopic enrichment factor equal to the sum of ε^* (equilibrium component) and ε_k (kinetic component) (Gibson and

Edwards, 2002; Edwards *et al.*, 2004), δ_I is the theoretical isotope composition of source water assumed to be equal to δ_P, and δ_E is the isotope composition of lake-specific water vapour.

Chapter 3. Results and Discussion

3.1 Radiometric dating

Similar stratigraphic variations in total ^{210}Pb activity were observed at AC1 and AC5. Total ^{210}Pb activity was relatively constant in the upper 3.5 cm (~1.2 Bq/g) and 10.0 cm (~1.5 Bq/g) at AC 1 and AC5, respectively, after which activity declined rapidly (Figure 3.1). Below 19.0 cm at AC1 and 36.0 cm at AC5, total ^{210}Pb activities remained near-constant and approximated the mean activity of supported ^{210}Pb (^{226}Ra = 0.003 Bq/g and 0.013 Bq/g, respectively), which suggests background activity was reached. Based on the CRS model at AC1, with error ranging from 0.22 to 11.87 years (2-sigma), and linear extrapolation beyond the depth where background was reached, the basal date was estimated to be ca. 1100 CE. Based on the CRS model at AC5, with error ranging from 0.14 to 15.87 years (2-sigma), the linearly extrapolated basal date was ca. 1550 CE. At AC1 and AC5, peak ^{137}Cs activity corresponded with the CRS model date 1985 and 1969, respectively.

Stratigraphic variation in total ^{210}Pb activity was similar at AC3 and PC4. Total ^{210}Pb activity increased to ~1.7 Bq/g through the upper 2.5 cm and 7.0 cm at AC3 and PC4, respectively, before declining linearly to 10.0 cm (1.414 Bq/g) and 19.5 cm (0.011 Bq/g), respectively (Figure 3.1). At both lakes, ^{210}Pb activity then declined to 32.0 cm (0.024 Bq/g). Below 32.0 cm, total ^{210}Pb activity remained near-constant and approximated mean activity of supported ^{210}Pb (^{226}Ra = 0.010 Bq/g and 0.006 Bq/g), which suggests background activity was reached. Based on the CRS model at AC3, with error ranging from 0.10 to 19.28 years (2-sigma), the linearly extrapolated basal date was ca. 1350 CE. Based on the CRS model at PC4, with error ranging from 0.13 to 19.20 years (2-sigma), the linearly extrapolated basal date was ca. 850 CE. At AC3

and PC4, peak ^{137}Cs activity corresponded with the CRS model date 1978 and 1983, respectively.

Constant or increasing trends in measured ^{210}Pb activity with depth in the upper strata of each core are likely due to increasing sedimentation rate rather than sediment mixing since organic matter content increased through the upper strata of all cores (i.e., %OM was not constant as would be expected if the sediment was mixed) (Figure 3.1). Additionally, while peak measurements of ^{137}Cs activity differed from the expected year (1963; peak deposition from above-ground nuclear weapons testing), the approximation is reasonable given the likelihood for upward mobility of ^{137}Cs through organic-rich sediment (Appleby, 2001).

To apply radiometric dates to non-dated cores, organic matter profiles of both cores were compared and aligned (Table 2.2; Figure 3.1). Offset between organic matter profiles was observed at AC1, AC5, and PC4 and constant correction factors were applied (AC1-C2: 1.22, AC5-C2: 0.95, and PC4-C2: 1.07) to the bottom-depth values of the non-dated cores. CRS model dates were then applied to the adjusted depths by linear interpolation of the nearest depth-wise date.

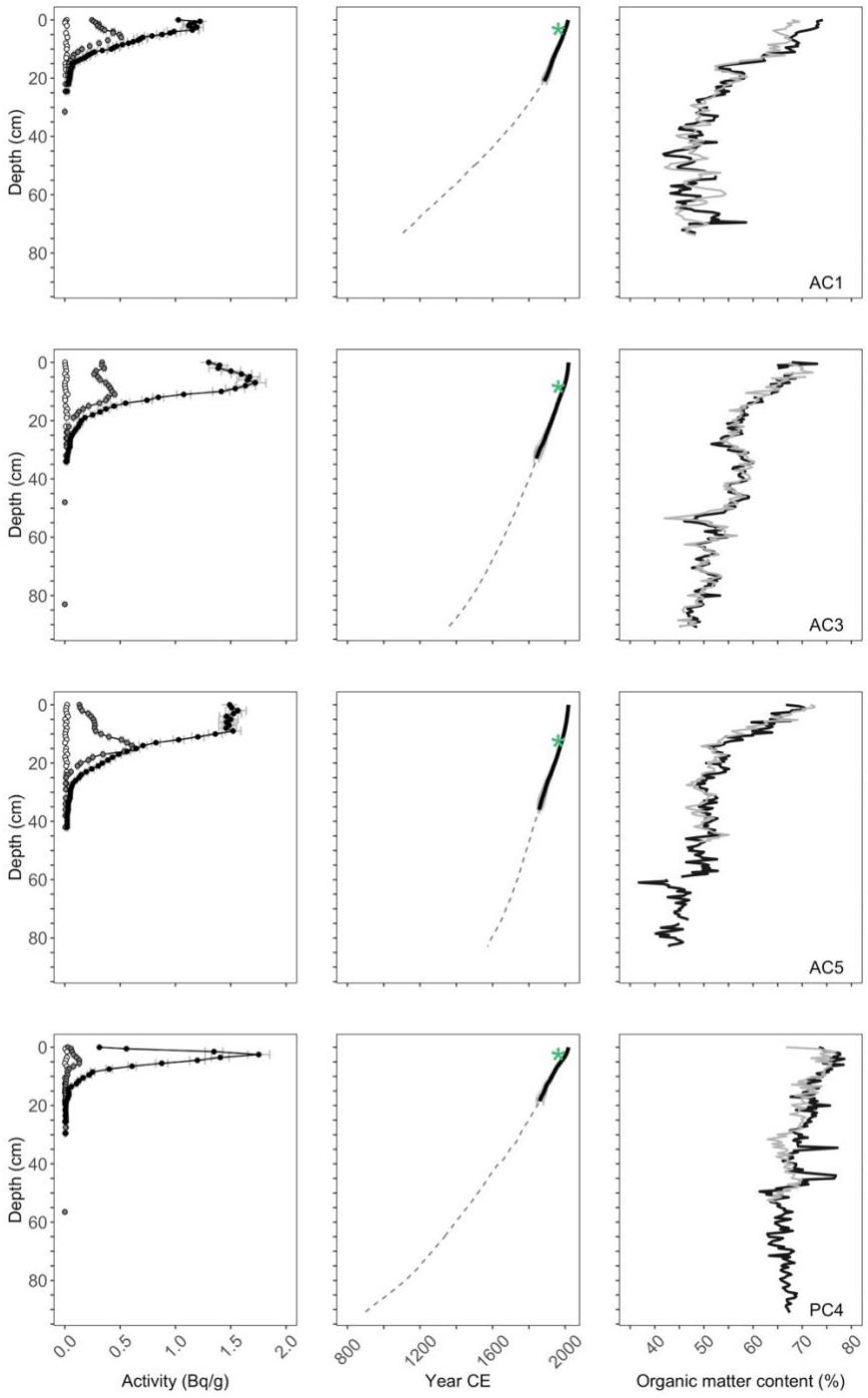

Figure 3.1. Graphs showing stratigraphic profiles of radioisotope activities, age-depth relations and organic matter content in cores from the study lakes AC1-C3, AC3-C1, AC5-C1, and PC4-C3. Activity profiles (left panel) are displayed for measured ^{226}Ra (white), ^{137}Cs (grey), and ^{210}Pb (black). CRS age model (middle panel; black) and linear extrapolation (grey) are displayed along with the depth of peak ^{137}Cs (green star) plotted at the CRS-defined date of 1963. Cross-matched radiometrically dated (right panel; black) and non-dated cores (grey; AC1-C2, AC3-C2, AC5-C2, and PC4-C2) are displayed by depth.

3.2 Assessment of organic matter source

Carbon-to-nitrogen ratios (C:N) and $\delta^{13}C_{org}$ were assessed to confirm that lake sediment organic matter was primarily aquatic in origin, ensuring oxygen isotope composition from extracted cellulose would reflect lake water oxygen isotope composition. Lake sediment records were organic-rich, ranging between 39% and 82% organic matter (Table 3.1; Figure 3.1). C:N ratios were below 15 and similar amongst all lakes, and $\delta^{13}C_{org}$ values ranged from -30.35 to -19.22 ‰ amongst all lakes (Table 3.1; Figure 3.2). Compared to published ranges of values for aquatic plants and algae, mean C:N and $\delta^{13}C_{org}$ values plotted within or near the range of algae (Figure 3.2; C:N < 15, -30‰ < $\delta^{13}C$ < -25‰; Meyers & Teranes; 2001). Thus, the sediment records are well suited to reconstruct lake water oxygen isotope composition from cellulose oxygen isotope composition.

Table 3.1. Summary statistics of organic matter content, C:N and $\delta^{13}C_{org}$ from the non-dated sediment cores at study lakes.

		AC1	AC3	AC5	PC4
Organic matter (%)	Mean	52.6	55.1	50.8	68.7
	Max.	69	72	73	77
	Min.	42	42	39	59
C:N	Mean	12.7	12.5	12.0	11.6
	Max.	15	14	13	12
	Min.	11	11	9	11
$\delta^{13}C_{org}$ (‰ VPDB ± 0.2‰)	Mean	-23.59	-23.04	-23.37	-27.89
	Max.	-21.0	-20.0	-19.2	-26.9
	Min.	-25.8	-25.7	-26.0	-30.4

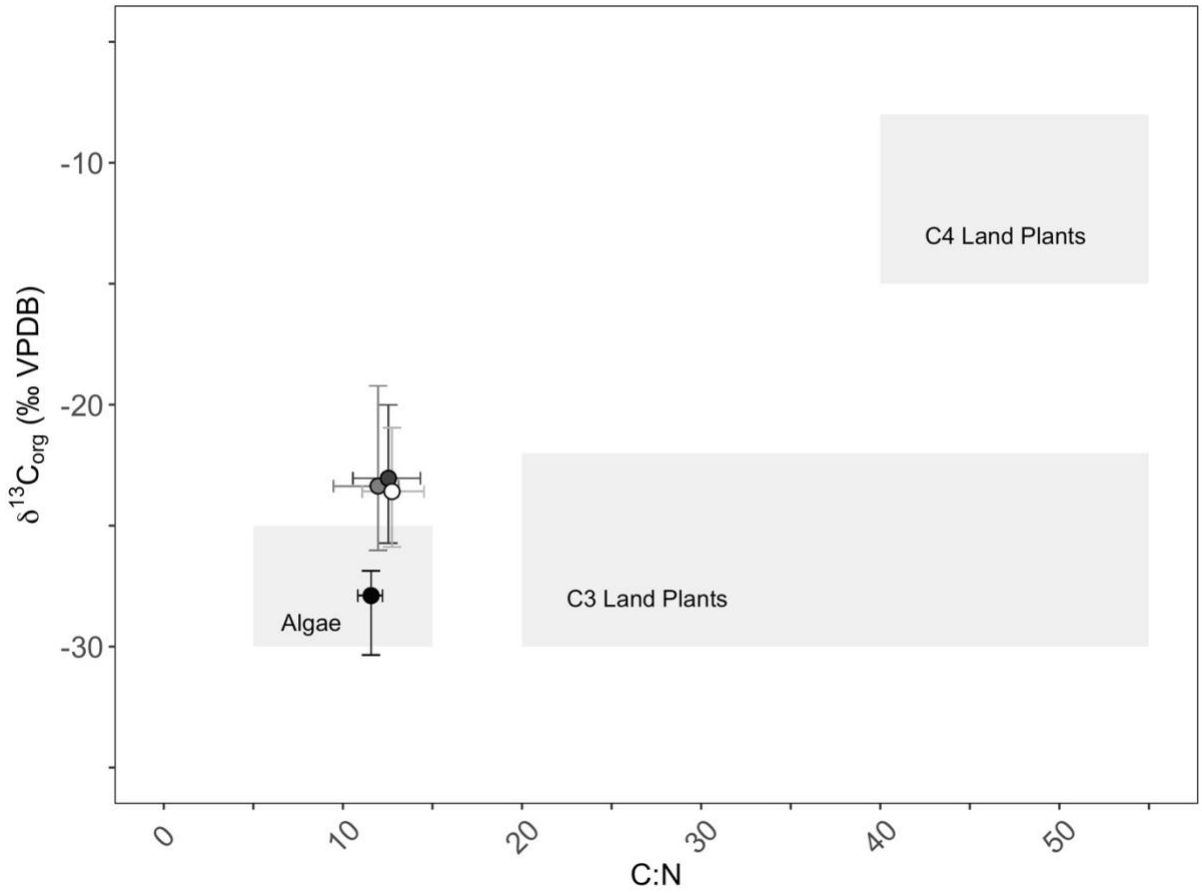

Figure 3.2. Mean $\delta^{13}C_{org}$ values and carbon-to-nitrogen ratios (C:N) from sediment cores at the study lakes (AC1: white, AC3: dark grey, AC5: grey, PC4: black) are displayed relative to ranges for algae, C3 land plants, and C4 land plants (shaded areas) reported by Meyers & Teranes (2001, p. 243). Horizontal and vertical bars around the mean values represent the range of values at each lake.

3.3 Reconciling relations between measured $\delta^{18}O_{lw}$ and cellulose-inferred $\delta^{18}O_{lw}$

Lake water isotope compositions at the four study lakes were measured in 2019 to inform interpretation of the cellulose-inferred lake water oxygen isotope reconstructions. At three of the four study lakes, measured lake water oxygen isotope composition (measured $\delta^{18}O_{lw}$) was higher than the range of cellulose-inferred lake water $\delta^{18}O$ in upper strata of the sediment core (since ca. 1999; Table 3.2). Measured $\delta^{18}O_{lw}$ was ~1.2-3.7‰ higher than cellulose-inferred $\delta^{18}O_{lw}$ in upper strata at AC1 and AC3, whereas measured $\delta^{18}O_{lw}$ was ~3.7-4.9‰ higher than cellulose-inferred

$\delta^{18}O_{lw}$ at PC4. At AC5, measured $\delta^{18}O_{lw}$ was within the range of cellulose-inferred $\delta^{18}O_{lw}$ in the upper strata of the sediment core.

To explore potential causes that may account for the discrepancies between measured $\delta^{18}O_{lw}$ and cellulose-inferred $\delta^{18}O_{lw}$ values at three of the four lakes, the isotope data were examined in $\delta^{2}H$-$\delta^{18}O$ space (Figure 3.3). The isotope composition of input water (δ_I) and evaporative flux (δ_E) were calculated using the May 2019 lake water isotope compositions for each study lake following methods described by Yi *et al.* (2008) and Remmer *et al.* (2020a). A lake-specific evaporation line was then established between δ_I in May of 2019 ($\delta_{I\text{-}May2019}$) and δ^* (theoretical isotope composition of the last drop of water in a lake due to evaporative drawdown; Remmer *et al.*, 2020a). The range of post-1999 cellulose-inferred $\delta^{18}O_{lw}$ at each lake was then projected along the lake-specific evaporation line with the assumption that corresponding lake water $\delta^{2}H$ values would likely plot close to this line. Thus, the green highlighted segments in Figure 3.3 represent the probable range of water balance conditions for each lake since 2000, which illustrates that evaporation during 2019 was greater for three of the study lakes compared to the stratigraphic interval since 1999. At the AC lakes, $\delta_{I\text{-}May2019}$ approximates the average annual isotope composition of precipitation (δ_P) and $\delta_{E\text{-}May2019}$ plots left of the Local Meteoric Water Line (LMWL) indicating evaporation did not exceed inflow at the time of sampling in May 2019. In contrast, at PC4, $\delta_{I\text{-}May2019}$ approximates the isotope composition of snow (δ_{Snow}) indicating the lake is normally supplied primarily by snowmelt. Moreover, $\delta_{E\text{-}May2019}$ plots to the right of the LMWL indicating evaporation exceeded inflow at the time of sampling in May 2019, likely a highly unusual condition for the early open-water season.

Characterization of May 2019 δ_I and water balance status are likely related to catchment characteristics, which regulate runoff and subsurface flow to the lakes, and to meteorological

conditions. The AC lakes are situated within permeable, sandy substrate and likely receive inflow directly via surface runoff, as well as indirect, delayed inflow via subsurface flows derived from both snowmelt and rainfall ($\delta_{I\text{-}May2019} \sim \delta_P$). Conversely, at PC4, the high-relief, bedrock catchment would likely normally promote substantial snowmelt runoff to the lake ($\delta_{I\text{-}May2019} \sim \delta_{Snow}$). However, examination of meteorological data for 2019 reveals strong divergence from the 1981-2010 climate normal. A sharp temperature increase in mid-March occurred for several days when the daily average temperature was well above 0 ºC, which raised the average monthly temperature above the climate normal (1981-2010; Figure 3.3). Field observations in late March 2019 identified that ice-covered lakes were barren of snow (Figure 3.4) suggesting snowmelt occurred in March, before ice-off.

Upon consideration of the isotope data and derived water balance metrics, catchment characteristics, and rapid snowmelt prior to ice-off in 2019, the observed offset between measured $\delta^{18}O_{lw}$ and cellulose-inferred $\delta^{18}O_{lw}$ at three of the four study lakes was likely due to snowmelt bypass. This occurs when snowmelt does not enter an ice-covered lake or passes through a mostly-ice covered lake as a "sub-ice layer" without mixing with lake water since water colder than 4 ºC is less dense than typical winter lake water (Bergmann & Welch, 1985; Schiff & English, 1988; Cortés *et al.*, 2017). Without the influence of ^{18}O depleted snowmelt, lake water would be expected to be ^{18}O enriched reflecting the influence of evaporation during the prior year. The smaller offset between measured $\delta^{18}O_{lw}$ and cellulose-inferred $\delta^{18}O_{lw}$ at the AC lakes suggests they received inflow via subsurface flow through their permeable, sandy catchments and were only marginally influenced by snowmelt bypass. In contrast, the more substantial offset at PC4 suggests snowmelt bypass was more pronounced, consistent with its catchment characteristics and water balance strongly influenced by evaporation during the early

open-water season. Spring 2019 conditions were likely highly unusual since regular occurrence of snowmelt bypass would lead to rapid evaporative lake-level drawdown and perhaps desiccation, and little such evidence exists in the sediment core record of PC4 (see below). Thus, the cellulose-inferred $\delta^{18}O_{lw}$ stratigraphic profiles below are considered to provide records of water balance conditions reflecting shifting influence in the ratio of evaporation to inflow, with the latter predominantly characterized by snowmelt at PC4.

Table 3.2. Range and difference between cellulose-inferred $\delta^{18}O$ in upper strata of the sediment core and 2019 measured lake water $\delta^{18}O$ values at the four study lakes.

	Cellulose-inferred $\delta^{18}O$ in upper strata (±0.3‰ VSMOW)		2019 measured lake water $\delta^{18}O$ (±0.2‰ VSMOW)		Difference (‰ VSMOW)
	Min.	Max.	Min.	Max.	
AC1	-14.0	-12.8	-11.1	-10.1	1.8 - 2.9
AC3	-14.3	-11.9	-10.6	-10.1	1.2 - 3.7
AC5	-15.0	-11.0	-13.6	- 12.7	N/A
PC4	-15.7	-14.5	-10.8	-9.5	3.7 - 4.9

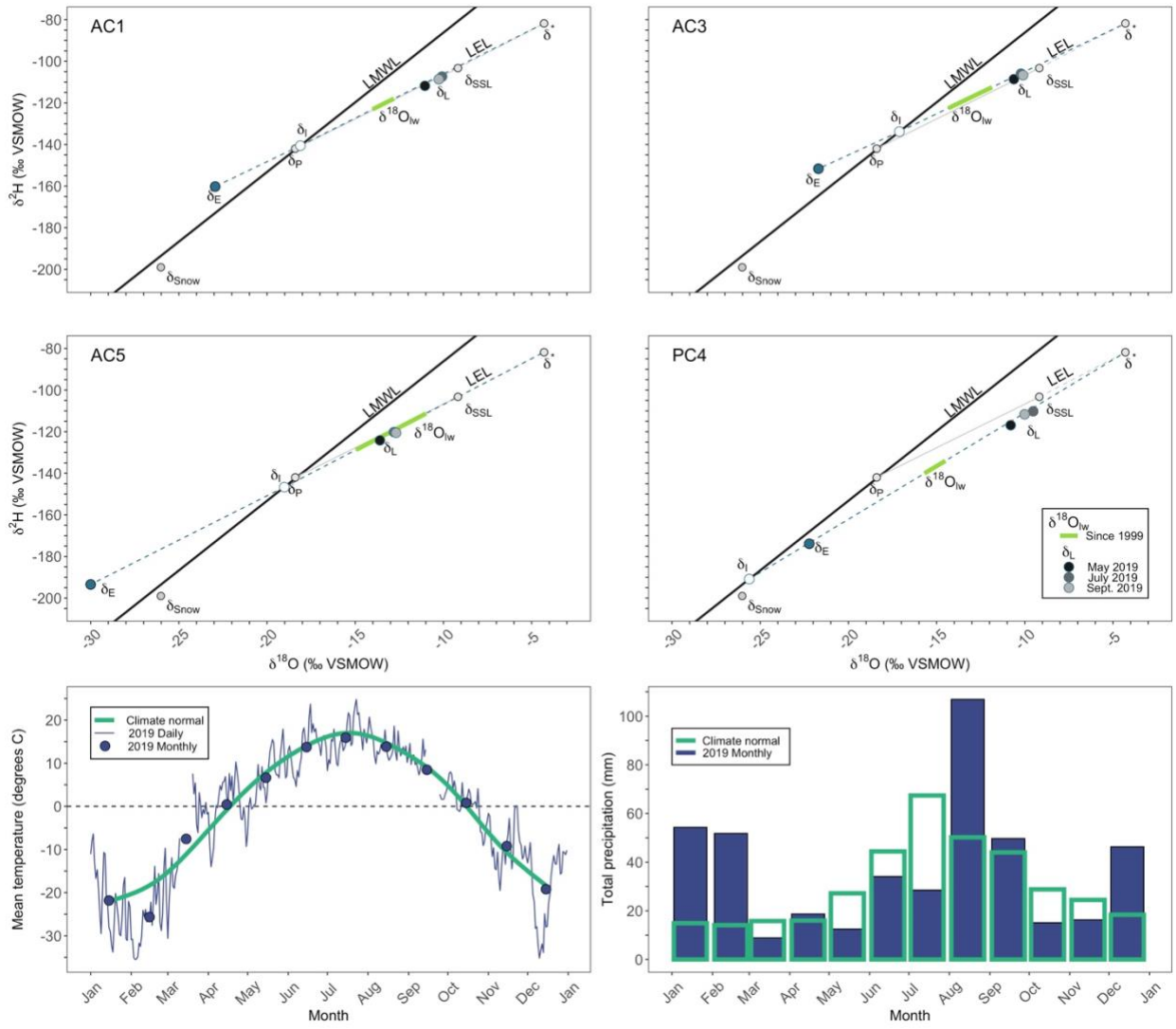

Figure 3.3. Panels AC1, AC3, AC5, and PC4 project stratigraphic profiles of cellulose-inferred lake water $\delta^{18}O$ since 1999 (light green) onto lake-specific evaporation lines defined by the May 2019 lake water isotope data and the 2015-2019 isotope framework developed by Remmer *et al.* (2020a) for the PAD. Included are the Local Meteoric Water Line (LMWL; solid black) and Local Evaporation Line (LEL; dashed light grey). Note that the range of cellulose-inferred $\delta^{18}O_{lw}$ values for the post-1999 stratigraphic records are lower than the measured lake water $\delta^{18}O$ values from 2019 for AC1, AC3, and PC4, likely a consequence of snowmelt bypass in 2019. Bottom panels include meteorological data where 2019 (dark blue) is compared to 1981-2010 climate normal (green). See text for explanation of labels.

Figure 3.4. Photos of the Peace-Athabasca Delta (March 30 and 31, 2019): lakes were ice-covered and there was little to no snow accumulation across the surrounding catchments, suggesting snowmelt occurred before ice-off in 2019 (Photos: A. Ghosh).

3.4 Evaluating paleohydrological responses of the study lakes to local hydroclimate since ca. 1600

3.4.1 Paleohydrological responses of the study lakes to local hydroclimate during the Little Ice Age

Cellulose-inferred lake water $\delta^{18}O$ profiles from all study lakes (AC1, AC3, AC5, PC4) displayed intervals of notably high values during the Little Ice Age (LIA; 1600-1900 CE; Figure 3.5). Individual cellulose-inferred $\delta^{18}O_{lw}$ values were compared to the long-term mean for each lake (ca. 1600 - 2019 at AC1, AC3, PC4, and ca. 1780 - 2019 at AC5), and stratigraphically adjacent groups of samples greater than one standard deviation above the mean within each record were identified (see shaded 'intervals of ^{18}O enrichment' in Figure 3.5). These were considered to be intervals when lake water balances were more strongly influenced by evaporation. At AC1, the long-term cellulose-inferred $\delta^{18}O_{lw}$ mean was -13.4‰ and values ranged from -16.2 to -9.7‰ during the LIA. Cellulose-inferred $\delta^{18}O_{lw}$ values increased early in the record and were relatively high (~ -11.9‰) during an interval of ^{18}O enrichment from ca. 1620 to ca. 1670. Values then decreased and were typically at or below the mean until ca. 1820, at which time values increased and remained high (~ -12.2‰). During this interval of ^{18}O enrichment, from ca. 1820 until ca. 1860, one value (ca. 1840) exceeded the lake water oxygen isotope composition (measured $\delta^{18}O_{lw}$) of samples collected in 2019 (> -10.0‰). Values then declined and approximated the mean throughout the rest of the LIA. At AC3, cellulose-inferred $\delta^{18}O_{lw}$ values ranged from -16.3 to -11.3‰ during the LIA. Values approximated the mean for the record (-13.5‰) through the early 1600s before rising ca. 1635 and remaining high (~ -12.5‰) during an interval of ^{18}O enrichment which persisted until ca. 1730. Values then declined and remained below the mean throughout the remainder of the LIA, with the exception

of a brief interval of ^{18}O enrichment between ca. 1860 and ca. 1880 when values increased to -12.2‰. Cellulose-inferred $\delta^{18}O_{lw}$ values had the greatest range at AC5 (-19.8 to -6.7‰) during the LIA, despite this also being the shortest record (extending only to ca. 1780). Values were lower than the mean for the record (-14.9‰) until ca. 1820. Values then rose, and an interval of ^{18}O enrichment continued until ca. 1870, with four values exceeding -10.0‰ and peaking at -6.7‰ ca. 1840. Values then declined below the mean and remained low until the end of the LIA. At PC4, cellulose-inferred $\delta^{18}O_{lw}$ values ranged from -18.4 to -12.1‰ during the LIA. Values were lower than the long-term mean (-15.4‰) until ca. 1710, at which time values increased and remained high during an interval of ^{18}O enrichment until ca. 1750, and then peaked at ca. 1725 at -12.1‰. Values then declined and approximated the mean throughout most of the remainder of the LIA, except during a brief interval of ^{18}O enrichment from ca. 1850 to ca. 1870 when values increased and peaked at -13.9‰ ca. 1857.

Comparison of cellulose-inferred $\delta^{18}O_{lw}$ records at the study lakes revealed that intervals of ^{18}O enrichment coincided at three or more lakes during two portions of the LIA, including the early LIA (ca. 1620 - ca. 1750) and late LIA (mid-1800s) (Figure 3.5). In the early LIA, intervals of ^{18}O enrichment were identified at three lakes (AC1, AC3, PC4). These were the longest intervals of ^{18}O enrichment identified, lasting ~40-85 years at each lake. The duration and timing of enrichment intervals differed amongst lakes, but intervals at AC1 (ca. 1620 - ca. 1670) and PC4 (ca. 1710 - ca. 1750) each overlapped with the longer intervals identified at AC3 (ca. 1635 - ca. 1730). Results suggest lake water balances were more influenced by evaporation for several decades, relative to the lake-specific long-term mean, during the early LIA. Intervals of ^{18}O enrichment during the early LIA (ca. 1620 - ca. 1730) align with tree ring reconstruction of low relative humidity from the headwaters of the Athabasca River (Edwards *et al.*, 2008; Figure 3.5)

and numerous prolonged intervals of drought in western Canada (Kerr *et al.*, 2021). During the late LIA, intervals of ^{18}O enrichment were identified at all four study lakes. These intervals were shorter than those in the early LIA, lasting ~20-50 years at each lake, and occurring between ca. 1820 and ca. 1870. Particularly short intervals were identified at AC3 (ca. 1860 - ca. 1880) and PC4 (ca. 1850 - ca. 1870), while slightly longer intervals were identified at AC1 (ca. 1820 - ca. 1860) and AC5 (ca. 1820 - ca. 1870). During this time, cellulose-inferred $\delta^{18}O_{lw}$ reached the highest values of the entire record at two lakes (AC1, AC5; Figure 3.5). These results suggest that evaporative influence on lake water balance was brief and intense during the late LIA. At this time, isotope analysis of tree ring reconstruction indicates that low relative humidity at the PAD (Bailey, 2008) may have been the primary driver of lake water balance. During the late LIA, drought intervals in western Canada were shorter and less frequent when compared to the early LIA (Kerr *et al.*, 2021).

3.4.2 Paleohydrological responses of the study lakes to local hydroclimate during the twentieth and twenty-first centuries

Cellulose-inferred $\delta^{18}O_{lw}$ profiles were constant at most of the study lakes during the twentieth (1900-1999 CE) and twenty-first (2000-2019 CE) centuries (Figure 3.5). Values often approximated the lake-specific long-term mean values, suggesting lake water balances were relatively stable. Exceptions include at PC4, when a short interval of ^{18}O enrichment was identified from ca. 1905 - ca. 1920 (~ -14.3‰). At AC3 and AC5, intervals of ^{18}O enrichment that span the late twentieth century and the twenty-first century were identified (beginning ca. 1995). During this interval, cellulose-inferred $\delta^{18}O_{lw}$ values were high but constant at AC3 (~ -12.8‰), while values at AC5 ranged from -15.0 to -11.0‰, with an increase of ~2.0‰ since the beginning of the twenty-first century, although this rising trend began ca. 1980. A Mann Kendall

trend test indicated that the increasing trend at AC5 during the twenty-first century was significant (Mann Kendall U_{AC5}; tau = 0.293, p = 0.001). No significant trends were identified at the other three study lakes for the 1900-1999 and post-2000 intervals (Appendix G).

Unlike during the LIA, cellulose-inferred $\delta^{18}O_{lw}$ records were largely constant across study lakes since ca. 1900, although intervals of ^{18}O enrichment occurred at two lakes during the twenty-first century. These results suggest the influence of evaporation during the twentieth century was comparatively low at the study lakes and is consistent with the higher, constant Athabasca River headwater relative humidity (Edwards *et al.*, 2008) and high local relative humidity (Bailey, 2008) records (Figure 3.5). Additionally, increased precipitation since ca. 1950 could have offset a longer ice-free season mitigating the severity of evaporation (Figure 2.1). Intervals of ^{18}O enrichment identified during the early twenty-first century at AC3 and AC5 suggest that lake water balance was more influenced by evaporation relative to the lake-specific long-term mean. These early twenty-first century intervals of ^{18}O enrichment correspond with lower local relative humidity (Bailey, 2008), although high cellulose-inferred $\delta^{18}O_{lw}$ values of the twenty-first century are lower than values at all lakes during the LIA.

3.4.3 Reconciling paleohydrological records at the study lakes

Broad temporal correspondence amongst intervals of ^{18}O enrichment across the study lakes builds confidence in cellulose-inferred $\delta^{18}O_{lw}$ and radiometric dating results, while differences in magnitude and precise timing of intervals of greater evaporative influence on lake water balance may be due to lake-specific factors such as uncertainty associated with linear extrapolation of the inferred sedimentation rate. For instance, dates were linearly extrapolated below the depth of unsupported ^{210}Pb activity and therefore the sediment core chronologies before ca. 1860 should

be considered approximate especially for the intervals of ^{18}O enrichment during the early LIA (Figure 3.5).

Other lake-specific factors which may have influenced the sensitivity of cellulose-inferred $\delta^{18}O_{lw}$ to dry hydroclimatic episodes include catchment characteristics and depth of the basins. Since AC1, AC3, and AC5 are underlain by sandy substrate, snowmelt contributions may be limited. Therefore, small decreases in snow accumulation may have elicited a relatively strong evaporative response at the AC lakes, which may have occurred during the early and late LIA. These three lakes are located adjacent to and downhill from sand dunes which may conduct substantial groundwater input towards the lakes. In contrast, the relatively steep-sided bedrock catchment at PC4 likely captures and directs substantial snowmelt runoff to the lake, as suggested by the comparison of measured and cellulose-inferred $\delta^{18}O_{lw}$ (Figure 3.3). Thus, PC4 would likely be more resistant to episodes of low snow accumulation and dry hydroclimatic conditions, which may explain the lesser degree of ^{18}O enrichment during the early and late LIA. Given the inference of snowmelt bypass accounting for ^{18}O enrichment in the measured $\delta^{18}O_{lw}$ from 2019 (Figure 3.3), this may also account for intervals of ^{18}O enrichment in the PC4 stratigraphic record (Figure 3.5). Lastly, the study lakes, though shallow (<6 m), are deeper than lakes within the PAD (<2 m) and are located near expansive sand dunes that may provide a conduit for groundwater exchange with the lakes. This may account, to a degree, for the resistance of the study lakes to changes in local hydroclimatic conditions since ca. 1600.

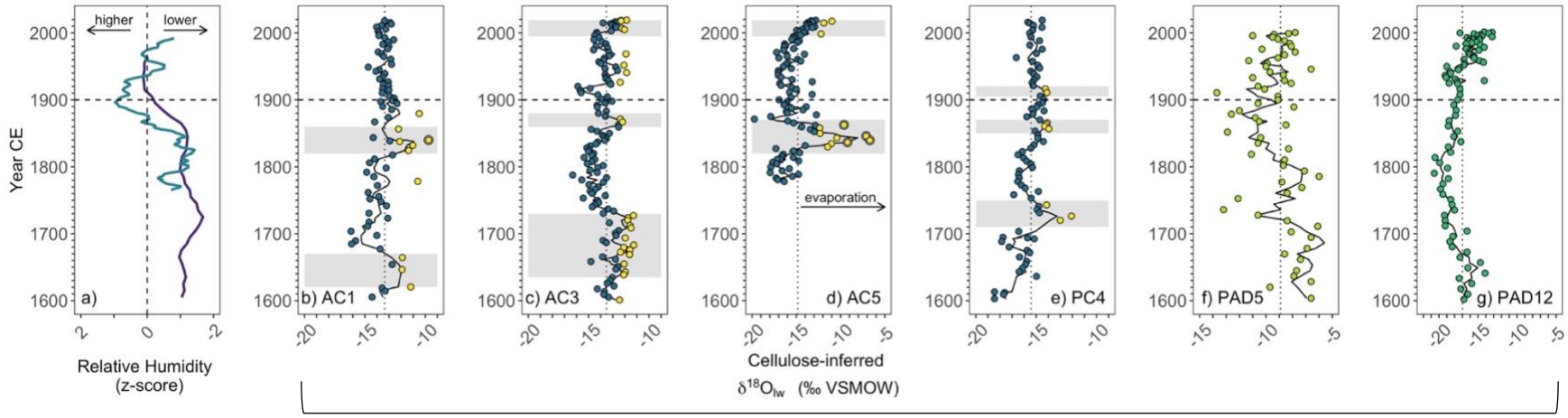

Figure 3.5. Tree-ring isotope-based reconstructions of a) relative humidity (Edwards *et al.*, 2008; Bailey, 2008) are displayed along with cellulose-inferred lake water $\delta^{18}O$ reconstructions for b-e) the study lakes and f-g) two perched lakes in the PAD near the Peace River (PAD 5, PAD 12; Wolfe *et al.*, 2008a). a) Long-term trends of relative humidity reconstructed from measurements of carbon and oxygen isotope composition of tree-rings at the headwaters of the Athabasca River by Edwards *et al.* (2008; dark purple) and within the Peace-Athabasca Delta by Bailey (2008; teal) are displayed using running means (5-point and 20-point, respectively). The dashed vertical line identifies the zero of z-scored data based on the full 1000-year record from Edwards *et al.* (2008). Note, the x-axis is reversed such that lower relative humidity is to the right. b-e) Cellulose-inferred lake water $\delta^{18}O$ records for the study lakes, including three-point running means (black line). Values greater than one standard deviation above the long-term mean were considered high (yellow circles) and are differentiated from the rest of the record (dark blue circles). Additionally, values exceeding lake water oxygen isotope composition (measured $\delta^{18}O_{lw}$) of samples collected in 2019 (> -10.0‰) are identified (bold outline). 'Intervals of ^{18}O enrichment', where high values were persistent, are identified at each study lake and are identified by the grey bars. A dotted vertical line identifies the 1600 to present average cellulose-inferred $\delta^{18}O_{lw}$ for each record. The end of the Little Ice Age (LIA; ~1600-1900 CE) is distinguished by a horizontal dashed line at 1900. The vertical dotted line identifies the 1600 to present average cellulose-inferred $\delta^{18}O_{lw}$.

3.5 Discerning the relative role of local hydroclimate on episodes of drying at lakes in the Peace-Athabasca Delta

To further explore the role of local hydroclimate on episodes of drying in the PAD, stratigraphic intervals of ^{18}O enrichment at the study lakes were characterized by estimating the associated ranges of evaporation-to-inflow ratios. During the early LIA intervals of ^{18}O enrichment (ca. 1620 - ca. 1730), E/I ratios among the study lakes ranged from 0.17 at AC3 to 0.53 at AC1 (Table 3.3). During the late LIA intervals of ^{18}O enrichment (ca. 1820 - ca. 1870), E/I ratios among the study lakes were encompassed by the broad range of 0.05 to >1.00 at AC5. Notably, high E/I ratios were reconstructed ca. 1840 at AC1 (E/I = 0.81) and AC5 (E/I >1.00) when cellulose-inferred $\delta^{18}O_{lw}$ values were greater than measured $\delta^{18}O_{lw}$ from 2019 samples (> -10.0‰). Since ca. 1995, when intervals of ^{18}O enrichment were identified at two lakes, E/I ratios were encompassed by the range of 0.16 to 0.57 at AC5.

Comparison of cellulose -inferred $\delta^{18}O_{lw}$ and E/I ratios from the study lakes to previously studied perched basins (PAD 5 and PAD 12) reveals that local hydroclimate played a varying role in episodes of drying in the PAD (Figure 3.4; Table 3.3). During the early LIA when intervals of ^{18}O enrichment were identified at study lakes (ca. 1620 – ca. 1730), lake water balance was moderately influenced by evaporation at two study lakes (E/I > 0.50; E/I_{MAX} = 0.53 at AC1, 0.52 at AC3; Table 3.3) in response to hydroclimatic factors (e.g., low relative humidity; Figure 3.5). At PAD 5, cellulose-inferred $\delta^{18}O_{lw}$ values were higher than the lake-specific long-term mean (since ca. 1600; Figure 3.5) and correspondingly E/I ratios were high (E/I range 0.63 to > 1.00). At this time, paleolimnological evidence suggests PAD 5 may have periodically desiccated (Wolfe *et al.*, 2005; 2008a). These results suggest local hydroclimate may have contributed, in part, to the intense and prolonged drying observed at PAD 5 during the early LIA. In contrast,

low E/I ratios ($\leq$ 0.22) at PAD 12 indicate the lake water balance was driven primarily by inflow because of the influence of river floodwaters and the expansion of Lake Athabasca (Wolfe *et al.*, 2008a).

During the late LIA (ca. 1820 - ca. 1870), lake water balances at all study lakes were subject to a short but variably intense interval of evaporative influence (Figure 3.5). E/I ratios at two of the study lakes suggest particularly strong influence of evaporation (E/I $\cong$ 1.00; E/I_{MAX} = 0.81 at AC1, > 1.00 at AC5; Table 3.3). At PAD 5 and PAD 12, however, cellulose-inferred $\delta^{18}O_{lw}$ was stable and lower than the lake-specific long-term mean during most of this interval, with mostly low E/I ratios at PAD 5 (0.33 to > 1.00) and PAD 12 (0.00 to 0.04). Although the range at PAD 5 exceeded 1.00 during this interval, most values were below 0.70 and only two of the six values were greater than 1.00 and occurred non-sequentially ca. 1830 and ca. 1865. Local hydroclimatic factors appear to have had little or no influence on evaporation at PAD lakes during the late LIA, likely due to the strong influence of river floodwaters (Wolfe *et al.*, 2005; 2008a).

For most of the twentieth century, relatively constant cellulose-inferred $\delta^{18}O_{lw}$ records at study lakes suggests local hydroclimate contributed very little to the observed increase in cellulose-inferred $\delta^{18}O_{lw}$ values and associated drying at PAD 5 and PAD 12 (Figure 3.5; Wolfe *et al.*, 2008a). However, since ca. 1995, E/I ratios at two study lakes (AC3, AC5) indicate evaporation has recently become more influential on the lake water balances (E/I $\cong$ 0.50; maximum of 0.44 at AC3 and 0.57 at AC5; Table 3.3), suggesting local hydroclimate may have played a role in more recent lake drying, which has been observed at PAD 5 (Remmer *et al.*, 2018). To explore drying trends in recent decades more directly, cellulose-inferred $\delta^{18}O_{lw}$ at AC5 and measured $\delta^{18}O_{lw}$ at PAD 5 and PAD 12 since ca. 2000 were compared (Figure 3.6). Significantly increasing cellulose-inferred $\delta^{18}O_{lw}$ values at AC5 may implicate local hydroclimate as a

contributor to the persistently high measured $\delta^{18}O_{lw}$ since 2000 and correspondingly high E/I ratios (Table 3.3) at PAD 5 and PAD 12. Overall, these results indicate that increased influence of evaporation due to hydroclimatic factors can have marked influence on lake water balance at the shallow PAD lakes, especially during intervals of reduced river flooding including the early LIA and early twenty-first century.

Table 3.3. Range of evaporation-to-inflow (E/I) ratios estimated for AC1, AC3, AC5, and PC4 during intervals of ^{18}O enrichment identified at two or more study lakes during the early LIA, late LIA, and ca. 1995 to 2019. Corresponding ranges of E/I ratios are also reported for PAD 5 and PAD 12. For PAD 5 and PAD 12, the early LIA was considered as ca. 1620 to ca. 1730 and the late LIA was considered as ca. 1820 to ca. 1870 (see Figure 3.5). E/I ratios above 0.50, where evaporation has more influence on lake water balance than inflow, are bolded. Early LIA, Late LIA, 1995 to 2000, and 1995 to 2019 E/I ratios are based on cellulose-inferred $\delta^{18}O_{lw}$ records and 2001 to 2019 E/I ratios are based on measured $\delta^{18}O_{lw}$.

		Early LIA	Late LIA	1995-2000	1995-2019	2001-2019
Study Lakes	AC1	0.34 to **0.53**	0.21 to **0.81**	N/A	N/A	N/A
	AC3	0.17 to **0.52**	0.26 to 0.40	N/A	0.19 to 0.44	N/A
	AC5	N/A	0.05 to **>1.00**	N/A	0.16 to **0.57**	N/A
	PC4	0.32 to 0.41	0.16 to 0.24	N/A	N/A	N/A
PAD Lakes	PAD 5	0.63 to **>1.00**	0.32 to **>1.00**	0.56 to **>1.00**	N/A	0.67 to **>1.00**
	PAD 12	0.00 to 0.22	0.00 to 0.04	0.04 to 0.26	N/A	0.53 to **>1.00**

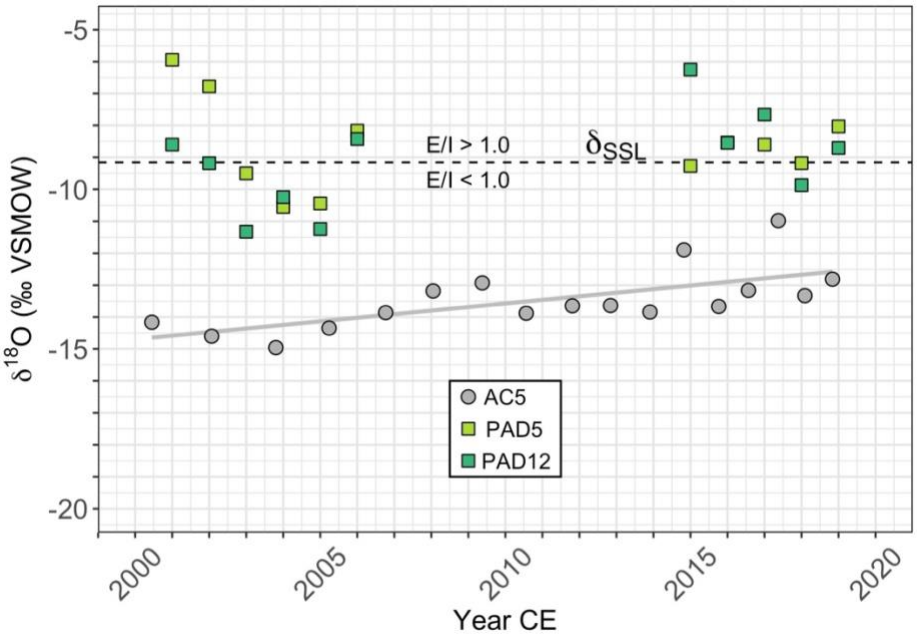

Figure 3.6. Average open-water season measured $\delta^{18}O$ for PAD 5 and PAD 12 (two lakes in the PAD near the Peace River) and cellulose-inferred $\delta^{18}O$ from the study lake AC5 for 2000-2019. A significant positive trend was identified at AC5 (Mann Kendall U test; AC5) since 2000 and a linear trendline visually displays this finding. Dashed line identifies the theoretical oxygen isotope composition of a terminal basin in steady state (δ_{SSL}) based on the 2000-2019 average lake water $\delta^{18}O$ value of PAD 18, a terminal lake considered to be in hydrological steady state (Yi *et al.*, 2008).

Chapter 4. Conclusions and Recommendations

4.1 Key findings

At the Peace-Athabasca Delta (PAD), multiple potential stressors converge with complicating negative implications for water availability that contribute to the challenges in distinguishing the relative role of local climate. This study employed paleolimnological techniques to reconstruct lake water oxygen isotope composition at four lakes adjacent to the PAD to assess temporal changes to lake water balance that can be attributed to local hydroclimate alone without the influence of other possible confounding factors that operate within the delta. These lakes were hydrologically isolated from deltaic processes and were therefore well suited to compare to PAD lakes to determine the relative role of local hydroclimate during episodic drying during the past 400 years. However, the greater depth and volume of the study lakes, and potential groundwater exchange at the AC lakes, may render the study lakes to be more resistant to climate-induced change in lake water balance.

Intervals when hydrological response (i.e., evaporative influence) was more pronounced were the focus of this study because of concern for observed lake drying at the PAD. At the four study lakes, stratigraphic intervals of cellulose-inferred lake water oxygen isotope composition (cellulose-inferred $\delta^{18}O_{lw}$) that were more than one standard deviation above the lake-specific long-term mean were defined as intervals of ^{18}O enrichment and were interpreted as episodes of greater evaporative influence. Intervals of ^{18}O enrichment and corresponding estimated evaporation-to-inflow (E/I) ratios at the study lakes were compared to previously studied PAD lakes (PAD 5 and PAD 12) to determine the relative role of local hydroclimate in episodic drying

events during the early and late Little Ice Age (LIA), twentieth century, and the first two decades of the twenty-first century.

Results of the study suggest that local hydroclimate does appear to contribute to episodic drying at PAD lakes; however, the role of this driver was limited to intervals of low relative humidity (reconstructed from isotope measurements of tree ring records; Edwards *et al.*, 2008; Bailey, 2008) and when contribution of river floodwaters to PAD lakes was also low. For instance, during the early LIA, high cellulose-inferred $\delta^{18}O_{lw}$ values at three study lakes and E/I ratios at two of these lakes indicated lake water balance was more influenced by evaporation in response to low relative humidity. These findings suggest evaporative influence due to local hydroclimate at this time and were compared to PAD records. While the strong evaporative influence at PAD 5 may have been, in part, influenced by local hydroclimate, the same could not be said for PAD 12 which was flood-prone at this time. During the late LIA, high cellulose-inferred $\delta^{18}O_{lw}$ values at all four study lakes and E/I ratios at two of these lakes indicated lake water balance was strongly influenced by evaporation in response to low local relative humidity. These findings suggest evaporative influence due to local hydroclimate also occurred at this time but when compared to PAD 5 and PAD 12 records there is little to no evidence of ^{18}O enrichment, likely due to the strong influence of river floodwaters. During the twentieth century, constant cellulose-inferred $\delta^{18}O_{lw}$ at the study lakes reveal local hydroclimate played little to no role in the drying of PAD lakes. Most recently, during the first two decades of the twenty-first century, intervals of ^{18}O enrichment determined by high cellulose-inferred $\delta^{18}O_{lw}$ at two study lakes identify a small role of local hydroclimate in recent observed lake drying at the PAD.

These conclusions assume water balance of the study lakes and lakes within the PAD are comparably responsive to variations in local hydroclimate. However, the study lakes are deeper

(ranging in depth from 2.4 to 6 m) compared to the depth of lakes within the PAD (<2 m) and three lakes (AC1, AC3, AC5) may receive groundwater input from nearby sand dunes that could offset evaporative water losses. Of note, increased influence of evaporation on lake water balance since 1920 has been reconstructed from paleolimnological analysis at McClelland Lake (located ~95 km south of the PAD), which is presently of similar depth (4.2 m deep) to the study lakes (Zabel *et al.*, 2022). Although water balance at the study lakes may be less responsive to hydroclimate than lakes in the PAD, the detection of evaporative influence elucidates intervals when PAD lakes may be particularly sensitive to evaporative water loss.

4.2 Implications

The variable role of local hydroclimate on lake water balance at the shallow and evaporatively-sensitive PAD lakes underscores the important and strong influence of flood frequency and magnitude on lake water balance at the PAD (Wolfe *et al.*, 2008a; Remmer *et al.*, 2018; 2020; WBNP, 2019; Neary *et al.*, 2021). For instance, during the early LIA (1600s) when conditions at PAD 5 were the driest during the past 400 years and flood frequency and magnitude declined, local hydroclimate may have contributed to drying. However, study lakes also indicate a drying event during the late LIA (ca. 1820 - ca. 1870) which was not captured at either PAD lake (PAD 5, PAD 12) due to offsetting influence of several high magnitude floods at this time on their water balance (Wolfe *et al.*, 2006; 2008a). Furthermore, during the twentieth and early twenty-first centuries, the strong influence of evaporation on lake water balance at the PAD appears to be primarily a response to lower flood frequency and magnitude (Wolfe *et al.*, 2006, 2020). Higher local relative humidity during most of the twentieth century and increased precipitation since ca. 1950 may have mitigated the severity of evaporation at PAD lakes. Most recently, evidence at two study lakes (AC3, AC5) indicates drying at PAD lakes during the early twenty-

first century may be responsive to local hydroclimatic factors that have led to greater evaporation.

Prolonged evaporative influence due to arid local hydroclimatic conditions would have serious negative consequences for the interconnection, floodplain ecosystem function, and navigation at the PAD (Prowse & Conly, 2002; Wolfe *et al.*, 2008a; MCFN, 2014; Remmer *et al.*, 2018; Straka *et al.*, 2018). Projected uncertainty in longevity of floodwater contributions (DeBeer *et al.*, 2016; Chernos *et al.*, 2020; Lamontange *et al.*, 2021) and increased urban and industrial water demand upstream would increase risk of periodic desiccation of lakes in the delta, as occurred during the 1600s at PAD 5 and has recently been observed at lakes across the delta (e.g., PAD 9; Remmer *et al.*, 2018). The uncertainty in floodwater delivery leaves a greater potential influence for local hydroclimate to play either a mitigating role (e.g., high relative humidity and precipitation) or could place lakes at greater risk during arid (e.g., low relative humidity and precipitation) intervals due to the potential for strong evaporative water losses from the shallow PAD lakes. With these uncertainties, continued monitoring of hydrologically diverse lakes across the PAD is integral to ecosystem conservation efforts under the Action Plan (WBNP, 2019; Remmer *et al.*, 2020b).

4.3 Recommendations

The current recommended PAD monitoring framework provides a spatially and temporally comprehensive isotope-based lake water sampling regime across the delta but does not currently include lakes that solely capture the influence of local hydroclimate (Remmer *et al.*, 2020; Neary *et al.*, *in prep.*). With 400 years of baseline information, the addition of the four study lakes within this Thesis to the monitoring framework would allow assessment of the relative role of

local hydroclimate on evaporative influence at the PAD. For instance, water samples at these lakes could be collected during mid-summer sampling efforts and E/I ratios calculated. Based on this study's findings, these data could be used to better understand the role of local hydroclimate on lake drying in the PAD especially when flood frequency or magnitude are low.

Additional analysis of lake sediment cores could be undertaken to further quantify paleohydrological and potential hydroecological responses at study lakes to local hydroclimate. For example, diatom abundances could be enumerated to assess if changes in community composition have occurred in conjunction with intervals of ^{18}O enrichment, where shifts from planktonic to benthic taxa may indicate deeper light penetration or epiphytic taxa may indicate increased macrophyte growth as the lake-level became shallower over time, and vice versa (Smol *et al.*, 2005; Wolfe *et al.*, 2005). Additionally, pigment analysis could be performed to determine shifts in algal assemblages and carbon and nitrogen isotope composition data (Appendix D) could be further explored to determine shifts in nutrient source and cycling in relation to aquatic productivity (Meyer & Ishiwatari, 1993; Meyers & Teranes, 2001). Together these ecological indicators may provide additional hydroecological context to ecosystem changes associated with intervals of ^{18}O enrichment.

References

Appleby, P.G. (2001). *Chronostratigraphic techniques in recent sediments. Tracking Environmental Change Using Lake Sediments: Basin Analysis, Coring, and Chronological Techniques (Developments in Paleoenvironmental Research. 1)* ed) ed W. M. Last & J. P. Smol 1. Dordrecht: Kluwer Academic Publishers. 9 171-2030-7923-6482-1.

Appleby, P.G., & Oldfield, F. (1978). The calculation of lead-210 dates assuming a constant rate of supply of unsupported ^{210}Pb to the sediment. *CATENA, 5:* 1-8. https://www.doi.org/10.1016/S0341-8162(78)80002-2

Bailey, J.N.L. (2008). *Reconstruction of Paleoclimate Time-Series in the Peace-Athabasca Delta, Northern Alberta, from Stable Isotopes in Tree-Rings.* Master of Science Thesis. University of Waterloo. Waterloo, ON, Canada. Available from https://uwspace.uwaterloo.ca/

Beltaos, S. (2018). Frequency of ice-jam flooding of Peace-Athabasca Delta. *Canadian Journal of Civil Engineering, 45*(1): 71-75. dx.doi.org/10.1139/cjce-2017-0434

Bergmann, M.A., & Welch, W.E. (1985). Spring meltwater mixing in small arctic lakes. *Canadian Journal Fisheries and. Aquatic Sciences, 42*(11): 1789–1798. https://www.doi.org/10.1139/f85-224

Bill, L., Crozier, J., Surrendi, D., Flett, L.S., & MacDonald, D. (1996). *A report of wisdom synthesized from the Traditional Knowledge Component Studies.* Northern River Basins Study, Synthesis Report No. 12. Alberta Environmental Protection: Edmonton, Canada. Available from http://www.barbau.ca/content/northern-river-basins-study-project

Binford, M.W. (1990). Calculation and uncertainty analysis of ^{210}Pb dates for PIRLA project lake sediment cores. *Journal of Paleolimnology, 3*: 253-267. https://www.doi.org/10.1007/BF00219461

Birks, S. J., Edwards, T. W. D., Gibson, J. J., Drimmie, R. J., & Michel, F. A. (2004). Canadian Network for Isotopes in Precipitation. Available from http://www.science.uwaterloo.ca/˜twdedwar/cnip/ cniphome.html

Carroll, M.L., Townshend, J.R.G., DiMiceli, C.M., Lobado, T., & Sohlberg, R.A. (2011). Shrinking lakes of the Arctic: Spatial relationships and trajectory of change. *Geophysical Research Letters, 38*: L20406. https://www.doi.org/10.1029/2011GL049427

Chernos, M., MacDonald, R.J., Nemeth, M.W., & Craig, J.R. (2020). Current and future projections of glacier contribution to stream flow in the upper Athabasca River Basin. *Canadian Water Resources Journal/Revue Canadienne des ressources hydriques. 45*(4): 324-344. https://doi.org/10.1080/07011784.2020.1815587

Coplen, T. B. (1996). New guidelines for reporting stable hydrogen, carbon, and oxygen isotope-ratio data. *Geochimica et Cosmochimica Acta, 60*: 3359–3360. https://www.doi.org/10.6028/jres.100.021

Cortés, A., MacIntyre, S., & Sadro, S. (2017). Flowpath and retention of snowmelt in an ice-covered arctic lake. *Limnology and Oceanography, 62*(5): 2023–2044. https://www.doi.org/10.1002/lno.10549

Craig, H., & Gordon, L. I. (1965) Deuterium and oxygen 18 variations in the ocean and marine atmosphere. *In* Tongiorgi, E. (ed.), *Stable Isotopes in Oceanographic Studies and Paleotemperatures.* Pisa, Italy: Laboratorio di Geologia Nucleare, 9–130.

Cutforth, H., O'Brien, E.G., Tuchelt, J., & Rickwood, R. (2004). Long-term changes in the frost-free season on the Canadian prairies. *Canadian Journal of Plant Science, 84*: 1085-1091. https://www.doi.org/10.4141/P03-169

DeBeer, C.M., Wheater, H.S., Carey, S.K., & Chun, K.P. (2016). Recent climatic, cryospheric, and hydrological changes over the interior of western Canada: a review and synthesis. *Hydrology and Earth System Science, 20:* 1573-1598. https://www.doi.org/10.5194/hess-20-1573-2016

Edwards, T.W.D., Birks, S.J., Luckman, B.H., & MacDonald, G.M. (2008). Climatic and hydrologic variability during the past millennium in the eastern Rocky Mountains and northern Great Plains of western Canada. *Quaternary Research, 70*(2): 188-197. https://doi.org/10.1016/j.yqres.2008.04.013

Edwards, T.W.D., Wolfe, B.B., Gibson, J.J., & Hammarlund, D. (2004). Use of water isotope tracers in high-latitude hydrology and paleohydrology. In: Pienitz, R., Douglas, M., Smol, J.P. (Eds.), *Long-term Environmental Change in Arctic and Antarctic Lakes, Developments in Paleoenvironmental Research, vol. 7.* Springer.

Gibson, J.J. Birks, S.J., Yi, Y., & Vitt, D.H. (2015). Runoff to boreal lakes linked to land cover, watershed morphology and permafrost thaw: a 9-year isotope mass balance assessment. *Hydrological Processes, 29*: 3848-3861. https://www.doi.org/10.1002/hyp.10502

Gibson, J.J., & Edwards, T.W.D. (2002) Regional water balance trends and evaporation-transpiration partitioning from a stable isotope survey of lakes in northern Canada. *Global Biogeochemical Cycles, 16*(2): 1026. https://www.doi.org/10.1029/2001GB001839

GoC (Government of Canada). (2021, November 18). *Adjusted and homogenized Canadian climate data*. Canada.ca. Available from https://www.canada.ca/en/environment-climate-change/services/climate-change/science-research-data/climate-trends-variability/adjusted-homogenized-canadian-data.html

Heiri, O., Lotter, A. F., & Lemcke, G. (2001). Loss on ignition as a method for estimating organic and carbonate content in sediments: reproducibility and comparability of results. *Journal of Paleolimnology, 25:* 101–110. https://www.doi.org/10.1023/A:1008119611481

Johnston, J.W., Köster, D., Wolfe, B.B., Hall, R.I., Edwards, T.W.D., Endres, A.L., Martin, M.E., Wiklund, J.A., & Light, C. (2010). Quantifying Lake Athabasca (Canada) water level during the 'Little Ice Age' highstand from palaeolimnological and geophysical analyses of a transgressive barrier-beach complex. *The Holocene, 20*(5): 801-911. https://www.doi.org/10.1177/0959683610362816

Kay M.L., Wiklund, J.A., Remmer, C.R., Neary, L.K., Brown, K., Ghosh, A., MacDonald, E., Thomson, K., Vucic, J.M., Wesenberg, K., Hall R.I., & Wolfe, B.B. (2019). Bi-directional hydrological changes in perched basins of the Athabasca Delta (Canada) in recent decades caused by natural processes. *Environmental Research Communications, 1:* 08 11001. https://www.doi.org/10.1088/2515-7620/ab37e7

Kerr, S.A., Andreichuk, Y., & Sauchyn D. (2021). Warm and cool season reconstruction and assessment of the long-term hydroclimatic variability of the Canadian prairie provinces through the development of the Canadian Prairies Paleo Drought Atlas. *International Journal of Climatology,2021*: 1-22. https://www.doi.org/10.1002/joc.7034

Lamontagne, J.R., Jasek, M., & Smith, J.D. (2021). Coupling physical understanding and statistical modeling to estimate ice jam flood frequency in the northern Peace-Athabasca Delta under climate change. *Cold Regions Science and Technology, 192*: 103383. https://doi.org/10.1016/j.coldregions.2021.103383

Leng, M.J., Lamb, A.L., Heaton, T.H.E., Marshall, J.D., Wolfe, B.B., Jones, M.D., Holmes, J.A., & Arrowsmith, C. (2006). Isotopes in Lake Sediments. In: Leng, M.J. (Eds.), Isotopes in Paleoenvironmental Research. Developments in Paleoenvironmental Research, vol 10. Springer, Dordrecht. https://doi.org/10.1007/1-4020-2504-1_04

MacDonald, L.A., Turner, K.W., McDonald, I., Kay, M.L., Hall, R.I., & Wolfe, B.B. (2021). Isotopic evidence of increasing water abundance and lake hydrological change in Old Crow Flats, Yukon, Canada. *Environmental Research Letters, 16*: 124024. https://www.doi.org/10.1088/1748-9326/ac3533

MCFN (Mikisew Cree First Nation). (2014). Petition to the World Heritage Committee requesting Inclusion of Wood Buffalo National Park on the List of World Heritage in Danger. 1–18. Available from https://cpawsnab.org/wood-buffalo-np/

McLeod, A.I. (2011). Kendall: Kendall rank correlation and Mann-Kendall trend test. R package version 2.2. Available from https://CRAN.R-project.org/package=Kendall

Meyers, P.A., & Lallier-Vergès, E. (1999). Lacustrine sedimentary organic matter records of Late Quaternary paleoclimates. *Journal of Paleolimnology, 21*: 345-372. https://www.doi.org/10.1023/A:1008073732192

Meyers, P.A., & Teranes, J.L. (2001). Sediment Organic Matter. *In:* Last, W.M., Smol, J.P. (Eds.), *Tracking Environmental Change using Lake Sediments, Vol. 2: Physical and Chemical Techniques*. Kluwer Academic Publishers, Dordrecht.

Neary, L.K., Remmer, C.R., Kay, M.L., Owca, T., Savage, C.A.M., Imran, A., Hall, R.I., & Wolfe, B.B. (*in prep*). An adaptive framework for monitoring hydrology, limnology and contaminant deposition in lakes across the Peace-Athabasca Delta.

Peters, D.L., Prowse, T.D., Marsh, P., Lafleur, P.M., & Buttle, J.M. (2006). Persistence of water within perched basins of the Peace-Athabasca Delta, Northern Canada. *Wetlands Ecology and Management, 14:* 221-243. https://www.doi.org/10.1007/s11273-005-1114-1

Prowse, T.D., & Conly, F.M. (1998). Effects of climatic variability and flow regulation on ice-jam flooding of a northern delta. *Hydrological Processes, 1610*(March): 1589-1610. https://www.doi.org/https://doi.org/10.1002/(SICI)1099-1085(199808/09)12:10/11%3C1589::AID-HYP683%3E3.0.CO;2-G

Prowse, T.D., & Conly, F.M. (2002). A review of hydroecological results of the Northern River Basins Study, Canada. Part 2. Peace-Athabasca Delta. *River Research and Applications, 18:* 447-460. https://www.doi.org/10.1002/rra.682

R Core Team (2019). R: A language and environment for statistical computing. R Foundation for Statistical Computing, Vienna, Austria. Available from http://www.r-project.org/

R Studio Team. (2019). RStudio: Integrated development for R. RStudio, Inc., Boston, MA; [accessed 2020 June 10]. Available from www.rstudio.com

Rasouli, K., Hernández-Henríquez, M.A., & Déry, S.J. (2013). Streamflow input to Lake Athabasca, Canada. *Hydrology and Earth System Science, 17:* 1681-1691. https://www.doi.org/10.5194/hess-17-1681-2013

Remmer, C.R., Klemt, W.H., Wolfe, B.B., & Hall, R.I. (2018). Inconsequential effects of flooding in 2014 on lakes in the Peace-Athabasca Delta (Canada) due to long-term drying. *Limnology and Oceanography, 63*(4): 1502-1518. https://www.doi.org/10.1002/lno.10787

Remmer, C.R., Neary, L.K., Kay, M.L., Wolfe, B.B., & Hall., R.I. (2020a). Multi-year isoscapes of lake water balances across a dynamic northern freshwater delta. *Environmental Research Letters, 15:* 104066. https://doi.org/10.1088/1748-9326/abb267

Remmer, C.R., Neary, L.K., Wolfe, B.B., & Hall, R.I. (2020b). *Technical Report for Monitoring Lakes in the Peace-Athabasca Delta, Alberta.* Wood Buffalo National Park.

Romero-Lankao, P., Smith, J.B., Davidson, D.J., Diffenbaugh, N.S., Kinney, P.L., Kirshen, P., Kovacs, P., & Ruiz, L.V. (2014). North America. *In: Climate Change 2014: Impacts, Adaptation, and Vulnerability. Part B: Regional Aspects. Contribution of Working Group II to the Fifth Assessment Report of the Intergovernmental Panel on Climate Change* [Barros, V.R., C.B. Field, D.J. Dokken, M.D. Mastrandrea, K.J. Mach, T.E. Bilir, M. Chatterjee, K.L. Ebi, Y.O. Estrada, R.C. Genova, B. Girma, E.S. Kissel, A.N. Levy, S. MacCracken, P.R. Mastrandrea, and L.L.White (eds.)]. Cambridge University Press, Cambridge, United Kingdom and New York, NY, USA, pp. 1439-1498. Available from https://www.ipcc.ch/site/assets/uploads/2018/02/WGIIAR5-Chap26_FINAL.pdf

QGIS.org. (2020). QGIS Geographic Information System. Open Source Geospatial Foundation Project. Available from http://qgis.org/

Sanchez-Cabeza, J. A. & Ruiz-Fernandez, A.C. (2012). ^{210}Pb sediment radiochronology: an integrated formulation and classification of dating models. *Geochimica et Cosmochimica Acta, 82*: 183–200. https://www.doi.org/10.1016/j.gca.2010.12.024

Savage, C.A.M., Remmer, C.R., Telford, J.V., Kay, M.L., Mehler, E., Wolfe, B.B., & Hall, R.I. (2021). Field testing cellulose-water oxygen isotope relations in periphyton for paleohydrological reconstructions. *Journal of Paleolimnology, 66*: 297-312.

Schiff, S.L., & English, M.C. (1988). Deuterium/hydrogen as a tracer of snowmelt mixing in a small subarctic and a small northern temperate lake. *In: Interaction between groundwater and surface water*. International symposium., pp. 136–170, Ystad, Sweden.

Schindler, D.W., & Donahue, W.F. (2006). An impending water crisis in Canada's western prairie provinces. *Proceedings of the National Academy of Science of the United States of America, 103*(19): 7210-7216. https://doi.org/10.073/pnas.0601568103

Serreze, M.C., Walsh, J.E., Chapin III, F.S., Osterkamp, T., Dyurgerov, M., Romanovsky, V., Oechel, W.C., Morison, J., Zhang, T., & Barry, R.G. (2000). Observational evidence of recent change in the northern high-latitude environment. *Climatic Change, 46:* 159-207. https://www.doi.org/10.1023/A:1005504031923

Sinnatamby, R.N., Yi, Y., Sokal, M.A., Clogg-Wright, K.P., Asada, T., Vardy, S.R., Karst-Riddoch, T.L., Last, W.M., Johnston, J.W., Hall, R.I., Wolfe, B.B., & Edwards, T.W.D. (2010). Historical and paleolimnological evidence for expansion of Lake Athabasca (Canada) during the Little Ice Age. *Journal of Paleolimnology, 43*: 705-717. https://www.doi.org/10.1007/s10933-009-9361-4

Smol, J.P., & Douglas, M.S.V. (2007). Crossing the final ecological threshold in high arctic ponds. *Proceedings of the National Academy of Sciences of the United States of America, 104*(30): 12395-12397. https://www.jstor.org/stable/25436310

Smol, J.P., Wolfe, A.P., Birks, H.J.B., Douglas, M.S.V., Jones, V.J., Korhola, A., Pienitz, R., Rüland, K., Sorvari, S., Antoniades, D., Brooks, S.J., Fallu, M.A., Hughes, M., Keatley, B.E., Laing, T.E., Michelutti, N., Nazarova, L., Nyman, M., Paterson, A.M., Perren, B., Quinlan, R., Rautio, M., Saulnier-Talbot, E., Siitonen, S., Solovieca, N., & Weckström, J. (2005). Climate-driven regime shifts in the biological communities of arctic lakes. *Proceedings of the National Academy of Science of the United States of America, 102*(12): 4397-4402. https://www.doi.org/10.1073/pnas.0500245102

Straka, J.R., Antoine, A., Bruno, R., Campbell, D., Campbell, R., Campbell, R., Cardinal, J., Gibot, G., Gray, Q.Z., Irwin, S., Kindopp, R., Ladouceur, R., Ladouceur, W., Lankshear, J., Maclean, B., Macmillan, S., Marcel, F., Marten, G., Marten, L., McKinnon, J., Patterson, L.D., Voyageur, C., Voyageur, M., Whiteknife, G.S., & Wiltzen, L. (2018). "We

Used to Say Rats Fell from the Sky After a Flood": Temporary Recovery of Muskrat Following Ice Jams in the Peace-Athabasca Delta. *Arctic, 71*(2): 218-228. https://www.doi.org/10.14430/arctic4714

Telford, J.V.K., Kay, M.L., Van der Heide, H.C., Wiklund, J.A., Owca, T.J., Faber, J.A., Wolfe, B.B., & Hall, R.I. (2021). Building upon open-barrel corer and sectioning systems to foster the continuing legacy of John Glew. *Journal of Paleolimnology, 65*: 271-277. https://doi.org/10.1007/s10933-020-00162-w

Timoney, K. (2002). A dying delta? A case study of wetland paradigm. *Wetlands, 22*(2): 282-300. https://www.doi.org/10.1672/0277-5212(2002)022[0282:ADDACS]2.0.CO;2

Timoney, K. (2013). *The Peace-Athabasca Delta: a portrait of a dynamic ecosystem.* Edmonton, AB: University of Alberta Press.

Timoney, K., & Lee, P. (2016). Changes in the areal extent of the Athabasca River, Birch River, and Cree Creek Deltas, 1950-2014, Peace-Athabasca Delta, Canada. *Geomorphology, 258*: 95-107. http://dx.doi.org/10.1016/j.geomorph.2016.01.011

Timoney, K., Smith, J.D., Lamontagne, J.R., & Jasek, M. (2018). Discussion of "Frequency of ice-jam flooding of Peace-Athabasca Delta". *Canadian Journal of Civil Engineering, 46*(3). https://doi.org/10.1139/cjce-2018-0409

Thompson, R., Clark, R.M., & Boulton, G.S. (2012). Core Correlation. In: Birks, H.J.B., Lotter, A.F., Juggins, S., Smol, J.P. (Eds.), *Tracking Environmental Change using Lake Sediments, Vol. 5: Data Handling and Numerical Techniques*. Springer.

Ward, E.M., & Gorelick, S.M. (2018). Drying drives decline in muskrat population in the Peace-Athabasca Delta, Canada. *Environmental Research Letters, 13*: 124026. https://doi.org/10.1088/1748-9326/aaf0ec

Watson, V.T., & Medeiros, A.S. (2021). The value of paleolimnology in reconstructing and managing ecosystem vulnerability: a systematic map. *FACETS, 6*(1). https://doi.org/10.1139/facets-2020-0067

WHC/IUCN. (2017). Reactive monitoring mission to Wood Buffalo National Park, Canada; mission report, March 2017. United Nations Educational, Scientific and Cultural Organization. Available from http://whc.unesco.org/en/documents/156893

Wickham, H., Averick, M., Bryan, J., Chang, W., McGowan, L.D., François, R., Grolemund, G., Hayes, Aa., henry, L., Hester, J., Kuhn, M., Pedersen, T.L., Miller, E., Bache, S.M., Müller, K., Ooms, J., Robinson, D., Seidel, D.P., Spinu, V., Takahashi, K., Vaughan, D., Wilke, C., Woo, K., & Yutani, H. (2019). Welcome to the tidyverse. *Journal of Open Source Software, 4*(43): 1686. https://doi.org/10.21105/joss.01686

WBNP (Wood Buffalo National Park). (2019). World Heritage Site Action Plan. Parks Canada. Available from https://www.pc.gc.ca/en/pn-np/nt/woodbuffalo/info/action

Wolfe, B.B., Edwards, T.W.D., Beuning, K.R.M., & Elgood, R.J. (2001). Carbon and oxygen isotope analysis of lake sediment cellulose: methods and applications. In: Last, W.M., Smol, J.P. (Eds.), *Tracking Environmental Change using Lake Sediments, Vol. 2: Physical and Chemical Techniques*. Kluwer Academic Publishers, Dordrecht.

Wolfe, B.B., Hall, R.I., Edwards, T.W.D., & Johnston, J.W. (2012). Developing temporal hydroecological perspectives to inform stewardship of a northern floodplain landscape subject to multiple stressors: paleolimnological investigations of the Peace-Athabasca Delta. *Environmental Reviews, 20*: 191-210. https://www.doi.org/10.1139/A2012-008

Wolfe, B.B., Hall, R.I., Wiklund, J.A., & Kay, M.L. (2020). Past variation in Lower Peace River ice-jam flood frequency. *Environmental Reviews, 28*(3): 209-217. dx.doi.org/10.1139/er-2019-0047

Wolfe, B.B., Falcone, M.D., Clogg-Wright, K.P., Mongeon, C.L., Yi, Y., Brock, B.E., St. Amour, N.A., Mark, W.A., & Edwards, T.W.D. (2007). Progress in isotope paleohydrology using lake sediment cellulose. *Journal of Paleolimnology, 37:* 221-231. https://www.doi.org/10.1007/s10933-006-9015-8

Wolfe, B.B., Hall, R.I., Edwards, T.W.D., Jarvis, S.R., Sinnatamby, R.N., Yi, Y., & Johnston, J.W. (2008a). Climate-driven shifts in quantity and seasonality of river discharge over the past 1000 years from the hydrographic apex of North America. *Geophysical Research Letters* 35, L24402. https://www.doi.org/10.1029/2008GL036125

Wolfe, B.B., Hall, R.I., Edwards, T.W.D., Vardy, S.R., Falcone, M.D., Sjunneskog, C., Sylvestre, F., McGowan, S., Leavitt P.R., & van Driel, P. (2008b). Hydroecological responses of the Athabasca Delta, Canada, to changes in river flow and climate during the 20th century. *Ecohydrology 1,* 131-148. https://www.doi.org/10.1002/eco.13

Wolfe, B.B., Hall, R.I., Last, W.M., Edwards, T.W.D., English, M.C., Karst-Riddoch, T.L., Paterson, A., & Palmini, R. (2006). Reconstruction of multi-century flood histories from oxbow lake sediments, Peace-Athabasca Delta, Canada. *Hydrological Processes 20*, 4131-4153. https://doi.org/10.1002/hyp.6423

Wolfe, B.B., Karst-Riddoch, T.L., Vardy, W.R., Falcone, M.D., Hall, R.I., & Edwards, T.W.D. (2005). Impacts of climate and river flooding on the hydro-ecology of a floodplain basin, Peace-Athabasca Delta, Canada since A.D. 1700. *Quaternary Research 64*, 147-162. https://www.doi.org/10.1016/j.yqres.2005.05.001

Wrona, F.J., Johansson, M., Culp, J.M., Jenkins, A., Mård, J., Myers-Smith, I.H., Prowse, T.D., Vincent, W.F., & Wookey, P.A. (2016). Transitions in Arctic ecosystems: Ecological implications of a changing hydrological regime. *Journal of Geophysical Research: Biogeosciences 121*, 650-674. https://doi.org/10.1002/2015JG003133

Yi, Y., Brock, B.E., Falcone, M.D., Wolfe, B.B., & Edwards, T.W.D. (2008). A coupled isotope tracer method to characterize input water to lakes. *Journal of Hydrology, 350*: 1-13. https://www.doi.org/10.1016/j.jhydrol.2007.11.008

Zabel, N.A., Soliguin, A.M., Wiklund, J.A., Birks, S.J., Gibson, J.J., Fan, X., Wolfe, B.B., & Hall, R.I. (2022). Paleolimnological assessment of past hydro-ecological variation at a shallow hardwater lake in the Athabasca Oil Sands Region before potential onset of industrial development. *Journal of Hydrology: Regional Studies, 39*: 100977. https://doi.org/10.1016/j.ejrh.2021.100977

Zhang, X., Flato, G., Kirchmeier-Young, M., Vincent, L., Wan, H., Wang, X., Rong, R., Fyfe, J., Li, G., & Kharin, V.V. (2019). Changes in Temperature and Precipitation Across Canada; Chapter 4 in Bush, E. and Lemmen, D.S. (Eds.) *Canada's Changing Climate Report*. Government of Canada, Ottawa, Ontario, pp 112-193. Available from www.nrcan.gc.ca

Appendix A: Water isotope and limnological data

Table A1. Water isotope data for the four study lakes, obtained in 2019.

		AC1	AC3	AC5	PC4
May	$\delta^{18}O$	-11.05	-10.60; -10.64	-13.60	-10.80
	$\delta^{2}H$	-111.80	-108.68; -108.54	-124.18	-116.89
July	$\delta^{18}O$	-10.08	-10.21; -10.22	-12.85; -12.76	-9.60; -9.47; -9.50
	$\delta^{2}H$	-107.34	-106.01; -105.90	-120.29; -120.09	-110.29; -109.95; -110.35
September	$\delta^{18}O$	-10.26	-10.10	-12.66; -12.71	-10.01
	$\delta^{2}H$	-108.64	-106.69	-120.47; -120.61	-111.65

Table A2. Water chemistry data from the four study lakes sampled in July 2019. Water samples were filtered, kept refrigerated, and shipped to the University of Alberta Biogeochemical Analytical Service Laboratory (BASL) for analysis.

	AC1	AC3	AC5	PC4
NO_2+NO_3 (µg/L as N)	< 2	< 2	< 2	< 2
TN (µg/L as N)	1650	1120	954	1100
TDN (µg/L as N)	851	870	788	850
TKN (µg/L as N)	1645	1118	952	1098
Silica (mg/L as Si)	0.31	0.46	0.50	0.05
TP (µg/L as P)	36	20	19	20
TDP (µg/L as P)	7	9	6	5
DOC (mg/L)	11.2	10.0	10.3	17.4
DIC (mg/L)	2.9	2.7	3.3	2.6
Ca (mg/L)	1.43	1.94	2.28	3.21
K (mg/L)	0.51	0.73	0.54	0.6
Mg (mg/L)	0.70	0.81	1.12	0.97
Na (mg/L)	0.75	0.78	0.65	0.64
Cl (mg/L)	1.21	0.30	0.54	0.61
SO_4 (mg/L)	1.74	1.69	1.59	0.86
pH	6.6	6.9	7.0	6.8
Gran Alkalinity (mg/L)	5.7	8.0	9.6	9.8
Bicarbonate (mg/L as HCO_3)	8.4	11.2	13.1	13.2

Appendix B: Compiled chronology data

Table B1: Measured ^{210}Pb, ^{137}Cs, and ^{226}Ra and CRS age model of sediment core C3 from lake AC1 collected in 2019. The age model was linearly extrapolated (grey) after reaching supported ^{210}Pb. Some ^{210}Pb values were interpolated (orange). ^{226}Ra is reported as the weighted mean of ^{214}Bi and ^{214}Pb.

Depth (cm)	CRS Age Model (Year CE)	CRS age model ± error 2 Sigma (Year CE)	^{210}Pb (dpm/g)	^{210}Pb ± error 1 standard deviation (dpm/g)	^{137}Cs (dpm/g)	^{137}Cs ± error 1 standard deviation (dpm/g)	^{226}Ra (dpm/g)	^{226}Ra ± error 1 standard deviation (dpm/g)
0.5	2016.73	0.22	61.5979	2.4119	14.6993	0.4327	0.9553	0.2590
1	2014.68	0.31	73.3235	3.4719	15.6338	0.6448	0.3013	1.1012
1.5	2012.64	0.37	70.2186	2.9856	16.8647	0.5342	0.1211	1.0429
2	2010.79	0.43	67.7698	3.1666	18.5048	0.6053	-0.8978	0.6772
2.5	2008.58	0.51	67.2713	3.5700	17.7519	0.7208	1.1277	0.3811
3	2005.62	0.61	71.5677	3.5323	19.0259	0.6848	-0.8896	0.4261
3.5	2002.75	0.71	69.5184	3.5227	20.2664	0.7377	-0.6099	0.8252
4	1999.79	0.81	69.1563	3.4638	21.5500	0.7473	-0.0732	0.0330
4.5	1996.92	0.91	59.1372	3.6152	26.2002	0.8810	-0.5764	0.5459
5	1993.96	1.02	57.0753	3.2991	26.1414	0.8350	0.6158	0.2405
5.5	1991.19	1.13	52.7387	2.8758	29.5684	0.7218	-0.6250	0.5871
6	1988.09	1.25	47.2662	4.0845				
6.5	1985.18	1.37	42.1860	2.9005	30.5867	0.8384	1.3749	0.7379
7	1982.44	1.49	40.9311	3.6201				
7.5	1978.77	1.68	39.7013	2.1661	23.3221	0.5470	-0.6758	0.5349
8	1975.13	1.86	37.0452	3.1445				
8.5	1971.89	2.06	34.5103	2.2795	18.5640	0.5535	0.5594	0.1890
9	1968.67	2.25	31.2415	3.1493				
9.5	1965.05	2.50	28.1859	2.1731	13.4874	0.4901	1.2273	0.3521
10	1961.12	2.76	26.6782	2.8741				
10.5	1956.72	3.15	25.2252	1.8811	9.2986	0.3976	0.9904	0.2816
11	1953.17	3.46	20.3012	2.5263				
11.5	1949.95	3.79	16.0639	1.6863	7.0103	0.3460	-1.0101	0.4904
12	1946.47	4.13	14.4150	2.1386				
12.5	1942.63	4.62	12.8830	1.3153	4.7643	0.2625	1.1199	0.2927
13	1939.80	4.99	11.7068	1.7895				
13.5	1935.70	5.61	10.6045	1.2133	4.2230	0.2416	0.7514	0.2210
14	1932.93	6.04	8.7506	1.6599				
14.5	1929.56	6.62	7.1266	1.1328	2.9023	0.2217	-0.6948	0.3598

15	1926.86	7.00	5.4666	1.6043				
15.5	1924.45	7.39	4.0869	1.1360	2.2206	0.2232	0.2365	0.0797
16	1922.15	7.73	4.0848	1.4812				
16.5	1919.09	8.31	4.0826	0.9505	2.1157	0.1878	0.6457	0.1759
17	1916.15	8.75	3.5837	1.3219				
17.5	1913.23	9.31	3.1273	0.9187	1.9932	0.1793	0.4969	0.1474
18	1910.06	9.53	3.0218	1.5411				
18.5	1907.11	9.98	2.9187	1.2373				
19	1904.07	10.26	2.8179	1.4893				
19.5	1900.69	11.00	2.7195	0.8289	1.6231	0.1613	0.3152	0.0983
20	1897.23	11.16	2.6204	1.5550				
20.5	1892.89	11.34	2.5237	1.3157				
21	1888.88	11.87	2.3375	1.0217				
21.5	1883.71	11.51	2.1608	1.1836				
22	1877.66		2.0758	1.3258				
22.5	1869.97		1.9931	0.5974	1.1463	0.1134	0.3386	0.0920
23	1864.83							
23.5	1860.17							
24	1856.18							
24.5	1851.14							
25	1846.23		1.3435	0.7936	0.6904	0.1478	0.3091	0.0951
25.5	1840.80							
26	1835.79							
26.5	1830.39							
27	1824.78							
27.5	1819.23							
28	1813.46							
28.5	1807.68							
29	1801.96							
29.5	1794.94							
30	1789.55							
30.5	1783.46							
31	1778.68							
31.5	1772.52							
32	1766.39							
32.5	1760.00							
33	1754.16							
33.5	1747.91							
34	1741.88							
34.5	1735.72							
35	1729.40							

35.5	1723.76							
36	1717.18							
36.5	1710.07							
37	1702.81							
37.5	1695.77							
38	1687.67							
38.5	1679.22							
39	1672.85							
39.5	1666.31							
40	1658.42							
40.5	1651.47							
41	1645.08							
41.5	1637.36							
42	1630.81							
42.5	1624.01							
43	1617.55							
43.5	1610.04							
44	1602.71							
44.5	1595.99							
45	1588.57							
45.5	1580.70							
46	1572.67							
46.5	1563.70							
47	1555.23							
47.5	1547.32							
48	1539.78							
48.5	1532.07							
49	1524.49							
49.5	1516.93							
50	1508.33							
50.5	1497.39							
51	1488.13							
51.5	1479.88							
52	1471.92							
52.5	1463.83							
53	1456.90							
53.5	1449.90							
54	1443.20							
54.5	1436.33							
55	1428.10							
55.5	1419.51							

56	1412.28							
56.5	1403.13							
57	1394.17							
57.5	1385.29							
58	1377.66							
58.5	1366.93							
59	1357.56							
59.5	1349.15							
60	1340.97							
60.5	1332.69							
61	1323.99							
61.5	1316.82							
62	1308.20							
62.5	1299.24							
63	1289.62							
63.5	1281.02							
64	1273.04							
64.5	1263.29							
65	1253.39							
65.5	1244.97							
66	1234.97							
66.5	1226.98							
67	1218.92							
67.5	1208.24							
68	1201.05							
68.5	1193.98							
69	1187.37							
69.5	1179.42							
70	1170.41							
70.5	1162.47							
71	1155.94							
71.5	1140.87							
72	1133.12							
72.5	1124.16							
73	1115.52							
73.5	1107.71							
74	1099.12							

Table B2: Measured ^{210}Pb, ^{137}Cs, and ^{226}Ra and CRS age model of sediment core C1 from lake AC3 collected in 2019. The age model was linearly extrapolated (grey) after reaching supported ^{210}Pb. Some ^{210}Pb values were interpolated (orange). ^{226}Ra is reported as the weighted mean of ^{214}Bi and ^{214}Pb.

Depth (cm)	CRS Age Model (Year CE)	CRS age model ± error 2 Sigma (Year CE)	^{210}Pb (dpm/g)	^{210}Pb ± error 1 standard deviation (dpm/g)	^{137}Cs (dpm/g)	^{137}Cs ± error 1 standard deviation (dpm/g)	^{226}Ra (dpm/g)	^{226}Ra ± error 1 standard deviation (dpm/g)
1	2018.67	0.10	78.0747	4.5900	20.2057	0.6544	0.0552	0.1005
2	2017.31	0.19	83.9348	4.8168	20.0422	0.6169	0.2491	0.1263
3	2015.78	0.27	83.1480	4.9974	21.3759	0.7486	0.5300	0.3251
4	2013.95	0.35	90.0946	5.2532	16.9057	0.6232	0.7437	0.1852
5	2011.73	0.45	95.7979	5.5782	15.7991	0.6147	0.0327	0.0699
6	2008.51	0.57	100.2516	5.6217	17.8748	0.5672	1.0416	0.1825
7	2004.97	0.70	99.1227	5.5867	19.1738	0.6059	0.9193	0.1873
8	2000.89	0.83	103.2598	5.8279	22.1590	0.6835	0.0429	0.1177
9	1996.00	0.97	97.9962	5.4155	23.6777	0.6396	0.0164	0.2267
10	1990.34	1.14	92.4309	5.1742	24.8091	0.6918	0.3064	0.0854
11	1983.35	1.33	84.8667	4.6356	25.6913	0.6296	0.6296	0.1119
12	1977.59	1.51	64.4686	3.7592	27.0288	0.7431	1.5217	0.2125
13	1971.67	1.73	50.7098	2.8981	23.5105	0.5974	0.0275	0.0265
14	1965.50	1.99	44.5420	2.6990	22.2044	0.6232	0.1773	0.1534
15	1959.89	2.26	32.9591	2.2823	18.7467	0.6232	-0.0295	0.0656
16	1953.77	2.63	26.6993	1.6549	12.8819	0.3642	0.4286	0.0873
17	1949.82	2.92	22.2896	1.6546	9.9074	0.3821	1.3554	0.1896
18	1943.70	3.42	19.1075	1.2845	7.4785	0.2570	0.7244	0.1141
19	1937.56	4.00	15.0634	1.2054	6.5457	0.2764	1.4340	0.1756
20	1931.92	4.62	10.8614	0.9128	4.6022	0.2048	0.9826	0.1307
21	1926.21	5.21	8.9690	1.1941				
22	1920.17	5.72	8.1114	1.4207				
23	1913.99	6.67	7.3103	0.7698	2.1910	0.1699	0.5655	0.1192
24	1907.48	7.61	6.0202	0.9633				
25	1901.41	8.82	4.8915	0.5791	1.3697	0.1367	0.9709	0.1232
26	1894.77	9.92	3.8673	0.7283				
27	1889.39	11.08	2.9971	0.4416	1.2372	0.1232	0.7287	0.0978
28	1883.24	12.32	2.8810	0.6075				
29	1876.41	14.21	2.7680	0.4171	1.0343	0.1165	0.8568	0.1056
30	1866.23	17.56	2.7951	0.3989	0.9327	0.1101	1.1182	0.1176
31	1859.21	19.27	2.0406	0.4927				
32	1852.82	19.28	1.7206	0.5713				

33	1847.20	18.35	1.4359	0.2892	0.6409	0.1054	0.7838	0.0965
34	1841.67	13.45	1.2784	0.3955				
35	1837.57		1.1328	0.2698	0.5117	0.1247	0.6738	0.0969
36	1830.89							
37	1825.85							
38	1819.90							
39	1814.20							
40	1807.62							
41	1801.91							
42	1795.84							
43	1787.07							
44	1780.76							
45	1773.07							
46	1766.75							
47	1760.26							
48	1753.36							
49	1746.02							
50	1740.49							
51	1733.59							
52	1727.50							
53	1720.17							
54	1712.47							
55	1704.58							
56	1697.15							
57	1690.16							
58	1683.18							
59	1675.66							
60	1669.09							
61	1661.62							
62	1655.15							
63	1647.06							
64	1638.72							
65	1630.53							
66	1621.75							
67	1613.42							
68	1605.10							
69	1596.97							
70	1588.68							
71	1579.46							
72	1572.17							
73	1564.68							

74	1554.95							
75	1546.42							
76	1537.11							
77	1528.26							
78	1519.38							
79	1510.03							
80	1498.83							
81	1488.79							
82	1478.47							
83	1466.72							
84	1455.64							
85	1445.61							
86	1434.97							
87	1421.97							
88	1408.86							
89	1395.53							
90	1381.68							
91	1368.09							
92	1353.85							
93	1345.08							

Table B3: Measured ^{210}Pb, ^{137}Cs, and ^{226}Ra and CRS age model of sediment core C1 from lake AC5 collected in 2019. The age model was linearly extrapolated (grey) after reaching supported ^{210}Pb. Some ^{210}Pb values were interpolated (orange). ^{226}Ra is reported as the weighted mean of ^{214}Bi and ^{214}Pb.

Depth (cm)	CRS Age Model (Year CE)	CRS age model ± error 2 Sigma (Year CE)	^{210}Pb (dpm/g)	^{210}Pb ± error 1 standard deviation (dpm/g)	^{137}Cs (dpm/g)	^{137}Cs ± error 1 standard deviation (dpm/g)	^{226}Ra (dpm/g)	^{226}Ra ± error 1 standard deviation (dpm/g)
1	2018.14	0.14	89.4278	4.2341	7.9171	0.3730	1.2334	0.3051
2	2016.75	0.19	90.5803	4.1545	8.2798	0.3394	0.8109	0.2412
3	2015.09	0.26	93.8485	4.5383	9.3603	0.4438	0.6221	0.3709
4	2013.25	0.32	91.5470	4.3574	12.6030	0.4842	1.1107	0.2843
5	2011.15	0.38	87.6730	3.8808	14.1885	0.3993	1.6672	0.2743
6	2008.73	0.44	89.9487	4.0121	15.4983	0.4447	0.1460	0.0566
7	2006.27	0.51	87.7029	4.1592	16.0775	0.5469	0.9744	0.2858
8	2003.25	0.58	89.1317	3.9604	16.3038	0.4557	0.3753	0.1966
9	2000.11	0.66	87.4523	3.8831	16.1200	0.4506	1.0982	0.2170
10	1996.38	0.75	91.2743	4.2245	16.7299	0.5350	0.4752	0.1440
11	1992.61	0.85	81.6206	3.7497	19.6298	0.5699	0.1787	0.1343
12	1988.34	0.96	72.1785	3.3352	23.9004	0.6506	0.4790	0.1369
13	1984.03	1.09	61.7225	2.9377	30.7547	0.8074	0.8970	0.1946
14	1979.66	1.23	49.4089	2.2937	33.7261	0.8135	0.0977	0.2247
15	1974.84	1.40	42.4234	2.1478	36.4069	0.9178	-0.0702	0.1264
16	1969.36	1.62	38.6874	1.8975	37.1040	0.8995	0.6753	0.1536
17	1964.27	1.85	33.7440	1.7607	32.2844	0.8159	0.4511	0.1223
18	1959.83	2.09	29.2271	1.4969	20.6565	0.5247	1.3235	0.1799
19	1954.76	2.39	25.8871	1.5139	15.1014	0.4506	0.1105	0.2749
20	1949.02	2.81	23.4124	1.2405	12.7352	0.3459	0.5874	0.1246
21	1943.42	3.28	20.2791	1.1582	8.5582	0.2627	1.2126	0.1716
22	1936.88	3.92	18.0989	0.9856	6.8309	0.2052	0.7314	0.1304
23	1931.04	4.53	14.5941	1.3282				
24	1925.35	5.26	11.5739	0.8903	3.3326	0.1595	0.9771	0.1585
25	1919.44	6.15	8.8943	0.6369	1.6433	0.0928	0.8220	0.1201
26	1912.66	7.36	7.6382	0.5313	0.6989	0.0665	0.5444	0.1031
27	1905.54	8.59	5.8346	0.7200				
28	1899.77	9.67	4.3402	0.4860	0.4137	0.0703	0.8919	0.1194
29	1894.70	10.57	3.7577	0.6567				
30	1889.85	11.58	3.2299	0.4417	0.4393	0.0658	0.8173	0.1213

31	1885.03	12.55	3.0198	0.6469				
32	1880.23	13.55	2.9183	0.8012				
33	1874.07	15.21	2.8191	0.4726	0.4221	0.0743	0.6640	0.1134
34	1869.28	15.87	2.2875	0.6018				
35	1865.21	15.20	1.8273	0.3725	0.3150	0.0587	0.9576	0.1122
36	1860.98	12.92	1.8165	0.5329				
37	1855.77	5.33	1.8057	0.3811	0.3135	0.0607	1.0047	0.1162
38	1850.29		1.5127	0.8085				
39	1844.46		1.2533	0.3365	0.2152	0.0540	0.8293	0.1010
40	1839.72		1.2572	0.6081				
41	1834.50		1.2611	0.5065				
42	1829.11		1.2650	0.6323				
43	1824.32		1.2689	0.3785	0.1822	0.0613	1.0173	0.1146
44	1819.52							
45	1816.14							
46	1811.40							
47	1806.01							
48	1801.06							
49	1795.61							
50	1790.86							
51	1785.32							
52	1780.47							
53	1775.58							
54	1770.34							
55	1765.79							
56	1760.83							
57	1756.21							
58	1751.85							
59	1746.89							
60	1743.19							
61	1736.13							
62	1729.84							
63	1724.28							
64	1718.57							
65	1713.46							
66	1707.50							
67	1701.27							
68	1694.90							
69	1687.77							
70	1681.22							
71	1673.67							

72	1667.57							
73	1662.20							
74	1655.47							
75	1647.40							
76	1639.50							
77	1630.57							
78	1621.90							
79	1612.75							
80	1603.05							
81	1594.07							
82	1586.20							
83	1578.03							
83.5	1573.14							

Table B4: Measured ^{210}Pb, ^{137}Cs, and ^{226}Ra and CRS age model of sediment core C3 from lake PC4 collected in 2019. The age model was linearly extrapolated (grey) after reaching supported ^{210}Pb. Some ^{210}Pb values were interpolated (orange). ^{226}Ra is reported as the weighted mean of ^{214}Bi and ^{214}Pb.

Depth (cm)	CRS Age Model (Year CE)	CRS age model ± error 2 Sigma (Year CE)	^{210}Pb (dpm/g)	^{210}Pb ± error 1 standard deviation (dpm/g)	^{137}Cs (dpm/g)	^{137}Cs ± error 1 standard deviation (dpm/g)	^{226}Ra (dpm/g)	^{226}Ra ± error 1 standard deviation (dpm/g)
0.0	2018.50	0.13	18.7453	1.3297	1.8157	0.1700	1.3252	0.1820
0.5	2016.72	0.28	33.3923	2.1463	3.4097	0.2435	0.2301	0.1239
1.5	2012.26	0.61	80.9158	4.7837	3.9203	0.3346	1.1624	0.3646
2.5	2004.81	1.00	105.1586	5.9714	4.6505	0.3418	-0.0167	0.0436
3.5	1995.54	1.37	84.3237	4.8358	6.3682	0.3497	1.1122	0.2264
4.5	1982.74	1.74	71.9042	4.1457	7.8390	0.3660	0.5124	0.1479
5.5	1971.01	2.04	52.5683	3.2475	7.7946	0.3964	0.0024	0.2214
6.5	1958.19	2.42	36.4582	2.1855	4.6620	0.2328	0.9441	0.1633
7.5	1948.67	2.78	24.0324	1.7820	2.3242	0.2534	1.4735	0.2123
8.5	1939.94	3.20	15.0170	1.2564	1.3572	0.1861	-0.0507	0.0247
9.5	1931.56	3.68	13.1606	1.2437	1.4492	0.2181	-0.0265	0.1210
10.5	1922.84	4.39	9.8780	0.9198	0.8197	0.1554	0.0244	0.0385
11.5	1913.96	5.34	7.5856	0.7113	0.6551	0.1249	0.6861	0.1062
12.5	1902.24	7.00	6.2671	0.6643	0.5181	0.1262	0.0011	0.0017
13.5	1893.77	8.52	3.5484	0.4699	0.3084	0.1068	0.3355	0.0633
14.5	1888.90	9.62	1.8301	0.3023	0.5019	0.1063	0.1072	0.0229
15.5	1881.95	11.31	2.1825	0.3614	0.5358	0.1147	0.0053	0.0767
16.5	1872.72	14.14	2.1983	0.3201	0.4125	0.0940	0.3639	0.1007
17.5	1864.72	17.26	1.5776	0.2787	0.4540	0.1070	0.3307	0.0617
18.5	1860.71	19.20	0.9152	0.1776	0.3569	0.0981	0.0233	0.0243
19.5	1851.17		0.6340	0.1381	0.4133	0.0957	0.0792	0.1359
20.5	1841.94		0.5496	0.1743				
21.5	1831.88		0.4730	0.1064	0.3828	0.0919	0.1448	0.0887
22.5	1822.23		0.5334	0.1677				
23.5	1812.83		0.5986	0.1297	0.2695	0.0889	0.3420	0.0586
24.5	1803.64		0.6738	0.2019				
25.5	1793.99		0.7550	0.1548	0.3307	0.0889	0.0534	0.1660
26.5	1783.26							
27.5	1773.48		-0.1036	-0.0288	0.3679	0.0872	0.6633	0.0931
28.5	1763.81							
29.5	1754.07		0.5050	0.1111	0.2482	0.0784	0.1346	0.0812
30.5	1749.10							

31.0	1744.23							
31.5	1739.52							
32.0	1734.81							
32.5	1729.82							
33.0	1724.05							
33.5	1709.44							
34.0	1704.23							
34.5	1699.02							
35.0	1696.31							
35.5	1691.16							
36.0	1684.94							
36.5	1680.48							
37.0	1676.02							
37.5	1669.84							
38.0	1664.47							
38.5	1659.22							
39.0	1653.89							
39.5	1648.56							
40.0	1642.16							
40.5	1623.61							
41.0	1619.06							
41.5	1614.51							
42.0	1608.51							
42.5	1603.11							
43.0	1596.89							
43.5	1590.54							
44.0	1584.20							
44.5	1579.05							
45.0	1573.75							
45.5	1568.81							
46.0	1563.67							
46.5	1558.54							
47.0	1553.21							
47.5	1547.71							
48.0	1542.05							
48.5	1536.43							
49.0	1530.82							
49.5	1524.26							
50.0	1518.91							
50.5	1513.50							
51.0	1507.62							

51.5	1501.73							
52.0	1495.99							
52.5	1489.82							
53.0	1484.06							
53.5	1478.46							
54.0	1472.87							
54.5	1465.98							
55.0	1458.89							
55.5	1453.13							
56.0	1446.31							
56.5	1439.50							
57.0	1434.11							
57.5	1427.67							
58.0	1421.22							
58.5	1415.16							
59.0	1409.10							
59.5	1403.21							
60.0	1396.45							
60.5	1390.78							
61.0	1384.28							
61.5	1377.78							
62.0	1372.65							
62.5	1364.74							
63.0	1359.21							
63.5	1353.15							
64.0	1347.09							
64.5	1341.58							
65.0	1334.90							
65.5	1329.20							
66.0	1322.54							
66.5	1315.89							
67.0	1308.93							
67.5	1301.12							
68.0	1294.86							
68.5	1287.79							
69.0	1280.72							
69.5	1272.91							
70.0	1266.47							
70.5	1260.35							
71.0	1253.72							
71.5	1247.09							

72.0	1239.93							
72.5	1232.27							
73.0	1224.59							
73.5	1217.98							
74.0	1211.37							
74.5	1204.74							
75.0	1197.79							
75.5	1191.19							
76.0	1183.93							
76.5	1176.67							
77.0	1169.15							
77.5	1160.09							
78.0	1150.84							
78.5	1143.37							
79.0	1135.91							
79.5	1127.74							
80.0	1119.02							
80.5	1109.84							
81.0	1099.98							
81.5	1090.12							
82.0	1080.63							
82.5	1070.27							
83.0	1061.03							
83.5	1051.31							
84.0	1041.59							
84.5	1030.75							
85.0	1020.52							
85.5	1010.27							
86.0	999.62							
86.5	988.97							
87.0	976.10							
87.5	965.80							
88.0	956.13							
88.5	945.55							
89.0	934.96							
89.5	924.54							
90.0	915.99							
90.5	905.84							
91.0	894.08							
91.5	882.33							
92.0	874.02							

92.5	863.41							
93.0	851.88							
93.5	842.26							

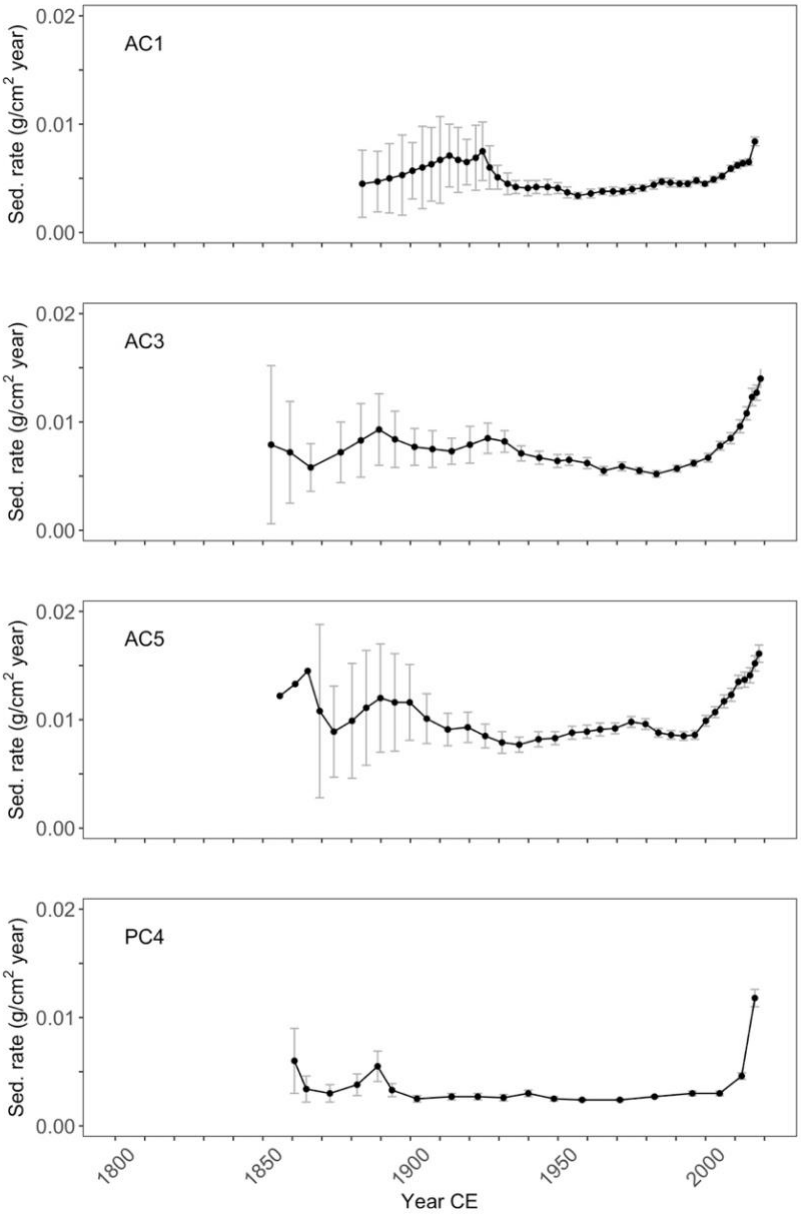

Figure B1. Total sedimentation rate plotted by depth determined using cores AC1-C3, AC3-C1, AC5-C1, and PC4-C3.

Appendix C: Compiled loss-on-ignition data

Table C1: Loss-on-ignition results of sediment core C2 from lake AC1.

Depth (cm)	Total Dry Sediment (g)	H_2O (%)	Organic Matter (%)	Mineral Matter with $CaCO_3$ (%)	Mineral Matter (%)	$CaCO_3$ (%)
0.0	1.0967	98.14	67.88	32.12	29.31	2.82
0.5	0.5848	97.77	69.43	30.57	28.79	1.78
1.0	0.5053	97.88	66.98	33.02	28.53	4.49
1.5	0.6603	97.67	67.81	32.19	31.61	0.58
2.0	0.8299	97.35	66.79	33.21	31.25	1.96
2.5	0.6008	97.74	66.67	33.33	31.01	2.32
3.0	0.6595	97.26	64.10	35.90	32.91	2.99
3.5	0.6784	97.59	64.88	35.12	31.75	3.37
4.0	0.8567	97.43	65.77	34.23	31.62	2.62
4.5	0.8567	97.52	67.32	32.68	30.00	2.68
5.0	0.7107	97.45	66.42	33.58	31.55	2.03
5.5	0.6651	97.30	67.69	32.31	31.26	1.05
6.0	0.7286	97.30	67.46	32.54	31.46	1.08
6.5	0.8507	97.11	66.67	33.33	31.59	1.74
7.0	0.8507	97.01	63.01	36.99	32.33	4.66
7.5	0.8777	96.92	65.36	34.64	31.08	3.56
8.0	0.9444	96.86	63.41	36.59	33.27	3.32
8.5	0.8772	96.93	65.52	34.48	29.79	4.69
9.0	0.8954	96.71	62.80	37.20	33.05	4.15
9.5	0.8954	96.53	62.71	37.29	33.45	3.84
10.0	0.8584	96.86	66.44	33.56	27.17	6.39
10.5	0.8853	96.68	61.54	38.46	36.72	1.74
11.0	0.9416	96.54	61.80	38.20	32.85	5.35
11.5	1.2588	96.13	57.46	42.54	39.54	3.01
12.0	1.2588	96.17	56.90	43.10	38.41	4.69
12.5	1.0447	96.19	54.19	45.81	42.01	3.80
13.0	1.2527	95.85	52.28	47.72	45.64	2.07
13.5	1.2547	95.54	52.81	47.19	43.06	4.12
14.0	1.2591	95.57	52.29	47.71	43.96	3.74
14.5	1.2591	95.53	54.78	45.22	42.26	2.96
15.0	1.3069	95.49	55.87	44.13	41.58	2.55
15.5	1.2504	95.63	57.53	42.47	39.98	2.48
16.0	1.2977	95.83	58.80	41.20	38.69	2.52
16.5	1.2365	95.57	55.45	44.55	40.84	3.71

17.0	1.2365	96.00	57.62	42.38	39.14	3.24
17.5	1.1812	95.77	56.04	43.96	40.68	3.29
18.0	1.5397	95.40	55.70	44.30	40.12	4.18
18.5	1.3570	94.92	54.02	45.98	42.85	3.13
19.0	1.5270	94.85	54.15	45.85	42.90	2.95
19.5	1.5270	94.94	53.28	46.72	40.79	5.94
20.0	1.7716	94.63	52.26	47.74	43.14	4.60
20.5	1.3926	94.62	53.23	46.77	36.9	9.87
21.0	1.3492	95.30	52.16	47.84	43.74	4.10
21.5	1.7164	94.42	52.10	47.90	43.62	4.28
22.0	1.7164	94.80	51.50	48.50	43.89	4.60
22.5	1.7402	94.22	50.17	49.83	45.62	4.21
23.0	1.7653	94.69	50.19	49.81	46.10	3.70
23.5	1.5292	94.29	50.34	49.66	45.50	4.16
24.0	1.7960	94.25	47.33	52.67	49.04	3.63
24.5	1.7960	93.63	48.29	51.71	48.45	3.26
25.0	1.8772	93.96	49.69	50.31	45.69	4.62
25.5	1.2194	94.91	51.09	48.91	43.99	4.93
26.0	1.5086	94.38	49.01	50.99	46.96	4.03
26.5	1.7182	94.41	48.48	51.52	49.23	2.29
27.0	1.7182	94.80	49.39	50.61	45.10	5.51
27.5	1.6251	94.49	49.01	50.99	47.23	3.76
28.0	1.7761	93.98	48.40	51.60	47.73	3.87
28.5	2.0798	93.76	49.19	50.81	48.61	2.20
29.0	1.0937	94.41	51.09	48.91	44.97	3.94
29.5	1.0937	94.38	51.35	48.65	43.92	4.73
30.0	1.0787	94.18	45.78	54.22	50.25	3.97
30.5	2.0465	94.20	47.81	52.19	48.07	4.12
31.0	1.7156	94.03	48.52	51.48	48.46	3.02
31.5	1.8508	94.06	48.16	51.84	45.93	5.91
32.0	1.8508	93.63	47.68	52.32	48.72	3.60
32.5	1.9641	93.26	44.38	55.62	52.18	3.44
33.0	2.1885	92.96	45.03	54.97	50.99	3.98
33.5	1.9269	93.33	47.22	52.78	50.26	2.52
34.0	2.0722	93.16	50.00	50.00	46.99	3.01
34.5	2.0722	92.98	46.92	53.08	47.89	5.18
35.0	1.9293	93.69	49.67	50.33	47.20	3.13
35.5	1.8217	93.78	47.56	52.44	48.29	4.15
36.0	1.8747	93.72	45.78	54.22	49.36	4.86

36.5	1.8810	93.37	48.38	51.62	48.81	2.81
37.0	1.8810	93.32	47.87	52.13	49.23	2.90
37.5	1.8051	93.75	46.95	53.05	47.81	5.25
38.0	1.9817	93.20	48.92	51.08	46.45	4.63
38.5	1.8424	94.04	49.49	50.51	45.93	4.58
39.0	1.6287	94.19	50.85	49.15	45.90	3.25
39.5	1.6287	93.84	47.77	52.23	48.49	3.74
40.0	2.1016	93.55	46.26	53.74	50.50	3.24
40.5	2.0948	92.83	43.11	56.89	51.59	5.29
41.0	2.2793	92.55	43.02	56.98	53.81	3.16
41.5	2.0223	92.54	42.00	58.00	54.89	3.11
42.0	2.0223	93.10	43.40	56.6	52.33	4.28
42.5	1.8693	92.83	47.98	52.02	49.09	2.93
43.0	1.9789	93.73	53.42	46.58	40.99	5.59
43.5	2.0652	93.01	48.97	51.03	47.84	3.19
44.0	2.1682	93.09	49.54	50.46	46.30	4.16
44.5	2.1682	93.39	49.14	50.86	45.81	5.05
45.0	2.0102	93.41	47.62	52.38	48.57	3.81
45.5	2.1062	92.65	45.99	54.01	48.76	5.25
46.0	2.1761	92.49	46.02	53.98	49.58	4.40
46.5	2.0412	93.05	46.44	53.56	49.69	3.87
47.0	2.0412	93.09	48.38	51.62	48.01	3.61
47.5	1.9198	93.45	50.50	49.50	44.04	5.46
48.0	2.1100	93.36	53.44	46.56	42.31	4.25
48.5	1.8886	93.71	54.04	45.96	42.16	3.80
49.0	1.8843	93.97	54.46	45.54	41.95	3.59
49.5	1.8843	93.46	53.77	46.23	43.23	2.99
50.0	1.7399	93.20	50.29	49.71	46.22	3.5
50.5	2.1465	93.29	47.60	52.40	49.95	2.44
51.0	1.9114	93.43	50.48	49.52	46.91	2.61
51.5	2.0303	92.80	50.57	49.43	46.71	2.72
52.0	2.0303	93.16	49.22	50.78	47.81	2.97
52.5	2.4749	92.27	44.58	55.42	51.99	3.43
53.0	2.4764	92.18	44.10	55.90	52.41	3.49
53.5	2.1492	92.01	45.73	54.27	50.19	4.08
54.0	2.3479	92.25	44.87	55.13	50.59	4.54
54.5	2.3479	92.29	44.31	55.69	50.98	4.71
55.0	1.9064	92.94	45.14	54.86	50.97	3.89
55.5	1.7565	92.13	45.75	54.25	49.75	4.49

56.0	2.6474	92.35	45.85	54.15	49.87	4.29
56.5	1.9957	92.44	48.05	51.95	47.36	4.59
57.0	1.9957	92.64	49.73	50.27	45.90	4.36
57.5	2.1468	92.85	50.90	49.10	46.32	2.78
58.0	2.4988	92.49	49.33	50.67	45.93	4.74
58.5	2.7516	91.63	45.81	54.19	48.85	5.34
59.0	2.1879	91.65	47.20	52.80	48.99	3.81
59.5	2.1879	91.42	46.27	53.73	48.51	5.22
60.0	2.5070	91.27	46.67	53.33	49.58	3.75
60.5	2.5478	91.54	48.38	51.62	47.89	3.73

Table C2: Loss-on-ignition results of sediment core C3 from lake AC1.

Depth (cm)	Total Dry Sediment (g)	H2O (%)	Organic Matter (%)	Mineral Matter with CaCO3 (%)	Mineral Matter (%)	CaCO3 (%)
0.0	1.2421	97.84	74.21	25.79	21.48	4.31
0.5	0.7526	97.34	73.06	26.94	24.43	2.51
1.0	0.7353	97.16	73.09	26.91	23.45	3.46
1.5	0.6487	97.67	73.33	26.67	23.83	2.83
2.0	0.7326	97.36	72.89	27.11	23.12	3.99
2.5	0.8518	96.89	73.21	26.79	25.17	1.62
3.0	0.7762	97.19	72.36	27.64	24.67	2.97
3.5	0.7362	97.25	71.17	28.83	25.92	2.90
4.0	0.7616	97.16	69.58	30.42	25.66	4.76
4.5	0.7431	97.32	68.73	31.27	26.33	4.95
5.0	0.6895	97.25	68.82	31.18	27.77	3.41
5.5	0.7854	97.36	68.23	31.77	28.33	3.44
6.0	0.7511	97.33	67.81	32.19	30.33	1.86
6.5	0.6694	97.34	67.38	32.62	29.73	2.89
7.0	0.8352	97.21	68.24	31.76	24.41	7.35
7.5	0.7928	97.11	68.92	31.08	27.41	3.68
8.0	0.6819	97.20	69.33	30.67	27.95	2.72
8.5	0.6757	97.44	68.75	31.25	29.13	2.12
9.0	0.7576	97.29	69.12	30.88	28.88	2.00
9.5	0.7745	97.19	66.67	33.33	30.31	3.02
10.0	0.8039	97.38	67.42	32.58	30.52	2.06
10.5	0.7139	97.32	67.88	32.12	28.15	3.97
11.0	0.7396	97.22	68.49	31.51	26.85	4.66
11.5	0.8027	97.32	63.89	36.11	32.33	3.78
12.0	0.8846	97.09	62.24	37.76	33.96	3.80
12.5	0.6486	97.31	61.87	38.13	35.19	2.94
13.0	0.9324	96.95	62.11	37.89	29.44	8.45
13.5	0.6886	97.13	61.90	38.10	35.32	2.78
14.0	0.9396	96.86	62.42	37.58	34.28	3.30
14.5	0.9010	96.87	60.00	40.00	36.70	3.30
15.0	1.0080	96.29	57.21	42.79	40.76	2.03
15.5	0.8933	96.60	54.55	45.45	42.16	3.3
16.0	1.0929	96.26	53.00	47.00	43.60	3.40
16.5	1.1008	95.84	52.91	47.09	43.43	3.66
17.0	1.1520	96.21	55.38	44.62	41.13	3.49

17.5	1.1817	95.80	53.81	46.19	42.30	3.89
18.0	1.0361	96.24	57.79	42.21	38.11	4.10
18.5	1.0120	96.26	58.21	41.79	37.73	4.06
19.0	1.0559	96.47	57.30	42.70	39.76	2.94
19.5	1.0098	96.19	57.44	42.56	37.68	4.88
20.0	1.1732	96.02	58.22	41.78	37.95	3.83
20.5	1.0335	95.65	57.01	42.99	40.45	2.54
21.0	1.2609	95.61	54.38	45.62	36.22	9.40
21.5	1.2946	95.61	53.46	46.54	41.53	5.01
22.0	1.3903	95.29	54.47	45.53	39.74	5.79
22.5	1.3573	95.21	55.51	44.49	41.50	3.00
23.0	1.2283	95.56	52.53	47.47	43.08	4.39
23.5	1.0526	95.35	54.03	45.97	42.68	3.29
24.0	1.3292	95.23	52.53	47.47	44.33	3.13
24.5	1.2956	95.33	55.11	44.89	43.08	1.81
25.0	1.4335	95.09	53.59	46.41	43.54	2.87
25.5	1.3211	95.24	54.26	45.74	42.69	3.05
26.0	1.4248	94.91	52.35	47.65	39.31	8.35
26.5	1.4804	94.88	51.30	48.70	44.65	4.04
27.0	1.4631	94.85	50.56	49.44	45.40	4.04
27.5	1.5229	94.68	48.58	51.42	48.04	3.38
28.0	1.5246	94.50	48.80	51.20	46.85	4.35
28.5	1.5085	94.54	49.28	50.72	49.25	1.47
29.0	1.8506	94.26	48.89	51.11	47.08	4.03
29.5	1.4214	94.85	54.21	45.79	42.30	3.49
30.0	1.6077	94.31	50.87	49.13	44.43	4.71
30.5	1.2598	95.60	49.10	50.90	48.45	2.45
31.0	1.6268	94.12	49.32	50.68	47.00	3.68
31.5	1.6168	93.90	49.32	50.68	47.90	2.78
32.0	1.6852	94.59	48.48	51.52	46.36	5.15
32.5	1.5410	94.22	49.49	50.51	47.28	3.23
33.0	1.6483	94.32	52.81	47.19	42.26	4.94
33.5	1.5918	94.31	52.10	47.90	44.10	3.80
34.0	1.6244	94.22	52.10	47.90	44.10	3.80
34.5	1.6685	94.16	51.96	48.04	43.2	4.84
35.0	1.4876	94.45	48.89	51.11	47.08	4.03
35.5	1.7359	94.13	48.21	51.79	47.90	3.89
36.0	1.8749	93.93	46.35	53.65	50.63	3.02
36.5	1.9148	93.14	46.47	53.53	50.91	2.62

37.0	1.8578	93.08	45.12	54.88	50.93	3.95
37.5	2.1371	93.00	44.96	55.04	48.77	6.27
38.0	2.2278	93.36	48.09	51.91	49.11	2.79
38.5	1.6812	93.45	49.37	50.63	48.05	2.58
39.0	1.7245	93.68	49.24	50.76	47.87	2.89
39.5	2.0822	93.26	49.73	50.27	46.21	4.07
40.0	1.8337	93.62	46.99	53.01	48.72	4.29
40.5	1.6848	93.75	48.47	51.53	47.78	3.75
41.0	2.0363	93.71	48.25	51.75	49.16	2.59
41.5	1.7293	93.86	47.35	52.65	48.33	4.33
42.0	1.7917	93.70	52.61	47.39	45.61	1.78
42.5	1.7043	93.35	48.06	51.94	48.29	3.65
43.0	1.9812	93.31	49.16	50.84	48.18	2.66
43.5	1.9354	93.40	48.61	51.39	47.18	4.21
44.0	1.7716	93.55	48.40	51.60	47.68	3.92
44.5	1.9564	93.35	45.99	54.01	49.97	4.04
45.0	2.0784	93.22	44.16	55.84	53.26	2.57
45.5	2.1182	92.42	43.10	56.90	53.88	3.01
46.0	2.3653	92.5	41.79	58.21	51.58	6.63
46.5	2.2340	92.56	42.13	57.87	53.88	3.99
47.0	2.0859	92.80	45.91	54.09	50.51	3.58
47.5	1.9903	92.88	47.35	52.65	49.24	3.41
48.0	2.0324	93.13	47.19	52.81	48.56	4.25
48.5	2.0019	93.13	48.13	51.87	48.35	3.53
49.0	1.9921	93.09	47.58	52.42	47.89	4.53
49.5	2.2695	92.56	46.63	53.37	48.02	5.35
50.0	2.8866	90.73	45.38	54.62	49.59	5.03
50.5	2.4434	91.43	44.63	55.37	51.39	3.98
51.0	2.1748	91.65	45.31	54.69	50.44	4.25
51.5	2.1003	92.44	48.40	51.60	49.06	2.55
52.0	2.1336	92.70	50.43	49.57	45.70	3.87
52.5	1.8277	94.16	58.44	41.56	36.26	5.30
53.0	1.8474	94.17	55.07	44.93	42.96	1.97
53.5	1.7677	93.66	52.54	47.46	43.00	4.47
54.0	1.8117	93.63	52.29	47.71	44.22	3.50
54.5	2.1710	92.74	52.34	47.66	44.08	3.58
55.0	2.2668	92.60	47.44	52.56	48.69	3.86
55.5	1.9080	92.99	46.80	53.20	49.42	3.79
56.0	2.4137	92.21	48.46	51.54	51.54	0.00

56.5	2.3625	91.97	47.44	52.56	52.56	0.00
57.0	2.3431	91.71	43.37	56.63	52.69	3.93
57.5	2.0140	91.79	46.31	53.69	53.69	0.00
58.0	2.8305	91.23	47.29	52.71	52.71	0.00
58.5	2.4713	92.07	45.06	54.94	50.68	4.26
59.0	2.2186	91.89	45.22	54.78	50.88	3.90
59.5	2.1583	92.18	43.20	56.80	51.93	4.87
60.0	2.1827	92.28	45.43	54.57	49.99	4.58
60.5	2.2945	92.53	49.32	50.68	48.46	2.22
61.0	1.8931	92.67	48.46	51.54	46.66	4.88
61.5	2.2727	92.30	49.17	50.83	47.07	3.76
62.0	2.3649	92.53	47.67	52.33	48.32	4.01
62.5	2.5360	91.68	44.52	55.48	50.92	4.56
63.0	2.2690	91.98	46.32	53.68	49.75	3.94
63.5	2.1060	91.68	45.68	54.32	50.10	4.22
64.0	2.5717	91.76	46.19	53.81	50.46	3.35
64.5	2.6123	90.70	45.18	54.82	50.72	4.10
65.0	2.2221	91.59	47.46	52.54	49.54	3.00
65.5	2.6357	90.62	48.10	51.90	49.18	2.73
66.0	2.108	92.52	51.74	48.26	44.54	3.72
66.5	2.1281	92.65	53.12	46.88	44.51	2.37
67.0	2.8168	93.28	52.97	47.03	44.71	2.31
67.5	1.8970	93.06	51.98	48.02	44.95	3.07
68.0	1.8655	93.26	51.56	48.44	45.36	3.08
68.5	1.7419	93.09	52.99	47.01	43.91	3.10
69.0	2.0987	92.84	51.46	48.54	46.15	2.39
69.5	2.3770	93.17	58.56	41.44	30.54	10.90
70.0	2.0946	92.20	47.04	52.96	49.30	3.66
70.5	1.7215	92.25	47.22	52.78	49.00	3.78
71.0	3.9763	86.96	28.14	71.86	69.14	2.72
71.5	2.0451	93.41	63.07	36.93	29.20	7.73
72.0	2.3617	92.07	45.38	54.62	49.38	5.23
72.5	2.2798	91.65	46.90	53.10	51.08	2.02
73.0	2.0593	91.86	48.13	51.87	49.01	2.86
73.5	2.2662	91.59	47.46	52.54	48.64	3.90

Table C3: Loss-on-ignition results of sediment core C1 from lake AC3.

Depth (cm)	Total Dry Sediment (g)	H2O (%)	Organic Matter (%)	Mineral Matter with CaCO3 (%)	Mineral Matter (%)	CaCO3 (%)
0.0	0.4061	99.33	67.86	32.14	32.14	0.00
0.5	0.2769	98.85	73.02	26.98	24.83	2.16
1.0	0.4071	98.32	65.09	34.91	30.08	4.83
1.5	0.5784	97.62	67.08	32.92	31.22	1.70
2.0	0.6941	97.57	65.04	34.96	31.64	3.32
2.5	0.3686	98.26	NA	NA	NA	NA
3.0	0.6237	97.90	81.06	18.94	9.96	8.99
3.5	0.4898	98.11	68.20	31.80	28.38	3.41
4.0	0.6293	97.51	67.95	32.05	27.85	4.20
4.5	0.5608	97.87	66.38	33.62	28.93	4.69
5.0	0.7505	97.36	66.67	33.33	30.31	3.02
5.5	0.7676	97.28	68.66	31.34	30.33	1.01
6.0	0.6940	97.35	64.83	35.17	31.42	3.75
6.5	0.8255	97.28	66.92	33.08	31.04	2.05
7.0	0.6558	97.38	67.44	32.56	30.45	2.11
7.5	0.8351	97.05	63.64	36.36	31.95	4.42
8.0	0.8530	96.76	65.90	34.10	30.96	3.14
8.5	0.7877	96.98	65.19	34.81	31.37	3.44
9.0	0.8503	96.67	64.52	35.48	34.61	0.88
9.5	0.8582	96.86	65.16	34.84	32.21	2.63
10.0	1.0090	96.65	64.97	35.03	31.95	3.07
10.5	0.8796	96.60	63.86	36.14	32.05	4.10
11.0	0.8971	96.72	63.58	36.42	33.06	3.36
11.5	0.7858	97.37	NA	NA	NA	NA
12.0	0.9462	96.53	60.10	39.90	37.08	2.82
12.5	0.8909	96.58	61.75	38.25	36.02	2.23
13.0	0.9178	96.73	61.59	38.41	38.41	0.00
13.5	0.8938	96.64	61.96	38.04	36.37	1.67
14.0	0.8698	96.66	59.15	40.85	38.37	2.49
14.5	0.9892	96.29	58.88	41.12	36.97	4.14
15.0	1.09400	96.21	58.66	41.34	39.06	2.28
15.5	0.9994	96.20	58.80	41.2	38.28	2.92
16.0	0.8725	95.93	57.45	42.55	38.21	4.34
16.5	0.5174	98.06	58.10	41.90	38.67	3.24
17.0	1.0480	95.97	58.12	41.88	38.32	3.56

17.5	1.1100	95.79	57.73	42.27	39.46	2.80
18.0	1.1081	95.78	58.88	41.12	37.66	3.45
18.5	1.1819	95.46	57.62	42.38	41.73	0.65
19.0	1.2482	95.28	56.94	43.06	41.17	1.89
19.5	1.2217	95.28	58.14	41.86	41.23	0.63
20.0	1.4921	95.36	56.67	43.33	40.74	2.59
20.5	1.0839	95.58	57.73	42.27	41.04	1.24
21.0	1.2402	95.23	54.74	45.26	42.33	2.93
21.5	1.2840	95.57	56.40	43.60	40.38	3.22
22.0	1.0667	95.16	57.02	42.98	38.93	4.05
22.5	1.3221	94.81	54.92	45.08	41.18	3.90
23.0	1.2955	95.11	55.70	44.30	41.91	2.39
23.5	1.2660	95.33	57.60	42.40	40.52	1.88
24.0	1.2776	95.04	56.44	43.56	40.98	2.58
24.5	1.2020	95.19	57.80	42.20	40.33	1.87
25.0	1.8045	94.94	56.05	43.95	39.56	4.39
25.5	1.1384	94.99	54.12	45.88	43.22	2.67
26.0	1.3873	95.52	53.62	46.38	42.43	3.94
26.5	1.3044	94.87	53.31	46.69	43.32	3.37
27.0	1.1881	95.83	NA	NA	NA	NA
27.5	1.5100	94.49	54.09	45.91	41.55	4.36
28.0	1.2531	94.6	51.55	48.45	44.23	4.22
28.5	1.3283	95.57	53.08	46.92	43.7	3.22
29.0	1.4210	94.84	55.79	44.21	41.40	2.81
29.5	1.4967	94.52	56.16	43.84	42.36	1.48
30.0	1.4542	94.9	54.91	45.09	42.12	2.97
30.5	1.1860	95.26	56.28	43.72	40.78	2.94
31.0	1.4163	95.27	59.00	41.00	38.73	2.28
31.5	1.2472	95.28	57.08	42.92	39.82	3.11
32.0	1.1484	95.19	57.38	42.62	38.03	4.59
32.5	1.6028	94.97	57.85	42.15	37.46	4.69
33.0	1.0985	95.29	57.66	42.34	39.28	3.06
33.5	1.5984	95.32	58.26	41.74	37.8	3.93
34.0	1.0925	95.88	59.69	40.31	36.84	3.47
34.5	0.9691	95.54	60.00	40.00	37.47	2.53
35.0	1.4566	95.64	57.92	42.08	37.37	4.71
35.5	1.1535	95.49	58.15	41.85	38.85	3.00
36.0	0.6359	95.68	56.12	43.88	39.86	4.02
36.5	1.3313	95.57	55.84	44.16	40.62	3.53

37.0	1.1728	95.82	58.11	41.89	37.60	4.29
37.5	1.1500	95.54	58.42	41.58	38.89	2.69
38.0	0.8267	95.62	57.63	42.37	39.49	2.88
38.5	1.3975	95.86	57.08	42.92	39.82	3.11
39.0	1.4553	95.38	57.14	42.86	40.35	2.51
39.5	1.1147	95.71	57.89	42.11	38.85	3.25
40.0	1.2457	96.04	58.10	41.90	38.86	3.04
40.5	0.9834	95.73	58.69	41.31	38.76	2.55
41.0	1.2017	95.96	57.53	42.47	40.28	2.19
41.5	1.1705	95.27	55.69	44.31	37.91	6.40
42.0	1.8275	95.12	54.86	45.14	41.96	3.18
42.5	1.5934	94.76	55.19	44.81	42.56	2.26
43.0	1.1320	94.79	55.37	44.63	41.82	2.81
43.5	1.3337	94.96	55.47	44.53	41.55	2.98
44.0	1.2299	95.71	56.28	43.72	40.56	3.16
44.5	1.7712	95.01	55.02	44.98	40.61	4.37
45.0	0.9542	95.37	56.70	43.30	39.66	3.64
45.5	1.5120	95.50	57.33	42.67	38.44	4.23
46.0	1.0417	95.80	59.13	40.87	37.6	3.27
46.5	1.4932	95.31	59.13	40.87	36.73	4.14
47.0	1.2830	95.28	57.85	42.15	38.78	3.37
47.5	1.4092	94.93	57.03	42.97	38.19	4.78
48.0	1.2909	95.07	55.74	44.26	40.20	4.05
48.5	1.5768	94.80	55.24	44.76	40.37	4.39
49.0	1.0791	95.43	55.05	44.95	40.59	4.37
49.5	1.0780	95.98	56.41	43.59	40.10	3.49
50.0	1.3092	95.46	55.96	44.04	40.92	3.12
50.5	1.3848	94.93	54.51	45.49	42.70	2.79
51.0	1.1749	95.62	54.41	45.59	42.25	3.33
51.5	1.2029	95.70	54.09	45.91	42.82	3.09
52.0	1.4340	95.17	51.90	48.10	44.08	4.02
52.5	1.4302	94.83	49.63	50.37	46.31	4.06
53.0	1.0132	95.12	48.28	51.72	47.56	4.17
53.5	1.9903	94.07	48.56	51.44	47.53	3.91
54.0	0.8012	94.88	47.95	52.05	48.70	3.34
54.5	2.2809	94.18	46.03	53.97	46.63	7.34
55.0	1.3629	94.27	48.71	51.29	47.28	4.01
55.5	1.5382	94.54	50.20	49.80	44.96	4.84
56.0	1.4243	95.03	50.97	49.03	44.83	4.20

56.5	1.3059	95.23	53.04	46.96	44.76	2.20
57.0	1.5821	94.99	52.42	47.58	45.18	2.40
57.5	1.1401	94.86	53.56	46.44	40.84	5.60
58.0	1.4347	95.16	50.23	49.77	45.47	4.31
58.5	1.5019	94.64	52.55	47.45	43.72	3.73
59.0	1.5729	94.97	52.24	47.76	43.19	4.57
59.5	0.9926	95.42	55.02	44.98	41.16	3.82
60.0	1.5103	95.11	54.70	45.30	39.32	5.98
60.5	1.1253	95.24	50.84	49.16	44.02	5.14
61.0	1.4024	94.92	51.87	48.13	42.04	6.09
61.5	1.4388	94.81	51.20	48.80	44.99	3.81
62.0	1.7199	94.32	49.64	50.36	46.42	3.94
62.5	1.9270	93.81	47.88	52.12	49.46	2.66
63.0	1.3283	93.58	49.19	50.81	47.29	3.52
63.5	1.8505	94.32	50.19	49.81	46.10	3.70
64.0	1.3440	94.50	50.00	50.00	45.21	4.79
64.5	2.0035	93.83	50.66	49.34	46.06	3.28
65.0	1.4269	94.62	52.07	47.93	44.56	3.37
65.5	1.9492	93.97	51.68	48.32	45.82	2.50
66.0	1.3010	94.57	52.41	47.59	44.5	3.10
66.5	1.4344	94.44	50.20	49.80	44.38	5.42
67.0	1.8134	94.08	49.45	50.55	47.58	2.97
67.5	1.3514	94.22	48.41	51.59	46.78	4.81
68.0	1.8239	94.17	49.83	50.17	46.9	3.27
68.5	1.4459	94.30	49.46	50.54	45.14	5.40
69.0	1.7916	94.09	51.08	48.92	44.71	4.21
69.5	1.5678	93.66	50.16	49.84	47.18	2.66
70.0	2.0328	93.37	48.99	51.01	46.70	4.31
70.5	1.6933	93.74	47.60	52.40	48.05	4.35
71.0	1.1510	93.98	49.24	50.76	48.27	2.50
71.5	1.5915	93.09	49.30	50.70	47.27	3.43
72.0	1.3316	93.97	50.45	49.55	45.03	4.52
72.5	2.0919	94.24	50.86	49.14	44.93	4.21
73.0	1.7081	94.35	51.92	48.08	43.17	4.91
73.5	1.5959	94.35	53.49	46.51	43.35	3.16
74.0	1.7345	94.00	53.29	46.71	42.02	4.69
74.5	1.7673	93.08	51.00	49.00	44.27	4.74
75.0	1.8671	93.55	52.69	47.31	44.86	2.44
75.5	1.7195	93.61	51.92	48.08	46.48	1.60

76.0	1.7348	93.73	50.91	49.09	42.50	6.59
76.5	1.8306	93.58	52.05	47.95	44.22	3.73
77.0	1.6388	93.17	50.00	50.00	46.11	3.89
77.5	1.8502	93.48	50.32	49.68	46.22	3.46
78.0	1.7993	92.85	49.21	50.79	46.84	3.96
78.5	1.9312	93.25	48.19	51.81	46.89	4.92
79.0	2.4412	92.65	48.97	51.03	46.47	4.56
79.5	1.9059	91.65	49.44	50.56	47.22	3.33
80.0	2.0131	92.80	53.28	46.72	44.07	2.65
80.5	2.1208	92.13	49.41	50.59	47.04	3.55
81.0	1.9103	92.46	49.29	50.71	46.45	4.26
81.5	2.3374	91.57	48.69	51.31	47.09	4.22
82.0	2.2476	91.27	49.53	50.47	46.00	4.47
82.5	1.8492	92.51	49.08	50.92	47.35	3.57
83.0	2.4786	92.40	49.88	50.12	47.16	2.96
83.5	1.7274	92.54	49.42	50.58	47.04	3.54
84.0	2.1868	91.96	47.66	52.34	48.45	3.90
84.5	1.7644	92.39	46.63	53.37	49.77	3.60
85.0	2.3916	92.11	47.26	52.74	50.47	2.27
85.5	2.4436	90.08	47.70	52.30	47.87	4.43
86.0	2.6303	91.35	46.57	53.43	49.25	4.18
86.5	2.5397	90.66	46.91	53.09	49.04	4.05
87.0	2.5770	91.28	46.87	53.13	50.07	3.07
87.5	2.1604	90.84	47.84	52.16	47.45	4.71
88.0	3.0473	91.27	48.68	51.32	47.73	3.59
88.5	2.4603	91.18	47.25	52.75	47.45	5.30
89.0	2.9454	90.14	49.13	50.87	46.16	4.71
89.5	2.5863	90.64	46.93	53.07	47.26	5.80
90.0	2.7207	90.50	47.54	52.46	48.51	3.95
90.5	2.7040	90.37	48.23	51.77	47.86	3.91
91.0	2.8535	89.65	48.58	51.42	47.28	4.15
91.5	3.4264	89.01	45.86	54.14	49.28	4.86

Table C4: Loss-on-ignition results of sediment core C2 from lake AC3.

Depth (cm)	Total Dry Sediment (g)	H2O (%)	Organic Matter (%)	Mineral Matter with CaCO3 (%)	Mineral Matter (%)	CaCO3 (%)
0.0	0.6978	99.15	67.69	32.31	29.17	3.14
0.5	0.5087	97.90	67.29	32.71	28.90	3.81
1.0	0.5060	98.10	69.00	31.00	27.44	3.56
1.5	0.6236	97.72	69.58	30.42	27.02	3.40
2.0	0.5044	97.72	70.16	29.84	27.21	2.64
2.5	0.6398	97.86	69.70	30.30	26.18	4.12
3.0	0.5108	98.10	70.20	29.80	26.20	3.60
3.5	0.4691	97.76	72.17	27.83	NA	NA
4.0	0.5878	98.09	66.33	33.67	25.35	8.33
4.5	0.6833	97.71	NA	NA	5.81	14.19
5.0	0.9718	96.36	70.81	29.19	26.25	2.94
5.5	0.4737	97.41	63.85	36.15	26.74	9.42
6.0	1.0510	97.30	67.15	32.85	29.87	2.98
6.5	0.4912	97.41	66.17	33.83	30.77	3.07
7.0	1.1038	96.95	65.16	34.84	29.57	5.26
7.5	0.5918	96.92	65.61	34.39	30.06	4.33
8.0	0.8594	96.94	64.05	35.95	31.5	4.44
8.5	1.1062	96.77	62.58	37.42	34.09	3.34
9.0	0.9553	96.48	65.34	34.66	32.34	2.32
9.5	0.9118	96.68	65.29	34.71	34.71	0.00
10.0	0.9617	96.43	60.77	39.23	36.22	3.01
10.5	0.8962	96.44	58.56	41.44	38.43	3.01
11.0	1.1380	96.10	63.45	36.55	33.10	3.45
11.5	0.8607	96.66	62.35	37.65	33.65	4.00
12.0	1.2140	96.07	61.31	38.69	34.59	4.10
12.5	1.0243	96.06	60.71	39.29	33.04	6.24
13.0	0.9614	96.29	61.17	38.83	34.49	4.34
13.5	1.3320	95.96	60.49	39.51	34.20	5.31
14.0	0.9227	95.72	60.28	39.72	35.91	3.81
14.5	1.1960	95.68	59.72	40.28	36.5	3.78
15.0	1.2052	95.63	57.53	42.47	36.88	5.59
15.5	1.2065	95.44	58.52	41.48	37.33	4.16
16.0	1.3498	95.74	57.73	42.27	38.56	3.71
16.5	1.1497	95.27	55.23	44.77	38.51	6.26
17.0	1.4490	95.06	57.83	42.17	38.35	3.82

17.5	1.1215	95.36	57.87	42.13	38.66	3.47
18.0	1.4632	95.16	57.44	42.56	37.50	5.06
18.5	1.2844	95.05	57.59	42.41	38.71	3.70
19.0	1.5690	94.91	57.20	42.80	39.63	3.18
19.5	1.1955	94.83	56.70	43.30	38.08	5.21
20.0	1.4683	95.05	55.73	44.27	38.89	5.38
20.5	1.3017	94.83	57.14	42.86	38.66	4.20
21.0	1.4092	95.42	56.28	43.72	38.42	5.30
21.5	1.1122	95.38	55.46	44.54	41.11	3.43
22.0	1.1760	95.88	58.17	41.83	36.6	5.23
22.5	1.2948	94.94	57.42	42.58	38.33	4.25
23.0	1.2989	95.29	57.08	42.92	40.08	2.83
23.5	1.0927	95.61	57.27	42.73	37.78	4.95
24.0	1.2664	95.77	55.09	44.91	40.5	4.41
24.5	0.9673	95.75	57.14	42.86	39.1	3.76
25.0	1.4613	95.26	55.37	44.63	40.13	4.50
25.5	1.4053	95.27	56.02	43.98	40.03	3.95
26.0	1.2967	94.95	54.72	45.28	40.99	4.28
26.5	1.3628	95.10	54.80	45.20	38.67	6.53
27.0	1.4738	95.11	53.25	46.75	43.43	3.32
27.5	1.1427	95.19	54.96	45.04	41.67	3.37
28.0	1.3968	95.63	55.20	44.80	39.87	4.92
28.5	1.2497	95.65	55.96	44.04	40.92	3.12
29.0	1.3250	94.69	56.98	43.02	38.91	4.11
29.5	1.7348	95.16	55.51	44.49	39.49	5.00
30.0	1.2549	95.19	58.16	41.84	40.13	1.71
30.5	1.3083	95.40	58.19	41.81	37.12	4.69
31.0	1.2550	95.05	58.73	41.27	38.57	2.70
31.5	1.2744	95.32	56.78	43.22	36.88	6.34
32.0	1.3167	95.27	58.51	41.49	39.8	1.69
32.5	1.2743	95.29	58.90	41.10	37.64	3.46
33.0	1.3287	95.41	58.72	41.28	37.23	4.05
33.5	1.1995	95.53	59.21	40.79	36.61	4.18
34.0	1.2821	95.39	60.26	39.74	36.17	3.56
34.5	1.0119	96.27	59.69	40.31	36.75	3.56
35.0	1.2481	95.86	57.21	42.79	37.56	5.23
35.5	0.8675	95.63	59.19	40.81	38.98	1.83
36.0	1.4291	95.71	59.82	40.18	35.84	4.35
36.5	0.9597	96.21	58.95	41.05	38.91	2.15

37.0	1.3767	95.84	56.34	43.66	39.19	4.47
37.5	0.9506	95.78	58.02	41.98	37.49	4.49
38.0	1.2457	95.75	57.80	42.20	39.71	2.5
38.5	1.2136	96.23	58.85	41.15	35.48	5.67
39.0	0.9061	96.31	59.24	40.76	35.59	5.17
39.5	1.1526	95.83	59.15	40.85	37.65	3.19
40.0	1.2158	95.57	59.47	40.53	37.53	3.00
40.5	1.2612	95.63	57.34	42.66	38.29	4.37
41.0	1.3956	95.21	57.08	42.92	38.38	4.53
41.5	1.3285	95.42	54.30	45.70	40.78	4.92
42.0	1.3902	95.35	55.02	44.98	40.61	4.37
42.5	0.8143	95.13	54.01	45.99	39.68	6.31
43.0	1.6897	95.16	55.64	44.36	40.65	3.70
43.5	1.3515	95.04	54.24	45.76	42.31	3.46
44.0	1.5263	95.17	56.47	43.53	40.6	2.93
44.5	0.8679	95.67	55.92	44.08	39.56	4.51
45.0	1.3762	95.63	57.67	42.33	37.27	5.06
45.5	1.3605	95.48	56.40	43.60	38.45	5.16
46.0	1.3300	95.33	58.50	41.50	39.35	2.15
46.5	1.3382	95.01	56.28	43.72	39.32	4.40
47.0	1.2551	95.62	55.17	44.83	41.90	2.93
47.5	1.0627	95.55	55.51	44.49	42.10	2.40
48.0	1.3273	95.53	56.64	43.36	39.75	3.61
48.5	1.5498	95.17	56.90	43.1	37.41	5.69
49.0	0.894	95.54	54.29	45.71	40.53	5.18
49.5	1.5934	95.45	54.02	45.98	41.13	4.86
50.0	1.3697	95.35	56.00	44.00	41.82	2.18
50.5	1.0205	95.41	53.02	46.98	42.55	4.43
51.0	1.4277	94.85	51.08	48.92	44.52	4.40
51.5	1.8196	95.07	50.44	49.56	45.95	3.61
52.0	1.1842	95.3	49.19	50.81	46.94	3.87
52.5	1.5522	94.88	47.52	52.48	49.67	2.81
53.0	1.5445	94.61	45.21	54.79	50.1	4.69
53.5	1.5968	94.15	41.97	58.03	53.56	4.47
54.0	1.4803	94.61	47.33	52.67	48.8	3.87
54.5	1.3828	94.62	50.87	49.13	43.96	5.18
55.0	1.5520	94.97	51.72	48.28	44.11	4.17
55.5	1.3673	95.13	50.86	49.14	44.45	4.69
56.0	1.2990	94.91	52.33	47.67	43.46	4.22

56.5	1.4944	95.01	54.89	45.11	41.53	3.58
57.0	1.1323	95.18	52.61	47.39	42.82	4.57
57.5	1.2327	95.65	54.25	45.75	41.26	4.49
58.0	1.2241	95.23	54.32	45.68	41.76	3.92
58.5	1.9761	95.26	54.22	45.78	41.96	3.82
59.0	0.862	95.38	54.18	45.82	40.94	4.88
59.5	0.7622	96.12	56.77	43.23	39.69	3.54
60.0	1.4348	95.58	53.00	47.00	43.60	3.40
60.5	1.1520	95.45	51.26	48.74	43.03	5.71
61.0	1.5353	94.98	52.94	47.06	44.20	2.86
61.5	1.2645	95.12	50.21	49.79	45.74	4.05
62.0	1.9904	94.67	48.52	51.48	46.95	4.53
62.5	1.7103	93.88	46.08	53.92	49.48	4.44
63.0	1.3649	94.36	49.62	50.38	46.23	4.15
63.5	1.4685	94.29	49.81	50.19	45.5	4.69
64.0	1.9006	94.14	50.19	49.81	43.75	6.07
64.5	1.6051	94.24	50.68	49.32	44.66	4.66
65.0	1.5937	94.68	51.64	48.36	46.13	2.23
65.5	1.4777	94.76	52.61	47.39	43.84	3.55
66.0	1.5479	94.62	52.99	47.01	44.3	2.71
66.5	1.1385	95.03	51.08	48.92	44.8	4.12
67.0	1.0204	96.71	82.12	17.88	9.77	8.11
67.5	1.5564	94.51	50.55	49.45	46.49	2.97
68.0	0.9853	94.90	51.05	48.95	44.93	4.02
68.5	1.7827	94.70	49.45	50.55	46.59	3.96
69.0	1.9281	94.51	50.75	49.25	45.19	4.06
69.5	1.0007	94.62	48.89	51.11	46.07	5.04
70.0	1.8761	94.20	48.46	51.54	46.89	4.64
70.5	1.4964	93.76	49.83	50.17	46.41	3.76
71.0	1.9996	93.61	48.24	51.76	47.41	4.35
71.5	1.7532	93.96	49.34	50.66	45.71	4.95
72.0	1.7840	93.87	50.50	49.50	44.53	4.97
72.5	1.5573	94.27	52.25	47.75	43.04	4.71
73.0	1.9599	93.71	53.25	46.75	41.45	5.3
73.5	1.8757	93.62	53.58	46.42	42.18	4.24
74.0	1.5362	93.65	52.07	47.93	43.91	4.02
74.5	1.7261	93.26	51.70	48.30	43.67	4.63
75.0	1.8390	93.58	49.49	50.51	45.01	5.49
75.5	1.6274	93.38	52.49	47.51	42.54	4.97

76.0	1.8218	93.61	52.00	48.00	44.37	3.63
76.5	1.1639	94.00	51.74	48.26	44.01	4.25
77.0	1.8405	93.75	51.88	48.12	42.60	5.53
77.5	2.0666	93.31	50.00	50.00	46.51	3.49
78.0	2.3650	93.22	49.54	50.46	46.25	4.21
78.5	1.2841	93.30	49.69	50.31	45.69	4.62
79.0	1.9673	92.93	50.31	49.69	46.31	3.38
79.5	2.3139	92.69	48.22	51.78	47.31	4.47
80.0	2.1228	92.70	46.70	53.30	49.16	4.14
80.5	2.2087	92.45	49.71	50.29	45.18	5.11
81.0	1.9102	92.24	50.00	50.00	45.92	4.08
81.5	2.0160	92.47	48.50	51.50	46.31	5.19
82.0	2.1025	92.36	48.33	51.67	47.89	3.78
82.5	2.0684	92.59	48.34	51.66	47.52	4.13
83.0	2.0989	92.51	49.60	50.40	46.76	3.65
83.5	2.3705	92.37	48.27	51.73	48.11	3.63
84.0	1.5965	92.54	46.01	53.99	49.87	4.12
84.5	2.185	92.01	45.96	54.04	49.92	4.12
85.0	2.5187	92.32	45.62	54.38	50.05	4.33
85.5	2.1489	91.86	46.06	53.94	50.16	3.78
86.0	2.1675	91.74	45.73	54.27	49.43	4.83
86.5	1.4301	95.59	NA	NA	NA	NA
87.0	2.2394	91.94	47.64	52.36	47.63	4.72
87.5	2.4211	91.56	47.30	52.70	48.50	4.20
88.0	2.4348	91.44	47.45	52.55	48.73	3.82
88.5	2.5434	91.19	44.72	55.28	49.60	5.68
89.0	2.4162	91.39	48.40	51.60	46.57	5.04
89.5	2.8497	90.70	47.10	52.90	48.04	4.86
90.0	3.1619	90.13	48.3	51.7	47.65	4.05
90.5	3.1269	89.50	45.06	54.94	49.83	5.11
91.0	2.8338	89.09	45.54	54.46	49.71	4.74

Table C5: Loss-on-ignition results of sediment core C1 from lake AC5.

Depth (cm)	Total Dry Sediment (g)	H2O (%)	Organic Matter (%)	Mineral Matter with CaCO3 (%)	Mineral Matter (%)	CaCO3 (%)
0.0	0.7451	99.05	66.67	33.33	26.25	7.08
0.5	0.5357	98.14	69.43	30.57	29.16	1.41
1.0	0.5681	97.89	70.43	29.57	28.97	0.59
1.5	0.6367	97.83	70.56	29.44	28.85	0.59
2.0	0.6493	97.77	67.78	32.22	25.96	6.26
2.5	0.6753	97.48	67.69	32.31	28.12	4.18
3.0	0.7101	97.50	63.78	36.22	28.72	7.50
3.5	0.7136	97.39	64.86	35.14	32.19	2.96
4.0	0.8708	97.08	65.87	34.13	32.74	1.39
4.5	0.7250	97.00	64.92	35.08	33.4	1.67
5.0	0.8293	97.21	63.48	36.52	35.13	1.39
5.5	0.8459	97.09	67.65	32.35	31.35	1.00
6.0	0.8207	97.10	59.71	40.29	39.31	0.98
6.5	0.7860	97.11	64.33	35.67	32.2	3.46
7.0	0.9025	96.75	62.57	37.43	34.25	3.18
7.5	0.8872	97.03	63.95	36.05	35.13	0.93
8.0	0.8514	97.08	63.19	36.81	33.03	3.78
8.5	0.8667	96.90	61.11	38.89	34.69	4.20
9.0	0.8436	96.87	59.88	40.12	35.23	4.89
9.5	0.9132	96.94	63.87	36.13	30.86	5.26
10.0	0.8409	96.75	59.88	40.12	35.37	4.74
10.5	0.9268	96.75	60.00	40.00	39.20	0.80
11.0	0.9872	96.57	54.40	45.60	38.13	7.47
11.5	1.0087	96.49	57.40	42.60	39.38	3.22
12.0	0.8628	96.20	57.89	42.11	38.85	3.25
12.5	1.2022	96.07	55.40	44.60	42.05	2.55
13.0	1.0862	96.15	54.21	45.79	40.78	5.01
13.5	1.1944	95.60	54.17	45.83	43.00	2.83
14.0	1.3007	95.63	53.13	46.87	43.84	3.04
14.5	1.2356	95.33	50.87	49.13	43.81	5.32
15.0	1.3647	95.51	51.54	48.46	43.07	5.39
15.5	1.3409	95.3	52.42	47.58	43.74	3.84
16.0	1.1923	95.53	52.19	47.81	44.23	3.58
16.5	1.2863	95.81	53.74	46.26	39.91	6.36
17.0	1.0298	95.85	53.50	46.50	37.66	8.84

17.5	1.1165	96.04	55.17	44.83	42.15	2.68
18.0	1.2483	95.73	53.15	46.85	41.95	4.90
18.5	1.1472	95.60	54.59	45.41	42.29	3.12
19.0	1.2071	95.59	53.42	46.58	42.85	3.73
19.5	1.3328	95.62	54.15	45.85	44.66	1.19
20.0	1.0135	95.37	50.46	49.54	43.30	6.24
20.5	1.4220	95.12	53.36	46.64	42.07	4.57
21.0	1.3415	95.31	53.24	46.76	39.20	7.56
21.5	1.3197	95.43	53.60	46.40	45.17	1.23
22.0	1.0371	95.48	55.11	44.89	42.47	2.42
22.5	1.4249	95.42	54.09	45.91	41.58	4.33
23.0	1.2549	95.50	54.42	45.58	43.68	1.90
23.5	1.3050	95.09	53.10	46.90	46.30	0.60
24.0	1.4687	94.76	50.58	49.42	44.17	5.25
24.5	1.4581	94.75	49.80	50.20	48.55	1.65
25.0	1.7273	94.47	52.03	47.97	46.14	1.84
25.5	1.4912	94.51	49.30	50.70	43.57	7.13
26.0	1.9707	92.92	50.42	49.58	46.55	3.03
26.5	1.7841	94.19	48.69	51.31	48.76	2.55
27.0	1.8225	94.06	50.17	49.83	48.94	0.90
27.5	1.7388	94.34	48.55	51.45	49.48	1.97
28.0	1.4108	94.30	49.08	50.92	46.43	4.48
28.5	1.7480	94.31	49.30	50.70	47.85	2.85
29.0	1.4593	94.49	50.69	49.31	47.9	1.41
29.5	1.6773	94.58	50.53	49.47	46.13	3.34
30.0	1.3353	94.72	50.19	49.81	45.61	4.20
30.5	1.5516	94.76	50.36	49.64	45.2	4.43
31.0	1.4252	94.95	52.29	47.71	45.63	2.08
31.5	1.1424	95.08	52.36	47.64	45.3	2.33
32.0	1.7141	94.75	52.73	47.27	45.14	2.13
32.5	1.1716	94.96	51.98	48.02	46.40	1.62
33.0	1.4711	94.91	50.00	50.00	46.74	3.26
33.5	1.3102	94.68	52.61	47.39	45.20	2.18
34.0	1.6766	94.75	50.62	49.38	47.14	2.24
34.5	1.5396	94.49	50.00	50.00	46.93	3.07
35.0	1.6466	94.28	49.01	50.99	49.64	1.34
35.5	1.4171	94.43	51.76	48.24	41.54	6.70
36.0	1.9223	94.10	50.68	49.32	47.45	1.86
36.5	1.485	94.49	48.75	51.25	47.84	3.41

37.0	1.4895	94.40	50.00	50.00	46.53	3.47
37.5	1.4218	94.71	51.31	48.69	47.67	1.02
38.0	1.2926	94.66	50.76	49.24	44.61	4.64
38.5	1.8055	94.66	50.19	49.81	44.76	5.06
39.0	1.3986	94.95	52.76	47.24	44.03	3.21
39.5	1.1209	95.29	52.05	47.95	41.74	6.21
40.0	1.5078	95.18	51.43	48.57	45.8	2.78
40.5	1.2718	95.12	50.79	49.21	48.13	1.08
41.0	1.6618	95.02	49.78	50.22	41.97	8.24
41.5	1.2002	95.36	50.86	49.14	45.03	4.10
42.0	1.2373	95.73	50.00	50.00	45.31	4.69
42.5	1.3075	95.53	50.23	49.77	45.42	4.35
43.0	1.1308	95.55	52.29	47.71	41.47	6.24
43.5	1.4252	95.65	51.16	48.84	42.51	6.33
44.0	0.9523	95.65	50.93	49.07	41.44	7.63
44.5	0.8440	96.24	53.93	46.07	42.51	3.56
45.0	1.2968	95.71	51.34	48.66	45.63	3.04
45.5	1.2227	95.68	48.57	51.43	46.9	4.53
46.0	1.4844	95.02	46.38	53.62	50.72	2.89
46.5	1.3815	95.40	48.93	51.07	46.4	4.67
47.0	1.4233	95.16	50.19	49.81	43.98	5.82
47.5	1.2084	95.54	49.33	50.67	46.44	4.23
48.0	1.2150	95.33	49.10	50.90	45.39	5.51
48.5	1.6837	94.96	48.29	51.71	47.57	4.14
49.0	1.0630	95.09	46.72	53.28	53.28	0.00
49.5	1.4600	95.08	47.88	52.12	48.45	3.68
50.0	1.1767	95.08	46.99	53.01	48.41	4.6
50.5	1.7692	94.42	50.00	50.00	46.30	3.70
51.0	1.3733	94.77	49.60	50.40	43.92	6.48
51.5	1.2018	95.46	48.21	51.79	47.54	4.25
52.0	1.1328	95.66	49.32	50.68	45.1	5.59
52.5	1.4714	94.99	49.62	50.38	45.23	5.15
53.0	1.3588	95.05	52.67	47.33	46.21	1.12
53.5	1.4250	95.32	49.37	50.63	45.47	5.16
54.0	1.3865	95.69	46.41	53.59	48.38	5.21
54.5	1.0331	94.72	49.62	50.38	49.34	1.04
55.0	1.0103	94.84	50.96	49.04	47.48	1.56
55.5	1.6251	94.66	49.61	50.39	46.70	3.69
56.0	1.3893	94.94	51.18	48.82	47.21	1.61

56.5	1.0667	95.76	49.76	50.24	45.68	4.56
57.0	1.4679	95.10	52.80	47.20	45.57	1.63
57.5	0.8502	95.70	47.64	52.36	44.52	7.83
58.0	1.2663	95.99	50.75	49.25	48.58	0.68
58.5	1.3710	95.52	47.56	52.44	47.61	4.84
59.0	1.5417	94.89	45.39	54.61	49.59	5.02
59.5	0.4231	98.26	NA	NA	NA	NA
60.0	1.7584	94.16	42.11	57.89	53.6	4.29
60.5	1.9970	93.42	42.54	57.46	54.83	2.63
61.0	1.6509	93.76	36.77	63.23	58.19	5.04
61.5	1.6943	94.68	41.83	58.17	56.62	1.55
62.0	1.4886	94.84	42.91	57.09	51.73	5.35
62.5	1.4666	94.30	42.77	57.23	52.86	4.37
63.0	1.7070	94.54	45.02	54.98	52.97	2.01
63.5	1.3285	94.57	46.07	53.93	51.90	2.04
64.0	1.6013	94.37	44.59	55.41	50.35	5.05
64.5	1.1171	94.85	47.29	52.71	49.76	2.95
65.0	1.7066	94.02	46.31	53.69	49.68	4.01
65.5	1.4590	94.85	45.98	54.02	50.38	3.65
66.0	1.6429	94.29	42.65	57.35	51.99	5.36
66.5	1.6707	93.87	45.16	54.84	52.21	2.63
67.0	1.6649	93.89	47.00	53.00	49.83	3.17
67.5	1.7230	93.65	46.08	53.92	52.21	1.71
68.0	1.9838	93.41	44.29	55.71	51.44	4.27
68.5	1.8024	93.28	46.34	53.66	51.59	2.07
69.0	1.8145	93.95	45.60	54.40	51.30	3.10
69.5	1.6697	93.64	45.63	54.37	50.92	3.45
70.0	2.0732	93.05	44.93	55.07	53.10	1.97
70.5	1.9425	93.07	45.22	54.78	52.02	2.76
71.0	1.6432	93.98	44.03	55.97	51.8	4.18
71.5	1.5988	93.65	44.06	55.94	54.24	1.70
72.0	1.5369	94.61	45.00	55.00	51.60	3.40
72.5	1.3155	94.39	44.8	55.20	52.76	2.44
73.0	1.8138	94.27	45.52	54.48	52.04	2.44
73.5	1.7636	93.15	46.63	53.37	47.39	5.98
74.0	2.1104	92.50	46.74	53.26	50.42	2.84
75.0	2.0786	92.80	45.00	55.00	53.11	1.89
75.5	2.1235	91.80	44.60	55.40	52.53	2.87
76.0	2.2683	91.83	43.71	56.29	52.69	3.60

76.5	2.4766	91.54	41.30	58.70	53.77	4.93
77.0	1.9886	91.55	45.71	54.29	51.7	2.59
77.5	2.6226	91.16	44.12	55.88	52.81	3.08
78.0	2.4595	91.44	41.61	58.39	56.20	2.19
78.5	2.4036	90.83	40.18	59.82	55.02	4.80
79.0	2.6459	90.10	42.88	57.12	54.06	3.06
79.5	2.5100	90.67	41.08	58.92	54.54	4.39
80.0	2.4873	91.54	44.21	55.79	53.22	2.57
80.5	2.2884	91.69	44.39	55.61	51.96	3.65
81.0	2.2310	92.37	45.29	54.71	51.15	3.56
81.5	1.9507	92.84	45.73	54.27	51.65	2.62
82.0	1.7318	93.52	44.69	55.31	54.46	0.85
82.5	2.6128	91.26	42.99	57.01	53.32	3.69
83.0	2.6015	90.26	42.80	57.20	53.23	3.97

Table C6: Loss-on-ignition results of sediment core C2 from lake AC5.

Depth (cm)	Total Dry Sediment (g)	H2O (%)	Organic Matter (%)	Mineral Matter with CaCO3 (%)	Mineral Matter (%)	CaCO3 (%)
0.0	0.4257	99.29	71.62	28.38	24.70	3.68
0.5	0.3876	98.38	72.53	27.47	25.98	1.49
1.0	0.415	98.46	72.39	27.61	25.10	2.5
1.5	0.4581	98.40	70.00	30.00	24.90	5.10
2.0	0.4826	98.32	70.52	29.48	26.34	3.14
2.5	0.4294	98.39	68.24	31.76	26.16	5.60
3.0	0.5065	98.20	67.76	32.24	31.50	0.74
3.5	0.2997	98.87	67.74	32.26	28.97	3.29
4.0	0.5937	97.81	66.67	33.33	26.68	6.65
4.5	0.6201	97.77	63.82	36.18	31.76	4.42
5.0	0.6693	97.68	65.13	34.87	33.16	1.71
5.5	0.5989	97.71	69.11	30.89	23.15	7.74
6.0	0.8148	97.48	62.31	37.69	34.55	3.14
6.5	0.7135	97.36	62.60	37.40	34.08	3.32
7.0	0.7678	97.19	62.94	37.06	34.21	2.85
7.5	0.8133	97.25	60.96	39.04	34.38	4.66
8.0	0.7766	97.21	58.65	41.35	32.15	9.20
8.5	0.8684	97.07	60.90	39.10	34.74	4.36
9.0	0.8653	97.04	58.28	41.72	36.71	5.01
9.5	0.6786	97.15	55.70	44.30	39.73	4.56
10.0	0.8299	97.07	56.55	43.45	37.82	5.63
10.5	0.9283	96.91	57.96	42.04	35.97	6.06
11.0	0.9624	96.47	56.36	43.64	41.16	2.47
11.5	0.9659	96.6	54.75	45.25	44.49	0.76
12.0	0.9604	96.73	53.85	46.15	40.52	5.63
12.5	0.9556	96.61	53.75	46.25	40.30	5.95
13.0	0.882	96.4	52.94	47.06	43.42	3.64
13.5	1.2677	96.19	52.91	47.09	42.77	4.32
14.0	1.0114	96.23	53.73	46.27	42.21	4.06
14.5	1.0041	96.27	50.83	49.17	45.41	3.76
15.0	1.2473	95.94	49.51	50.49	44.54	5.94
15.5	1.1017	96.13	51.53	48.47	42.22	6.24
16.0	1.0296	96.30	51.65	48.35	42.37	5.98
16.5	0.9908	96.45	52.47	47.53	45.85	1.68
17.0	0.9243	96.59	51.65	48.35	42.37	5.98

17.5	0.9476	96.44	51.98	48.02	42.64	5.38
18.0	1.0863	96.27	54.64	45.36	41.86	3.51
18.5	1.1139	96.36	53.59	46.41	41.15	5.26
19.0	1.0134	96.47	52.20	47.80	44.81	2.99
19.5	0.9993	96.34	52.46	47.54	46.8	0.74
20.0	1.0848	96.23	51.93	48.07	43.56	4.51
20.5	1.0632	96.28	53.40	46.60	39.48	7.12
21.0	1.0089	96.01	50.72	49.28	47.33	1.95
21.5	1.2619	95.92	51.42	48.58	46.02	2.57
22.0	1.1167	96.10	51.24	48.76	44.70	4.06
22.5	1.0394	96.07	50.79	49.21	44.17	5.04
23.0	1.0812	96.29	52.13	47.87	43.53	4.34
23.5	1.3491	95.79	52.02	47.98	43.17	4.81
24.0	1.1423	95.97	52.31	47.69	44.21	3.49
24.5	1.1392	95.74	50.22	49.78	46.15	3.63
25.0	1.1623	95.47	49.57	50.43	48.10	2.32
25.5	1.1186	95.73	49.56	50.44	45.03	5.42
26.0	1.6283	95.03	49.55	50.45	46.8	3.64
26.5	1.4177	94.92	50.20	49.80	48.13	1.67
27.0	1.3387	94.84	48.62	51.38	48.16	3.23
27.5	1.6457	94.59	49.23	50.77	48.15	2.62
28.0	1.6894	94.82	47.37	52.63	50.98	1.65
28.5	1.5177	94.82	47.89	52.11	45.41	6.70
29.0	1.4699	94.58	46.46	53.54	48.72	4.82
29.5	1.535	94.59	48.78	51.22	47.43	3.79
30.0	1.5468	94.98	47.97	52.03	47.51	4.52
30.5	1.3244	95.20	48.66	51.34	50.73	0.61
31.0	1.3869	95.16	49.39	50.61	45.65	4.96
31.5	1.3133	95.42	50.21	49.79	46.28	3.50
32.0	1.1893	95.52	50.00	50.00	45.10	4.90
32.5	1.1837	95.45	52.47	47.53	45.09	2.44
33.0	1.0812	95.58	50.91	49.09	45.38	3.71
33.5	1.5741	95.33	50.83	49.17	43.55	5.62
34.0	1.228	95.46	50.68	49.32	46.86	2.46
34.5	1.3363	95.12	50.61	49.39	43.34	6.06
35.0	1.1886	95.25	50.59	49.41	46.75	2.67
35.5	1.6448	95.21	49.37	50.63	46.04	4.59
36.0	1.1318	95.32	49.38	50.62	50.62	0.00
36.5	1.3544	94.76	47.78	52.22	47.69	4.53

37.0	1.6025	94.89	46.33	53.67	47.89	5.78
37.5	1.5269	94.7	46.89	53.11	49.13	3.99
38.0	1.3332	95.01	48.30	51.7	47.59	4.11
38.5	1.2892	95.19	50.20	49.80	49.26	0.54
39.0	1.0224	95.32	47.58	52.42	51.22	1.20
39.5	1.6469	94.92	47.74	52.26	47.65	4.6
40.0	1.3812	95.06	48.81	51.19	47.41	3.78
40.5	1.2724	95.01	50.59	49.41	48.35	1.07
41.0	1.4318	96.08	52.04	47.96	43.8	4.16
41.5	0.991	95.46	50.00	50.00	44.52	5.48
42.0	1.2796	95.64	50.45	49.55	45.91	3.64
42.5	1.2597	95.74	49.53	50.47	48.56	1.91
43.0	1.2436	95.55	49.79	50.21	45.66	4.55
43.5	1.2287	95.81	49.3	50.7	46.27	4.43
44.0	0.9599	96.49	48.04	51.96	51.96	0.00
44.5	1.0675	95.84	49.28	50.72	44.21	6.51
45.0	1.2364	95.97	50.7	49.3	44.83	4.47
45.5	1.1843	95.9	51.36	48.64	46.78	1.85
46.0	1.1741	95.91	51.82	48.18	43.24	4.95
46.5	0.9154	96.24	52.85	47.15	42.92	4.23
47.0	1.391	95.06	55.12	44.88	40.06	4.82
47.5	1.2867	96.14	53.23	46.77	39.32	7.44
48.0	0.7454	96.23	53.06	46.94	44.86	2.08
48.5	0.9848	96.01	50.71	49.29	46.07	3.22
49.0	1.4658	95.78	51.34	48.66	44.41	4.25
49.5	1.2554	95.86	49.03	50.97	46.35	4.62
50.0	1.0237	95.76	47.26	52.74	47.32	5.41
50.5	0.9387	96.19	51.72	48.28	44.93	3.35
51.0	1.4711	95.73	45.77	54.23	50.17	4.06
51.5	1.1546	95.74	49.49	50.51	47.76	2.75
52.0	1.1851	95.59	47.58	52.42	50.03	2.40
52.5	1.6623	95.16	47.95	52.05	51.43	0.62
53.0	0.8786	95.49	47.19	52.81	NA	NA
53.5	1.5831	95.09	48.03	51.97	50.9	1.07
54.0	1.3387	94.97	47.04	52.96	49.94	3.02
54.5	1.4497	95.21	50.21	49.79	48.05	1.74
55.0	1.0289	95.63	50.88	49.12	46.71	2.41
55.5	1.6525	95.05	50.64	49.36	45.31	4.05
56.0	1.1946	95.68	53.20	46.80	43.45	3.35

56.5	1.1104	95.44	51.69	48.31	44.37	3.94
57.0	1.3124	95.31	50.89	49.11	46.68	2.43
57.5	1.3196	95.23	49.36	50.64	47.14	3.50
58.0	1.5151	95.29	46.05	53.95	49.18	4.77
58.5	1.4184	94.72	46.21	53.79	47.61	6.18
59.0	1.1279	95.27	49.20	50.80	46.45	4.35
59.5	1.1343	95.23	51.21	48.79	47.15	1.65
60.0	1.4803	96.15	52.00	48.00	NA	NA
60.5	1.1237	95.94	50.76	49.24	43.72	5.52
61.0	0.7366	95.86	48.86	51.14	50.52	0.62
61.5	1.4303	95.79	51.44	48.56	47.90	0.65
62.0	1.1821	95.84	47.17	52.83	48.34	4.49
62.5	1.594	95.24	46.55	53.45	51.1	2.34
63.0	1.2654	95.53	45.61	54.39	52.12	2.28
63.5	1.4237	94.59	43.38	56.62	54.12	2.50
64.0	1.5986	94.92	42.74	57.26	54.52	2.74
64.5	1.3797	94.74	NA	NA	NA	NA
65.0	1.4777	95.07	38.82	61.18	NA	NA
65.5	1.8072	94.27	41.34	58.66	56.25	2.40
66.0	1.3868	95.17	44.86	55.14	NA	NA
66.5	1.3986	94.3	45.55	54.45	51.54	2.90
67.0	1.5275	94.31	45.91	54.09	51.19	2.90
67.5	2.0022	93.67	47.83	52.17	50.35	1.82
68.0	0.7395	97.28	90.78	9.22	2.47	6.75
68.5	1.0887	94.87	47.13	52.87	48.70	4.17
69.0	2.2393	94.27	46.62	53.38	49.99	3.39
69.5	1.5391	94.61	45.59	54.41	49.91	4.5
70.0	1.5819	94.29	45.02	54.98	50.46	4.52
70.5	2.0508	93.33	53.85	46.15	42.93	3.22
71.0	1.758	93.37	50.58	49.42	NA	NA
71.5	1.9942	93.47	45.32	54.68	51.5	3.18
72.0	2.0750	93.05	43.97	56.03	53.12	2.92
72.5	1.6354	93.35	44.12	55.88	51.88	4.00
73.0	1.9950	93.02	45.39	54.61	49.33	5.28
73.5	1.7456	93.39	43.96	56.04	52.39	3.65
74.0	1.7776	93.58	44.60	55.4	51.34	4.06
74.5	1.8975	93.44	43.67	56.33	53.61	2.72
75.0	1.9076	93.41	44.58	55.42	52.89	2.53
75.5	1.5211	93.55	44.20	55.8	51.11	4.69

76.0	2.296	93.17	44.76	55.24	52.22	3.02
76.5	1.5875	93.02	44.39	55.61	52.34	3.27
77.0	2.0980	93.16	42.94	57.06	52.66	4.40
77.5	2.4714	91.49	44.17	55.83	53.13	2.70
78.0	2.1008	92.57	42.82	57.18	NA	NA
78.5	2.228	92.15	41.39	58.61	55.03	3.58
79.0	2.2649	91.91	41.23	58.77	53.93	4.83
79.5	2.2223	91.66	41.77	58.23	56.94	1.30
80.0	2.4800	92.13	42.82	57.18	53.40	3.78
80.5	2.2846	91.90	42.12	57.88	56.21	1.67
81.0	2.3674	91.82	40.99	59.01	54.31	4.7
81.5	2.6230	91.00	41.12	58.88	NA	NA
82.0	2.5297	90.67	42.14	57.86	55.19	2.67
82.5	2.7707	89.85	41.54	58.46	55.25	3.20
83.0	2.8862	90.38	42.82	57.18	54.39	2.79
83.5	2.6023	91.06	44.24	55.76	54.53	1.23

Table C7: Loss-on-ignition results of sediment core C2 from lake PC4.

Depth (cm)	Total Dry Sediment (g)	H2O (%)	Organic Matter (%)	Mineral Matter with CaCO3 (%)	Mineral Matter (%)	CaCO3 (%)
0.0	0.6428	99.38	80.00	20.00	20.00	0.00
0.5	0.5759	98.10	73.30	26.70	23.14	3.56
1.0	0.4081	98.09	74.61	25.39	23.98	1.41
1.5	0.4755	98.11	76.80	23.20	23.20	0.00
2.0	0.4755	98.03	73.74	26.26	23.52	2.75
2.5	0.4438	98.02	74.11	25.89	18.98	6.90
3.0	0.6404	97.90	75.96	24.04	21.42	2.62
3.5	0.5732	97.79	71.82	28.18	21.38	6.80
4.0	0.6514	97.81	75.78	24.22	22.39	1.83
4.5	0.6514	97.51	72.73	27.27	20.82	6.45
5.0	0.8059	97.24	76.09	23.91	20.96	2.96
5.5	0.7218	97.44	75.40	24.60	22.44	2.16
6.0	0.6826	97.24	75.91	24.09	21.11	2.98
6.5	0.7092	97.07	75.16	24.84	19.50	5.33
7.0	0.7092	97.53	74.59	25.41	24.30	1.11
7.5	0.7326	97.34	74.45	25.55	19.59	5.96
8.0	0.6605	97.54	74.59	25.41	24.30	1.11
8.5	0.6757	97.49	73.98	26.02	23.80	2.21
9.0	0.7299	97.49	74.80	25.20	24.13	1.07
9.5	0.7299	97.46	73.39	26.61	22.23	4.39
10.0	0.6490	97.56	71.07	28.93	27.80	1.12
10.5	0.6363	97.60	70.59	29.41	22.55	6.86
11.0	0.7598	97.58	69.23	30.77	24.96	5.81
11.5	0.6915	97.56	70.83	29.17	23.50	5.67
12.0	0.6915	97.29	67.86	32.14	29.23	2.91
12.5	0.7138	97.10	73.97	26.03	22.30	3.73
13.0	0.6755	97.49	69.60	30.40	24.96	5.44
13.5	0.6229	97.62	72.58	27.42	24.13	3.29
14.0	0.8819	97.07	71.33	28.67	26.77	1.90
14.5	0.8819	97.18	73.24	26.76	21.97	4.79
15.0	0.6877	97.03	70.06	29.94	21.27	8.66
15.5	0.7736	97.20	68.57	31.43	27.54	3.89
16.0	0.7684	97.23	71.92	28.08	27.15	0.93
16.5	0.9318	96.76	69.82	30.18	27.76	2.41
17.0	0.9318	96.97	69.94	30.06	25.89	4.17

17.5	0.8017	97.20	70.20	29.80	28.90	0.90
18.0	0.5599	97.00	71.03	28.97	26.15	2.81
18.5	1.0819	97.15	67.88	32.12	24.18	7.94
19.0	0.8502	96.85	68.63	31.37	24.26	7.11
19.5	0.8502	97.02	70.67	29.33	26.61	2.72
20.0	0.7532	96.97	69.33	30.67	26.50	4.17
20.5	1.0456	97.08	69.44	30.56	25.83	4.72
21.0	0.8729	97.01	69.08	30.92	27.34	3.58
21.5	0.8025	97.04	67.53	32.47	26.29	6.18
22.0	0.8025	96.98	69.81	30.19	28.48	1.71
22.5	0.8200	97.03	70.75	29.25	25.55	3.70
23.0	0.8893	96.96	69.81	30.19	27.62	2.57
23.5	0.9774	96.92	70.20	29.80	25.30	4.50
24.0	0.7187	96.92	70.00	30.00	27.28	2.72
24.5	0.7187	96.87	69.57	30.43	27.06	3.38
25.0	0.8447	96.78	69.54	30.46	28.66	1.80
25.5	1.0552	96.93	69.23	30.77	29.03	1.74
26.0	0.5875	96.79	70.06	29.94	26.68	3.26
26.5	1.0790	96.45	69.06	30.94	29.44	1.50
27.0	1.0790	96.67	67.28	32.72	28.52	4.20
27.5	0.9254	96.88	67.76	32.24	30.45	1.79
28.0	1.0523	96.74	64.97	35.03	30.70	4.33
28.5	0.8173	96.75	66.87	33.13	28.02	5.10
29.0	0.8677	96.93	64.90	35.10	30.60	4.50
29.5	0.8677	96.61	62.94	37.06	28.26	8.80
30.0	0.9828	96.47	65.19	34.81	31.80	3.01
30.5	1.0583	96.35	65.88	34.12	33.32	0.80
31.0	0.9481	96.35	63.92	36.08	33.28	2.80
31.5	1.1339	96.44	66.31	33.69	30.05	3.64
32.0	1.1339	96.52	64.16	35.84	29.55	6.29
32.5	0.8698	96.84	66.67	33.33	23.92	9.41
33.0	1.0151	96.66	67.06	32.94	25.74	7.20
33.5	0.9397	96.56	66.67	33.33	27.86	5.47
34.0	0.9479	96.55	65.06	34.94	27.57	7.37
34.5	0.9479	96.53	67.76	32.24	29.27	2.97
35.0	0.9218	96.50	64.77	35.23	29.05	6.18
35.5	1.0265	96.66	65.58	34.42	28.23	6.18
36.0	0.9025	96.71	67.10	32.90	28.52	4.39
36.5	0.9258	96.83	67.30	32.70	29.28	3.42

37.0	0.9258	96.66	66.46	33.54	25.94	7.60
37.5	0.8205	96.92	68.03	31.97	31.05	0.93
38.0	0.8665	96.76	66.67	33.33	30.67	2.67
38.5	0.9190	96.80	66.29	33.71	29.83	3.89
39.0	1.0317	96.49	68.05	31.95	30.34	1.61
39.5	1.0317	96.58	66.85	33.15	29.39	3.76
40.0	1.2035	96.19	66.49	33.51	28.45	5.06
40.5	0.8684	96.24	68.51	31.49	29.24	2.25
41.0	1.1183	96.36	68.33	31.67	24.87	6.80
41.5	0.9799	96.32	68.13	31.87	29.63	2.24
42.0	0.9799	96.57	67.84	32.16	29.78	2.39
42.5	1.1768	96.35	69.94	30.06	26.91	3.14
43.0	0.9284	96.42	69.32	30.68	29.14	1.55
43.5	0.9641	96.37	69.61	30.39	23.62	6.76
44.0	1.1235	96.36	67.04	32.96	26.12	6.84
44.5	1.1235	96.64	69.36	30.64	27.49	3.14
45.0	0.9261	96.73	68.99	31.01	25.85	5.16
45.5	0.9866	96.48	66.49	33.51	26.16	7.35
46.0	0.9877	96.20	67.57	32.43	31.70	0.74
46.5	1.0704	96.22	64.86	35.14	29.25	5.88
47.0	1.0704	96.44	66.09	33.91	31.56	2.34
47.5	0.9804	96.51	64.07	35.93	32.67	3.26
48.0	1.0908	96.28	65.76	34.24	31.28	2.96
48.5	0.9027	96.44	64.50	35.50	31.48	4.02
49.0	1.0272	96.17	62.93	37.07	33.76	3.32
49.5	1.0272	96.06	64.48	35.52	30.32	5.20
50.0	0.9465	96.09	63.78	36.22	27.12	9.10
50.5	0.9742	96.20	68.11	31.89	23.81	8.09
51.0	0.8675	96.35	67.76	32.24	28.18	4.06
51.5	0.7378	96.89	68.13	31.87	28.62	3.25
52.0	0.7378	96.36	67.12	32.88	29.95	2.93
52.5	1.0381	95.54	63.46	36.54	32.18	4.37
53.0	1.0906	95.69	60.44	39.56	35.45	4.11
53.5	1.0428	95.41	64.89	35.11	27.01	8.10
54.0	0.9796	96.28	64.84	35.16	30.68	4.48
54.5	0.9796	95.66	66.56	33.44	29.54	3.90
55.0	1.2224	95.24	65.66	34.34	30.55	3.79
55.5	1.0110	96.08	67.21	32.79	28.38	4.42
56.0	1.1437	95.21	66.67	33.33	25.98	7.35

56.5	1.1706	95.28	66.94	33.06	30.03	3.02
57.0	1.1706	95.43	65.99	34.01	31.86	2.14
57.5	0.9773	95.74	59.47	40.53	37.37	3.16
58.0	1.0750	95.66	62.06	37.94	35.14	2.80
58.5	1.2835	94.84	66.11	33.89	31.93	1.96
59.0	0.8557	96.41	65.41	34.59	31.79	2.79
59.5	0.8557	94.39	64.82	35.18	34.15	1.03
60.0	1.1054	95.18	67.85	32.15	29.90	2.25
60.5	1.4261	94.87	64.42	35.58	33.46	2.12
61.0	1.3713	94.98	64.94	35.06	32.24	2.83
61.5	0.8802	95.30	65.45	34.55	31.71	2.85
62.0	0.8802	95.26	64.02	35.98	31.43	4.55
62.5	1.1483	95.20	64.09	35.91	32.52	3.39
63.0	1.1338	95.51	64.15	35.85	34.57	1.28
63.5	1.1331	95.07	63.33	36.67	33.10	3.56
64.0	1.0915	95.43	63.54	36.46	34.10	2.36
64.5	1.0915	95.47	65.90	34.10	32.76	1.34
65.0	1.2809	95.01	63.94	36.06	29.16	6.90
65.5	1.1526	94.76	64.79	35.21	33.30	1.92
66.0	1.3686	95.32	65.25	34.75	32.65	2.10
66.5	1.1753	94.92	65.63	34.37	31.65	2.71
67.0	1.1753	94.83	67.22	32.78	29.68	3.10
67.5	1.1022	95.66	73.36	26.64	15.61	11.03
68.0	1.3281	95.26	69.58	30.42	25.06	5.36
68.5	1.2178	94.80	67.85	32.15	25.85	6.30
69.0	1.1346	95.14	66.67	33.33	27.19	6.14
69.5	1.1346	94.96	65.89	34.11	27.29	6.82
70.0	1.2210	94.63	68.11	31.89	26.84	5.05
70.5	1.2069	94.92	66.34	33.66	26.93	6.73
71.0	1.2457	95.08	64.66	35.34	NA	NA
71.5	1.1843	94.91	63.24	36.76	NA	NA
72.0	1.1843	94.98	64.04	35.96	29.40	6.56
72.5	1.3169	94.72	65.77	34.23	26.54	7.69
73.0	1.3666	94.40	62.00	38.00	31.02	6.97
73.5	1.4645	94.25	62.75	37.25	31.32	5.93
74.0	1.2620	94.34	65.07	34.93	27.87	7.06
74.5	1.2620	94.65	64.10	35.90	27.06	8.85
75.0	1.4559	94.04	64.03	35.97	27.64	8.33
75.5	1.5726	93.75	60.42	39.58	35.12	4.46

76.0	1.4360	94.27	64.19	35.81	31.98	3.83
76.5	1.4004	94.36	66.29	33.71	28.66	5.05
77.0	1.4004	94.00	60.50	39.50	34.24	5.26
77.5	1.4689	94.35	66.20	33.80	30.01	3.79
78.0	1.4195	94.17	65.00	35.00	31.11	3.89
78.5	1.6928	93.31	61.50	38.50	35.22	3.27
79.0	1.6989	93.47	64.76	35.24	30.57	4.67
79.5	1.6989	93.61	65.71	34.29	29.66	4.63
80.0	1.5236	93.82	65.75	34.25	33.57	0.68
80.5	1.5575	94.11	65.63	34.37	28.74	5.62
81.0	1.5145	93.68	65.46	34.54	31.43	3.11
81.5	1.7206	93.39	65.05	34.95	29.45	5.49
82.0	1.7206	93.62	64.12	35.88	31.94	3.95
82.5	1.7311	93.34	64.50	35.50	32.33	3.17
83.0	1.5748	93.78	67.76	32.24	28.11	4.13
83.5	1.6733	93.82	64.33	35.67	32.10	3.57
84.0	1.6944	93.88	67.65	32.35	28.01	4.34
84.5	1.6944	92.54	66.32	33.68	30.00	3.68
85.0	1.5483	92.78	65.49	34.51	31.31	3.19
85.5	1.7807	93.19	65.34	34.66	30.93	3.73
86.0	2.0620	92.35	65.73	34.27	29.91	4.35
86.5	1.9531	91.87	64.63	35.37	30.79	4.58
87.0	1.9419	91.97	64.38	35.62	31.89	3.73
87.5	2.0615	92.49	66.24	33.76	29.45	4.31

Table C8: Loss-on-ignition results of sediment core C3 from lake PC4.

Depth (cm)	Total Dry Sediment (g)	H2O (%)	Organic Matter (%)	Mineral Matter with CaCO3 (%)	Mineral Matter (%)	CaCO3 (%)
0.0	1.0766	97.95	73.40	26.60	23.25	3.35
0.5	0.6941	97.75	74.24	25.76	22.20	3.56
1.0	0.4912	97.77	74.22	25.78	22.76	3.02
1.5	0.5508	97.95	75.86	24.14	20.12	4.02
2.0	0.5508	98.03	77.61	22.39	19.68	2.71
2.5	0.5653	97.76	77.73	22.27	18.11	4.16
3.0	0.6129	97.65	77.12	22.88	18.85	4.03
3.5	0.5070	97.81	75.78	24.22	18.12	6.10
4.0	0.9034	97.45	78.57	21.43	18.19	3.24
4.5	0.9034	97.15	77.16	22.84	19.07	3.76
5.0	0.7225	97.59	76.11	23.89	NA	NA
5.5	0.7327	97.32	74.26	25.74	18.74	7.00
6.0	0.6583	97.59	78.40	21.60	16.16	5.44
6.5	0.7512	97.92	75.68	24.32	21.87	2.45
7.0	0.7512	97.31	75.20	24.80	19.36	5.44
7.5	0.5884	97.62	76.07	23.93	20.44	3.49
8.0	0.6082	97.90	75.00	25.00	25.00	0.00
8.5	0.7542	97.38	75.36	24.64	21.68	2.96
9.0	0.5801	97.96	72.97	27.03	20.90	6.13
9.5	0.5801	97.67	73.77	26.23	19.54	6.69
10.0	0.5438	97.96	74.19	25.81	24.34	1.46
10.5	0.6353	97.89	71.84	28.16	24.19	3.96
11.0	0.5695	97.93	70.91	29.09	21.67	7.42
11.5	0.6151	97.74	73.73	26.27	22.81	3.46
12.0	0.6151	97.85	72.22	27.78	25.26	2.52
12.5	0.7439	97.32	70.21	29.79	23.04	6.75
13.0	0.7013	97.50	71.65	28.35	22.99	5.35
13.5	0.6933	97.52	70.99	29.01	23.82	5.19
14.0	0.7180	97.45	73.38	26.62	22.71	3.91
14.5	0.7180	97.52	71.31	28.69	25.34	3.34
15.0	0.7244	97.31	71.72	28.28	25.46	2.81
15.5	0.6605	97.59	70.16	29.84	27.65	2.19
16.0	0.7157	97.54	72.52	27.48	25.40	2.08
16.5	0.7049	97.28	71.22	28.78	24.86	3.91
17.0	0.7049	97.49	67.65	32.35	26.35	6.00
17.5	0.6848	97.40	72.54	27.46	21.72	5.75

18.0	0.7342	97.52	71.64	28.36	22.27	6.09
18.5	0.6246	97.48	73.11	26.89	23.46	3.43
19.0	0.6938	97.57	71.43	28.57	24.00	4.57
19.5	0.6938	97.38	72.36	27.64	24.33	3.32
20.0	0.8860	96.98	75.64	24.36	16.51	7.85
20.5	0.7863	97.15	71.22	28.78	21.93	6.85
21.0	0.7408	97.27	72.86	27.14	21.31	5.83
21.5	0.8327	97.03	68.75	31.25	23.60	7.65
22.0	0.8327	97.45	71.97	28.03	24.94	3.09
22.5	0.7878	97.27	72.99	27.01	26.01	0.99
23.0	0.8088	97.40	71.97	28.03	23.91	4.12
23.5	0.7474	97.36	72.79	27.21	20.21	7.00
24.0	0.8081	97.33	71.92	28.08	24.36	3.73
24.5	0.8081	97.68	NA	NA	NA	NA
25.0	0.7143	97.39	71.13	28.87	22.17	6.70
25.5	0.8128	97.30	71.85	28.15	23.11	5.04
26.0	0.7831	97.07	70.70	29.30	24.97	4.33
26.5	0.8879	97.13	70.39	29.61	25.13	4.47
27.0	0.8879	96.98	71.05	28.95	26.26	2.68
27.5	0.8728	96.98	69.74	30.26	27.58	2.68
28.0	0.7460	97.04	69.48	30.52	24.34	6.18
28.5	0.7530	97.17	67.55	32.45	28.85	3.60
29.0	0.8482	97.03	68.18	31.82	29.17	2.65
29.5	0.8482	96.98	68.59	31.41	27.92	3.49
30.0	0.7643	97.41	69.92	30.08	24.96	5.11
30.5	0.8220	96.91	69.29	30.71	23.91	6.80
31.0	0.8058	97.19	71.13	28.87	26.96	1.92
31.5	0.7799	97.12	68.59	31.41	25.31	6.10
32.0	0.7799	96.58	68.21	31.79	27.08	4.72
32.5	0.8262	96.95	69.70	30.30	24.53	5.77
33.0	0.9545	96.55	69.05	30.95	27.71	3.24
33.5	2.4176	91.01	22.02	77.98	76.14	1.83
34.0	0.8629	97.25	69.18	30.82	27.10	3.73
34.5	0.8629	97.33	77.17	22.83	12.13	10.71
35.0	0.4478	98.44	NA	NA	NA	NA
35.5	0.8522	97.00	68.32	31.68	25.76	5.91
36.0	1.0292	96.84	69.08	30.92	29.13	1.79
36.5	0.7385	97.17	67.57	32.43	23.24	9.19
37.0	0.7385	96.70	66.86	33.14	27.70	5.44

37.5	1.0228	96.80	68.02	31.98	29.60	2.37
38.0	0.8893	96.93	68.15	31.85	27.52	4.33
38.5	0.8676	96.95	67.10	32.90	25.88	7.02
39.0	0.8825	96.93	66.03	33.97	28.74	5.23
39.5	0.8825	96.92	66.87	33.13	27.17	5.95
40.0	1.0597	96.54	68.75	31.25	27.00	4.25
40.5	3.0704	96.86	68.75	31.25	25.58	5.67
41.0	NA	NA	NA	NA	NA	NA
41.5	0.7526	97.02	68.28	31.72	25.16	6.57
42.0	0.7526	96.54	70.12	29.88	25.73	4.15
42.5	0.9943	96.52	67.42	32.58	26.47	6.11
43.0	0.8932	96.84	70.24	29.76	24.90	4.86
43.5	1.0294	96.55	73.33	26.67	21.72	4.95
44.0	1.0503	96.26	76.85	23.15	20.47	2.68
44.5	1.0503	96.30	NA	NA	NA	NA
45.0	0.8524	96.49	76.50	23.50	19.78	3.72
45.5	0.8768	97.20	69.39	30.61	24.14	6.48
46.0	0.8176	97.17	71.05	28.95	24.47	4.47
46.5	0.8502	96.96	70.00	30.00	24.90	5.10
47.0	0.8502	96.88	71.25	28.75	25.35	3.40
47.5	0.8809	96.84	69.01	30.99	27.02	3.98
48.0	0.9110	96.81	66.89	33.11	28.51	4.59
48.5	0.9369	96.77	64.71	35.29	27.29	8.00
49.0	0.9294	96.70	65.84	34.16	28.25	5.91
49.5	0.9294	97.02	61.35	38.65	31.14	7.51
50.0	1.0860	96.41	63.74	36.26	30.29	5.98
50.5	0.8848	96.65	62.72	37.28	29.23	8.05
51.0	0.8953	96.76	64.85	35.15	29.38	5.77
51.5	0.9740	96.70	67.24	32.76	26.51	6.25
52.0	0.9740	96.53	65.14	34.86	28.64	6.22
52.5	0.9497	96.29	63.93	36.07	26.40	9.66
53.0	1.0212	96.53	63.54	36.46	29.70	6.76
53.5	0.9544	96.52	64.85	35.15	28.56	6.59
54.0	0.9259	96.62	65.48	34.52	27.24	7.29
54.5	0.9259	96.51	64.97	35.03	28.11	6.92
55.0	1.1399	96.11	65.62	34.38	28.71	5.67
55.5	1.1736	96.30	66.50	33.50	27.38	6.12
56.0	0.9541	96.46	66.30	33.70	27.78	5.91
56.5	1.1276	96.16	68.02	31.98	27.84	4.14

57.0	1.1276	96.60	66.48	33.52	29.72	3.80
57.5	0.8928	96.62	66.12	33.88	26.45	7.43
58.0	1.0649	96.34	65.45	34.55	29.57	4.98
58.5	1.0678	96.36	64.48	35.52	29.57	5.95
59.0	1.0031	96.35	67.66	32.34	19.48	12.86
59.5	1.0031	96.13	66.15	33.85	28.27	5.58
60.0	0.9753	96.21	64.57	35.43	26.88	8.55
60.5	1.1177	96.08	64.53	35.47	30.11	5.36
61.0	0.9391	96.42	65.24	34.76	25.30	9.45
61.5	1.0760	96.46	65.64	34.36	28.78	5.58
62.0	1.0760	96.23	67.23	32.77	26.62	6.15
62.5	0.8492	96.68	65.57	34.43	25.51	8.92
63.0	1.3089	96.08	68.08	31.92	26.18	5.75
63.5	0.9160	96.68	66.24	33.76	27.69	6.06
64.0	1.0028	96.68	62.92	37.08	27.15	9.93
64.5	1.0028	96.47	63.02	36.98	29.90	7.08
65.0	0.9114	96.40	63.27	36.73	29.80	6.94
65.5	1.1052	96.38	66.06	33.94	29.82	4.12
66.0	0.9444	96.47	65.50	34.50	27.35	7.16
66.5	1.1011	96.02	64.02	35.98	28.99	6.99
67.0	1.1011	96.01	63.59	36.41	28.88	7.52
67.5	1.1528	96.02	63.18	36.82	29.37	7.44
68.0	1.2913	95.66	64.45	35.55	28.45	7.09
68.5	1.0367	96.33	66.29	33.71	26.83	6.88
69.0	1.1705	95.81	65.22	34.78	27.69	7.10
69.5	1.1705	95.93	67.74	32.26	27.24	5.01
70.0	1.2923	95.71	68.28	31.72	26.93	4.79
70.5	1.0652	96.10	67.69	32.31	28.82	3.49
71.0	1.0141	96.38	67.36	32.64	28.41	4.23
71.5	1.0972	95.84	63.29	36.71	NA	NA
72.0	1.0972	96.01	67.51	32.49	28.35	4.14
72.5	1.1847	95.74	66.06	33.94	27.71	6.24
73.0	1.2680	95.41	66.81	33.19	26.66	6.53
73.5	1.2711	95.79	67.48	32.52	25.92	6.60
74.0	1.0942	96.14	68.42	31.58	27.28	4.29
74.5	1.0942	95.99	66.36	33.64	26.65	6.99
75.0	1.0976	96.18	65.82	34.18	27.94	6.24
75.5	1.1496	96.01	67.18	32.82	27.94	4.88
76.0	1.0925	95.92	66.01	33.99	26.62	7.37

76.5	1.2017	95.73	65.65	34.35	28.43	5.91
77.0	1.2017	95.83	66.19	33.81	29.28	4.53
77.5	1.2437	95.52	67.23	32.77	26.40	6.37
78.0	1.5007	95.32	67.76	32.24	26.69	5.55
78.5	1.5308	95.22	66.80	33.20	28.36	4.84
79.0	1.2357	95.28	66.52	33.48	26.89	6.59
79.5	1.2357	94.62	65.54	34.46	27.57	6.89
80.0	1.3509	95.12	65.77	34.23	27.43	6.80
80.5	1.4432	94.93	NA	NA	NA	NA
81.0	1.5195	94.76	66.92	33.08	27.32	5.75
81.5	1.6321	94.47	67.45	32.55	28.82	3.73
82.0	1.6321	94.04	67.11	32.89	27.97	4.92
82.5	1.5713	94.34	66.09	33.91	28.26	5.65
83.0	1.7138	94.39	66.45	33.55	27.79	5.76
83.5	1.5302	94.69	66.67	33.33	27.67	5.67
84.0	1.6087	94.29	67.24	32.76	26.73	6.03
84.5	1.6087	94.37	68.90	31.10	26.29	4.81
85.0	1.7933	94.01	68.45	31.55	26.83	4.72
85.5	1.6945	94.25	68.77	31.23	26.68	4.55
86.0	1.6951	94.38	68.42	31.58	27.55	4.03
86.5	1.7627	93.64	66.89	33.11	27.65	5.46
87.0	1.7627	NA	66.92	33.08	27.97	5.11
87.5	2.1304	93.62	67.08	32.92	28.32	4.60
88.0	1.7051	93.81	67.71	32.29	28.45	3.84
88.5	1.6002	93.91	66.78	33.22	27.45	5.77
89.0	1.7518	93.77	66.67	33.33	27.09	6.24
89.5	1.7518	93.70	66.96	33.04	27.92	5.12
90.0	1.7256	94.30	67.14	32.86	27.51	5.34
90.5	1.4139	94.42	67.25	32.75	27.54	5.21
91.0	1.6811	93.90	67.52	32.48	27.23	5.25
91.5	1.9450	93.52	67.23	32.77	26.34	6.43
92.0	1.9450	93.57	67.99	32.01	27.08	4.94
92.5	1.3762	93.57	67.24	32.76	28.07	4.69
93.0	1.7550	93.16	68.26	31.74	27.54	4.20
93.5	1.9086	93.36	67.44	32.56	27.47	5.10
94.0	1.5931	93.17	66.67	33.33	26.80	6.53

Appendix D: Compiled carbon and nitrogen elemental and isotope data

Table D1: Organic carbon and nitrogen elemental and isotope composition (‰ VPDB ±0.2‰; ‰ AIR ±0.3‰) results from sediment core C2 from lake AC1.

Depth (cm)	Carbon (%)	Nitrogen (%)	$\delta^{13}C_{org}$ (‰ VPDB)	$\delta^{15}N$ (‰ AIR)
0.0	34.35	3.08	-22.73	-0.08
0.5	34.99	3.16	-22.71	-0.08
1.0	34.99	3.13	-22.88	0.13
1.5	34.31	3.01	-22.96	0.59
2.0	34.70	3.02	-22.81	-0.18
2.5	35.21	3.03	-23.20	0.06
3.0	33.70	2.92	-23.16	0.58
3.5	35.02	3.06	-22.97	-0.08
4.0	35.74	3.13	-22.33	0.27
4.0	35.22	3.10	-22.18	0.10
4.5	37.23	3.36	-22.17	0.45
5.0	35.65	3.15	-22.21	0.23
5.5	35.23	3.14	-22.33	-0.08
6.0	35.82	3.14	-22.00	0.44
6.5	35.41	3.15	-22.34	0.62
7.0	35.08	3.14	-22.34	0.21
7.5	34.42	3.06	-22.38	0.30
8.0	33.45	2.98	-22.59	0.17
8.5	34.50	2.99	-22.87	0.74
9.0	34.70	3.00	-23.21	0.68
9.0	34.77	3.05	-23.16	0.41
9.5	30.64	2.65	-23.20	0.25
10.0	34.06	2.90	-23.42	-0.01
10.5	33.34	2.83	-23.22	0.48
11.0	32.37	2.77	-22.31	0.82
11.5	31.93	2.59	-21.63	1.19
12.0	30.99	2.49	-21.56	1.39
12.5	30.19	2.48	-21.51	1.28
13.0	26.77	2.15	-21.82	0.93
13.5	30.19	2.40	-21.99	0.60
14.0	29.93	2.40	-22.15	1.20
14.0	29.46	2.35	-22.03	1.07
15.0	30.62	2.50	-22.66	0.78
15.0	30.76	2.51	-22.66	0.57

15.5	31.71	2.54	-23.1	0.35
16.0	30.37	2.46	-22.44	0.04
16.5	31.86	2.56	-22.82	0.11
17.0	29.28	2.32	-22.37	0.24
17.5	29.79	2.37	-22.30	0.19
18.0	29.91	2.41	-22.51	0.87
18.5	30.05	2.45	-23.11	0.97
19.0	30.67	2.44	-23.12	0.67
19.0	30.71	2.41	-23.14	1.30
19.5	30.84	2.38	-22.56	1.52
20.0	30.61	2.33	-22.67	1.51
20.5	30.71	2.38	-23.01	1.45
21.0	30.16	2.41	-23.54	1.12
21.5	28.80	2.29	-23.69	1.08
22.0	28.71	2.27	-23.52	1.39
22.5	28.84	2.29	-23.61	1.37
23.0	29.50	2.27	-23.75	1.16
23.5	28.07	2.19	-23.94	1.62
24.0	28.96	2.28	-23.94	1.61
24.0	28.01	2.21	-23.86	1.30
24.5	28.02	2.22	-24.09	1.27
25.0	29.42	2.44	-24.21	1.19
25.5	28.28	2.39	-24.41	1.47
26.0	28.86	2.37	-24.32	1.77
26.5	26.85	2.18	-24.19	1.77
27.0	28.14	2.25	-23.72	1.75
27.5	27.97	2.22	-23.22	1.69
28.0	27.79	2.18	-23.23	1.51
28.5	28.02	2.14	-23.76	1.19
29.0	29.85	2.28	-24.50	0.67
29.0	29.51	2.29	-24.51	1.22
29.5	30.85	2.38	-24.94	1.12
30.0	29.77	2.37	-25.26	1.16
30.5	27.69	2.20	-24.82	0.94
31.0	27.83	2.26	-24.10	1.48
31.5	27.44	2.19	-23.78	1.66
32.0	27.54	2.16	-23.98	1.95
32.5	25.57	1.97	-24.24	2.31
33.0	26.91	2.03	-24.51	2.07

33.5	28.64	2.21	-24.77	1.77
34.0	28.02	2.17	-24.98	1.78
34.0	29.79	2.29	-25.09	1.76
34.5	30.33	2.33	-25.17	1.84
35.0	29.59	2.29	-25.29	1.92
35.5	28.14	2.18	-24.98	1.88
36.0	28.38	2.22	-24.74	1.99
36.5	27.29	2.14	-24.45	1.64
37.0	28.98	2.24	-24.29	1.66
37.5	28.16	2.19	-24.59	1.70
38.0	29.29	2.21	-24.93	1.25
38.5	29.20	2.19	-24.62	1.81
39.0	27.25	2.03	-23.95	1.35
39.0	28.99	2.11	-23.88	0.94
39.5	28.30	2.14	-23.91	1.45
40.0	26.33	2.03	-23.42	0.41
40.5	24.18	1.86	-23.41	1.53
41.0	23.25	1.77	-23.77	1.6
41.5	24.61	1.87	-24.03	1.53
42.0	23.11	1.76	-24.61	1.39
42.5	27.73	2.12	-25.41	1.71
43.0	26.25	1.99	-25.81	1.26
43.5	29.62	2.29	-25.88	1.95
44.0	28.75	2.19	-25.48	1.22
44.0	30.12	2.26	-25.61	0.86
44.5	28.77	2.16	-25.05	1.71
45.0	29.04	2.16	-24.43	1.73
45.5	28.39	2.06	-24.70	1.11
46.0	27.15	1.99	-25.17	1.41
46.5	26.84	1.95	-25.34	1.69
47.0	29.77	2.17	-24.86	1.36
47.5	29.90	2.20	-23.82	1.14
48.0	31.11	2.32	-22.80	0.68
48.5	31.58	2.38	-22.41	0.65
49.0	31.57	2.32	-21.61	0.44
49.0	32.03	2.37	-21.73	0.69
49.5	30.96	2.26	-21.34	0.72
50.0	29.80	2.17	-21.14	0.99
50.5	27.15	1.95	-20.95	0.92

51.0	27.25	1.97	-21.82	0.74
51.5	28.08	2.04	-22.11	1.10
52.0	25.83	1.91	-22.29	1.08
52.5	24.50	1.80	-22.68	1.14
53.0	26.30	1.95	-23.06	1.05
53.5	25.20	1.83	-23.64	1.35
54.0	25.21	1.85	-23.99	1.88
54.0	25.36	1.86	-24.02	1.47
54.5	26.71	2.04	-24.54	1.47
55.0	26.82	2.03	-25.20	1.16
55.5	25.96	1.90	-25.48	1.17
56.0	25.92	1.89	-25.58	1.41
56.5	28.77	2.09	-25.60	1.66
57.0	29.08	2.12	-25.30	1.05
57.5	29.26	2.15	-24.75	0.61
58.0	29.94	2.20	-23.91	1.10
58.5	26.88	1.97	-23.90	1.49
59.0	27.86	2.03	-24.76	1.36
59.0	27.56	1.99	-24.80	1.41
59.5	28.63	2.07	-24.54	2.03
60.0	29.20	2.01	-24.28	0.94
60.5	30.32	2.11	-23.67	0.86

Table D2: Organic carbon and nitrogen elemental and isotope composition (‰ VPDB ±0.2‰; ‰ AIR ±0.3‰) results from sediment core C2 from lake AC3.

Depth (cm)	Carbon (%)	Nitrogen (%)	$\delta^{13}C_{org}$ (‰ VPDB)	$\delta^{15}N$ (‰ AIR)
0.0	35.35	3.09	-25.02	1.50
0.5	34.90	3.05	-25.05	1.15
1.0	34.49	3.12	-25.28	0.74
1.5	35.55	3.35	-25.51	0.21
2.0	34.90	3.27	-25.58	0.18
2.5	35.03	3.32	-25.72	0.49
3.0	35.07	3.23	-25.59	0.83
3.5	35.27	3.22	-25.37	0.85
4.0	34.14	3.03	-25.34	0.99
4.0	35.51	3.19	-25.43	1.08
4.5	33.94	3.01	-25.16	1.09
5.0	33.93	3.01	-25.14	1.16
5.5	34.33	3.02	-25.02	1.58
6.0	33.45	2.79	-24.91	1.47
6.5	34.29	2.98	-24.91	1.79
7.0	33.46	2.82	-24.80	1.88
7.5	34.04	2.83	-24.78	1.36
8.0	33.51	2.82	-24.69	1.86
8.5	32.99	2.76	-24.69	2.11
9.0	33.60	2.72	-24.75	1.85
9.0	33.84	2.77	-24.82	2.11
9.5	32.31	2.66	-24.90	1.52
10.0	33.64	2.75	-24.77	2.37
10.5	32.19	2.64	-24.72	1.95
11.0	32.86	2.61	-24.81	1.85
11.5	32.14	2.59	-24.66	2.11
12.0	32.37	2.66	-24.71	2.00
12.5	32.46	2.62	-24.60	2.16
13.0	32.29	2.55	-24.55	2.51
13.5	31.26	2.52	-24.56	2.66
14.0	32.19	2.58	-24.41	2.39
14.0	32.06	2.56	-24.48	2.75
14.5	32.37	2.61	-24.45	2.67
15.0	30.92	2.47	-24.33	2.58
15.5	30.70	2.49	-24.28	3.11
16.0	17.25	1.42	-24.42	2.52

16.5	31.35	2.46	-24.30	3.32
17.0	31.62	2.47	-24.30	3.05
17.5	30.86	2.43	-24.41	3.29
18.0	30.06	2.32	-24.44	3.21
18.5	31.85	2.46	-24.67	3.29
19.0	30.49	2.35	-24.74	3.65
19.0	30.14	2.34	-24.75	3.19
19.5	29.56	2.29	-24.84	3.49
20.0	30.77	2.32	-24.85	3.69
20.5	30.62	2.34	-24.96	3.73
21.0	31.03	2.34	-24.87	3.70
21.5	29.53	2.20	-24.87	3.31
22.0	29.66	2.22	-24.83	3.48
22.5	29.47	2.20	-24.57	3.70
23.0	30.72	2.32	-24.69	3.42
23.5	29.99	2.27	-24.03	3.55
24.0	31.15	2.32	-23.17	3.22
24.0	29.85	2.26	-23.25	3.42
24.5	29.36	2.21	-22.75	3.24
25.0	29.86	2.29	-22.10	3.88
25.5	28.54	2.18	-21.49	3.72
26.0	29.39	2.28	-21.50	3.39
26.5	28.07	2.14	-21.25	3.12
27.0	28.65	2.18	-21.29	3.58
27.5	28.42	2.16	-21.44	3.22
28.0	27.69	2.08	-21.61	3.63
28.5	28.62	2.19	-21.55	3.31
29.0	28.68	2.17	-21.70	3.05
29.0	28.98	2.22	-21.73	3.19
29.5	28.74	2.21	-21.71	3.57
30.0	29.78	2.31	-21.82	3.02
30.5	28.30	2.17	-22.00	3.03
31.0	30.32	2.40	-21.95	3.15
31.5	29.55	2.40	-22.33	2.57
32.0	29.99	2.51	-22.83	2.50
32.5	29.82	2.48	-22.84	2.80
33.0	30.27	2.54	-23.03	2.23
33.5	29.92	2.55	-23.11	2.38
34.0	30.28	2.58	-22.43	2.62

34.0	30.02	2.54	-22.36	2.24
34.5	29.20	2.35	-21.96	2.63
35.0	29.20	2.32	-21.49	2.51
35.5	29.36	2.33	-21.33	2.89
36.0	29.90	2.37	-21.09	2.90
36.5	28.87	2.29	-20.73	2.77
37.0	29.47	2.4	-20.42	2.60
37.5	28.95	2.41	-20.31	3.18
38.0	28.95	2.46	-20.25	2.96
38.5	31.18	2.61	-20.25	2.95
39.0	30.47	2.55	-20.48	3.04
39.0	29.52	2.49	-20.46	3.65
39.5	29.86	2.51	-20.56	3.88
40.0	31.06	2.55	-20.75	3.73
40.5	30.26	2.45	-20.69	3.49
41.0	29.49	2.30	-20.89	3.61
41.5	30.36	2.34	-21.00	3.48
42.0	29.04	2.22	-20.88	3.90
42.5	29.91	2.32	-20.47	4.05
43.0	29.95	2.27	-20.01	3.85
43.5	29.54	2.32	-20.44	3.53
44.0	30.25	2.34	-20.38	3.72
44.0	29.80	2.29	-20.48	3.65
44.5	31.84	2.48	-20.55	3.78
45.0	30.23	2.40	-20.81	3.64
45.5	31.65	2.52	-21.05	3.33
46.0	30.15	2.36	-21.22	3.14
46.5	29.18	2.28	-21.50	2.93
47.0	30.03	2.35	-21.65	2.97
47.5	29.13	2.29	-21.77	3.18
48.0	29.58	2.30	-21.35	2.99
48.5	28.25	2.23	-21.09	2.69
49.0	28.91	2.23	-20.68	2.83
49.0	28.57	2.25	-20.76	2.79
49.5	28.92	2.25	-20.78	2.63
50.0	28.37	2.30	-20.73	2.98
50.5	27.19	2.24	-20.91	2.61
51.0	26.07	2.20	-21.09	2.96
51.5	26.13	2.18	-21.29	2.85

52.0	26.25	2.18	-21.52	2.81
52.5	24.46	2.03	-21.44	2.58
53.0	23.76	1.97	-21.67	2.29
53.5	23.81	1.96	-22.09	2.69
54.0	24.68	1.88	-21.93	2.85
54.0	24.90	1.9	-21.92	2.19
54.5	26.41	2.00	-22.32	2.95
55.0	26.79	2.04	-22.73	2.39
55.5	27.85	2.18	-23.00	2.14
56.0	27.17	2.10	-23.35	2.74
56.5	28.76	2.24	-23.39	2.39
57.0	27.54	2.13	-23.50	2.58
57.5	27.96	2.23	-23.33	2.43
58.0	28.22	2.29	-23.38	2.44
58.5	28.66	2.33	-23.39	2.74
59.0	27.32	2.26	-22.98	2.29
59.0	27.69	2.30	-23.17	2.38
59.5	28.79	2.47	-22.71	2.54
60.0	26.93	2.40	-22.62	2.64
60.5	27.46	2.49	-22.22	2.31
61.0	27.23	2.36	-22.18	2.71
61.5	26.31	2.31	-22.35	2.71
62.0	25.11	2.24	-22.32	2.48
62.5	24.71	2.13	-22.81	2.52
63.0	26.10	2.13	-23.20	2.70
63.5	25.93	2.14	-24.00	2.96
64.0	26.28	2.03	-24.51	2.63
64.0	27.79	2.09	-24.56	2.01
64.5	27.72	2.09	-24.86	2.54
65.0	27.29	2.04	-24.5	2.55
65.5	27.53	2.04	-24.11	2.34
66.0	27.80	2.07	-23.51	2.58
66.5	25.94	1.96	-22.90	2.67
67.0	26.48	1.98	-22.48	2.60
67.5	27.52	2.35	-22.15	3.55
68.0	27.70	2.25	-22.23	2.86
68.5	25.78	2.09	-22.14	2.93
69.0	26.21	2.19	-22.19	2.95
69.0	25.99	2.19	-22.19	2.79

69.5	26.18	2.19	-22.32	2.88
70.0	26.26	2.15	-22.38	2.95
71.0	25.28	1.97	-22.63	2.78
71.5	26.41	2.03	-22.83	3.02
72.0	27.96	2.24	-23.02	2.83
72.5	27.14	2.16	-23.30	2.76
73.0	28.59	2.34	-23.49	2.94
73.5	28.20	2.37	-23.74	2.65
74.0	27.85	2.30	-24.22	3.15
74.0	27.98	2.34	-24.24	3.29
74.5	27.68	2.22	-24.68	3.13
75.0	28.62	2.27	-25.12	3.04
75.5	27.30	2.15	-24.96	2.84
76.0	28.63	2.28	-23.91	3.25
76.5	26.64	2.13	-22.84	2.81
77.0	27.48	2.11	-22.65	2.53
77.5	26.91	2.02	-22.32	2.97
78.0	26.65	2.02	-22.14	3.24
78.5	26.52	2.04	-22.32	2.94
79.0	25.88	1.94	-22.59	2.79
79.0	26.43	2.05	-22.62	3.45
79.5	25.21	1.92	-23.02	3.07
80.0	26.42	2.01	-23.49	3.54
80.5	26.68	2.02	-23.83	3.86
81.0	28.29	2.07	-24.05	3.56
81.5	27.51	1.92	-24.13	3.30
82.0	26.41	1.88	-23.82	3.33
82.5	25.73	1.82	-23.40	2.88
83.0	25.70	1.90	-22.76	2.49
83.5	26.44	2.01	-22.36	2.75
84.0	25.43	1.96	-22.06	3.24
84.0	25.71	1.98	-22.03	3.16
84.5	25.94	2.00	-22.31	3.23
85.0	26.67	2.03	-22.46	3.21
85.5	24.91	1.93	-22.65	3.50
86.0	24.78	1.87	-23.21	3.34
86.5	26.37	2.02	-23.45	3.74
87.0	27.42	2.11	-23.66	3.50
87.5	25.87	2.04	-24.19	3.36

88.0	26.14	2.07	-24.82	3.40
88.5	25.61	2.02	-25.37	3.45
89.0	26.35	2.07	-25.14	3.21
89.0	30.03	2.25	-24.51	3.35
89.5	26.9	2.10	-24.95	3.79
90.0	27.00	2.09	-24.6	3.42
90.5	25.95	1.98	-24.23	3.91
91.0	25.93	2.03	-24.26	4.05

Table D3: Organic carbon and nitrogen elemental and isotope composition (‰ VPDB ±0.2‰; ‰ AIR ±0.3‰) results from sediment core C2 from lake AC5.

Depth (cm)	Carbon (%)	Nitrogen (%)	$\delta^{13}C_{org}$ (‰ VPDB)	$\delta^{15}N$ (‰ AIR)
0.0	35.05	3.70	-24.99	-0.89
1.0	36.27	3.72	-24.93	-0.79
1.5	35.23	3.53	-25.07	-0.69
2.0	35.00	3.49	-25.12	-1.03
2.5	34.66	3.42	-25.18	-1.13
3.0	34.41	3.33	-25.18	-1.01
3.5	33.93	3.24	-25.21	-0.91
4.0	33.35	3.15	-25.03	-0.64
4.5	32.41	3.11	-24.62	-0.56
5.0	31.74	2.93	-24.39	-0.31
5.5	32.94	3.04	-24.21	-0.44
6.0	32.50	3.00	-24.23	-0.81
6.5	31.97	2.89	-23.83	-0.62
7.0	32.85	2.97	-23.77	-0.33
7.5	32.28	2.88	-23.61	-0.18
8.0	31.66	2.82	-23.53	-0.43
9.0	31.13	2.76	-23.02	-0.22
9.5	30.59	2.74	-22.99	-0.33
10.0	29.75	2.60	-22.83	-0.06
10.5	30.00	2.62	-22.81	0.17
11.0	29.03	2.52	-22.80	0.30
11.5	29.25	2.51	-22.75	0.50
12.0	29.08	2.51	-22.79	0.20
12.5	29.62	2.50	-22.91	0.11
13.0	28.28	2.41	-23.21	0.42
13.5	28.07	2.34	-23.75	0.33
14.0	26.72	2.23	-23.92	0.07
14.5	27.69	2.33	-24.31	0.56
15.0	26.91	2.25	-24.57	0.69
15.5	27.64	2.31	-24.45	0.68
16.0	27.71	2.30	-24.32	0.13
16.5	28.37	2.35	-24.00	0.08
17.0	28.10	2.35	-23.67	-0.12
17.5	27.90	2.31	-23.10	-0.02
18.0	28.95	2.38	-22.79	0.33
18.5	28.03	2.31	-22.85	0.21

19.0	28.05	2.33	-22.81	0.26
19.5	28.28	2.33	-22.90	0.29
20.0	28.07	2.29	-23.48	0.05
20.5	27.75	2.27	-23.91	-0.01
21.0	27.90	2.27	-24.16	0.22
21.5	28.78	2.33	-24.18	0.03
22.0	28.08	2.30	-23.68	0.3
22.5	27.83	2.30	-23.30	0.74
23.0	27.35	2.22	-23.04	0.38
23.5	27.83	2.28	-22.70	0.32
24.0	28.23	2.32	-22.63	0.42
24.5	28.22	2.31	-22.88	0.71
25.0	27.51	2.26	-23.20	1.03
25.5	28.89	2.35	-23.40	1.34
26.0	28.03	2.27	-23.56	1.41
26.5	27.18	2.19	-23.98	1.28
27.0	29.03	2.34	-24.32	1.69
27.5	26.97	2.13	-24.74	1.68
28.0	26.70	2.06	-25.12	1.75
28.5	27.67	2.11	-25.60	1.93
29.5	26.92	2.08	-26.04	1.54
30.0	27.69	2.12	-25.96	1.39
30.5	28.41	2.20	-25.65	1.34
31.0	25.74	2.05	-25.20	0.87
31.5	27.99	2.22	-24.68	1.16
32.0	28.18	2.24	-24.31	1.25
32.5	28.51	2.32	-23.68	1.22
33.0	28.09	2.30	-23.34	1.08
33.5	28.35	2.32	-22.87	1.73
34.0	28.48	2.30	-22.81	1.83
34.5	28.73	2.34	-22.58	1.43
35.0	28.63	2.31	-22.35	1.54
35.5	27.56	2.23	-22.22	1.53
36.0	25.97	2.09	-22.14	1.77
36.5	25.97	2.08	-21.83	1.79
37.0	27.09	2.16	-21.64	1.82
37.5	24.81	1.97	-21.80	1.16
38.0	26.29	2.07	-21.6	1.17
38.5	28.81	2.29	-21.91	1.27

39.0	27.01	2.14	-22.21	1.46
39.5	27.29	2.16	-22.67	1.75
40.0	26.62	2.10	-22.89	1.29
40.5	28.29	2.23	-23.24	1.11
41.0	27.37	2.18	-23.46	0.97
41.5	27.45	2.21	-23.77	0.56
42.0	28.36	2.28	-23.63	0.99
42.5	26.84	2.17	-23.51	1.14
43.0	27.31	2.21	-23.38	0.97
43.5	27.30	2.18	-23.07	0.86
44.0	26.82	2.15	-22.85	0.93
44.5	25.96	2.06	-22.75	0.67
45.0	26.72	2.14	-22.56	0.68
45.5	27.33	2.16	-22.21	1.08
46.0	28.16	2.28	-22.00	0.68
46.5	27.67	2.21	-21.88	0.81
47.0	28.74	2.36	-21.31	0.65
47.5	29.06	2.37	-20.57	0.64
48.0	27.85	2.32	-20.00	0.72
48.5	26.87	2.27	-19.65	0.77
49.0	27.11	2.26	-19.31	1.65
49.5	26.77	2.13	-19.20	1.35
0.5	36.26	3.64	-24.96	-1.03
4.5	33.34	3.11	-24.55	-0.83
8.5	31.75	2.80	-23.12	-0.35
9.5	29.49	2.63	-22.83	-0.07
14.5	28.17	2.40	-24.15	0.81
19.5	28.55	2.37	-22.93	0.82
24.5	28.49	2.37	-22.76	1.48
29.0	26.79	2.07	-25.79	1.39
29.5	26.38	2.04	-26.00	1.90
34.5	27.84	2.28	-22.52	1.73
39.5	27.50	2.20	-22.49	1.78
44.5	26.27	2.08	-22.58	0.94
49.5	27.93	2.25	-19.24	1.64

Table D4: Organic carbon and nitrogen elemental and isotope composition (‰ VPDB ±0.2‰; ‰ AIR ±0.3‰) results from sediment core C2 from lake PC4.

Depth (cm)	Carbon (%)	Nitrogen (%)	$\delta^{13}C_{org}$ (‰ VPDB)	$\delta^{15}N$ (‰ AIR)
0.0	40.85	3.67	-28.71	-1.36
0.5	41.26	3.73	-28.83	-0.95
1.0	41.35	3.72	-29.01	-0.83
1.5	42.73	3.89	-29.54	-1.16
2.0	41.97	3.79	-29.53	-1.00
2.5	43.25	3.91	-30.14	-1.48
3.0	44.32	4.09	-30.35	-0.90
3.5	43.38	3.92	-29.95	-1.18
4.0	44.18	4.06	-30.32	-0.79
4.5	44.08	4.06	-30.28	-0.86
4.5	44.33	4.05	-30.33	-0.56
5.0	44.18	4.02	-29.83	-0.58
5.5	43.70	3.94	-29.53	-0.42
6.0	42.90	3.87	-28.87	-0.81
6.5	43.59	3.86	-28.31	-0.72
7.0	44.15	3.88	-28.04	-0.07
7.5	44.34	4.03	-28.01	-0.33
8.0	0.04	0.00	-28.29	-1.14
8.5	41.58	3.72	-28.41	-0.75
9.0	41.39	3.66	-28.40	-0.98
9.5	40.39	3.61	-28.50	-1.32
9.5	40.36	3.61	-28.56	-1.63
10.0	39.89	3.61	-28.37	-1.01
10.5	40.28	3.62	-28.19	-1.86
11.0	40.26	3.62	-28.08	-1.10
11.5	39.41	3.58	-28.02	-1.68
12.0	39.29	3.57	-28.09	-1.32
12.5	39.18	3.54	-28.18	-1.19
13.0	38.86	3.46	-28.07	-1.38
13.5	39.23	3.45	-27.92	-1.34
14.0	39.73	3.48	-27.93	-1.42
14.5	39.71	3.46	-27.61	-1.22
14.5	39.71	3.45	-27.77	-1.22
15.0	39.24	3.42	-27.67	-1.10
15.5	39.14	3.45	-27.33	-0.82
16.0	39.22	3.39	-27.47	-1.20
16.5	39.17	3.37	-27.27	-0.78
17.0	39.55	3.42	-27.30	-1.19
17.5	39.74	3.36	-27.22	-0.88
18.0	39.26	3.33	-27.20	-1.12
18.5	39.54	3.38	-27.33	-0.98
19.0	39.98	3.39	-27.36	-0.48

19.5	39.50	3.38	-27.37	-0.82
19.5	39.64	3.40	-27.24	-0.66
20.0	39.92	3.44	-27.36	-0.82
20.5	39.85	3.43	-27.32	-1.28
21.0	39.86	3.41	-27.31	-0.77
21.5	39.70	3.42	-27.40	-1.17
22.0	40.14	3.44	-27.35	-0.58
22.5	40.34	3.47	-27.42	-1.14
23.0	40.06	3.45	-27.53	-0.96
23.5	40.12	3.47	-27.41	-1.03
24.0	39.92	3.46	-27.58	-1.41
24.5	39.21	3.40	-27.44	-0.94
24.5	39.24	3.40	-27.42	-1.12
25.0	39.59	3.38	-27.41	-0.47
25.5	39.80	3.39	-27.23	-1.07
26.0	40.11	3.40	-27.06	-1.12
26.5	39.20	3.31	-27.09	-0.92
27.0	38.37	3.27	-27.31	-0.88
27.5	38.99	3.37	-27.49	-0.75
28.0	38.23	3.33	-27.58	-1.08
28.5	38.26	3.31	-27.79	-0.82
29.0	38.71	3.31	-27.74	-1.09
29.5	37.63	3.18	-27.70	-0.68
29.5	37.98	3.20	-27.66	-1.22
30.0	37.55	3.16	-27.35	-1.03
30.5	37.15	3.10	-27.48	-0.42
31.0	37.42	3.16	-27.70	-1.01
31.5	37.61	3.22	-27.92	-1.14
32.0	37.20	3.16	-27.83	-0.13
32.5	38.37	3.23	-27.75	-0.72
33.0	38.68	3.21	-27.37	-0.20
33.5	39.42	3.31	-27.14	-0.33
34.0	38.75	3.26	-27.20	-0.52
34.5	38.71	3.27	-27.84	-0.21
34.5	38.55	3.27	-27.79	-1.15
35.0	38.88	3.30	-28.07	-0.55
35.5	38.84	3.29	-27.89	-0.77
36.0	39.56	3.37	-27.73	-1.29
36.5	38.84	3.37	-27.81	-1.11
37.0	37.93	3.28	-27.88	-1.24
37.5	37.92	3.30	-27.91	-0.77
38.0	37.62	3.24	-27.98	-1.10
38.5	39.37	3.41	-27.71	-0.93
39.0	39.53	3.40	-27.98	-1.25
39.5	60.88	5.23	-27.65	-0.85

39.5	39.16	3.35	-27.96	-0.51
40.0	39.55	3.33	-27.73	-1.10
40.5	39.01	3.23	-27.43	-0.05
41.0	38.95	3.19	-27.34	-0.91
41.5	38.74	3.18	-27.16	-0.04
42.0	40.20	3.30	-27.35	-0.42
42.5	35.80	2.99	-27.40	0.20
43.0	40.29	3.35	-27.44	-0.34
43.5	41.21	3.45	-27.30	-0.75
44.0	40.65	3.35	-27.15	-0.50
44.5	40.68	3.44	-26.80	-0.75
44.5	41.05	3.41	-26.94	-0.89
45.0	40.13	3.43	-27.16	-0.77
45.5	38.95	3.27	-27.44	-0.58
46.0	38.83	3.28	-27.61	-1.42
46.5	38.28	3.28	-27.94	-0.49
47.0	39.05	3.32	-27.74	-1.06
47.5	37.78	3.24	-27.91	-0.83
48.0	38.14	3.24	-27.93	-0.84
48.5	36.92	3.08	-27.62	-0.37
49.0	38.41	3.24	-27.65	-0.92
49.5	38.41	3.17	-27.80	-0.67
49.5	38.77	3.21	-27.69	-0.76

Appendix E: Compiled cellulose oxygen isotope data

Table E1: Oxygen isotope composition (‰ VSMOW ± 0.3‰) of cellulose isolated from sediment core C2 from lake AC1.

Depth (cm)	Oxygen (%)	$\delta^{18}O$ (‰ VSMOW)
0.0	11.51	14.22
0.5	16.70	14.68
1.0	14.70	14.79
1.5	18.27	13.95
2.0	15.68	13.55
2.5	15.09	14.32
3.0	12.65	13.66
3.5	16.04	13.76
4.0	13.51	13.51
4.0	15.16	13.95
4.5	16.86	14.23
5.0	15.06	14.99
5.5	11.66	14.54
6.0	18.83	14.06
6.5	16.75	14.57
7.0	16.80	14.48
7.5	17.87	13.67
8.0	15.83	14.00
8.5	17.51	14.15
9.0	15.95	15.03
9.0	14.17	14.48
9.5	13.62	14.81
10.0	19.67	12.82
10.5	13.50	13.75
11.0	16.98	13.47
11.5	14.28	14.24
12.0	13.99	14.04
12.5	16.80	13.79
13.0	17.98	14.52
13.5	13.73	14.10
14.0	17.70	14.78
14.0	13.64	14.30
15.0	16.22	13.20
15.0	15.06	14.89
15.5	16.17	14.57
16.0	15.73	14.01
16.5	14.50	14.61

17.0	15.05	15.03
17.5	18.27	14.89
18.0	19.07	13.88
18.5	17.15	15.28
19.0	16.94	14.08
19.0	19.41	14.03
19.5	20.58	14.82
20.0	18.15	17.17
20.5	16.55	14.53
21.0	15.66	13.37
21.5	14.14	15.40
22.0	16.48	13.25
22.5	16.54	14.66
23.0	15.05	17.96
23.5	13.66	15.50
24.0	14.61	16.70
24.0	15.81	16.54
24.5	11.83	16.26
25.0	11.35	14.89
25.5	15.75	13.36
26.0	15.86	12.94
26.5	13.04	14.35
27.0	16.00	12.69
27.5	14.84	13.30
28.0	14.46	17.04
28.5	15.46	13.61
29.0	19.44	12.98
29.0	19.36	12.65
29.5	14.37	13.72
30.0	17.73	12.97
30.5	15.72	13.91
31.0	16.65	14.38
31.5	12.48	12.88
32.0	11.79	14.48
32.5	12.94	12.88
33.0	14.45	12.77
33.5	19.13	11.36
34.0	14.44	13.70
34.0	15.36	13.42
34.5	18.38	11.75
35.0	20.55	11.40

35.5	13.05	13.84
36.0	14.09	15.73
36.5	13.26	14.86
37.0	14.26	15.70
38.0	20.38	17.65
38.0	16.29	15.23
38.5	14.91	14.00
39.0	15.17	14.04
39.0	12.83	14.50
39.5	21.05	13.15
40.0	14.61	14.83
40.5	17.01	14.00
41.0	15.69	13.73
41.5	16.29	13.76
42.0	16.48	12.69
42.5	15.42	11.99
43.0	17.45	11.94
43.5	16.92	13.33
44.0	14.36	14.51
44.0	14.37	14.04
44.5	19.15	12.59
45.0	13.31	13.61
45.5	13.41	13.48
46.0	14.34	13.23
46.5	17.92	11.49
47.0	13.40	12.38
47.5	14.66	12.51
48.0	16.72	13.01
48.5	13.44	12.43
49.0	13.60	12.99
49.0	14.01	14.06
49.5	14.90	13.38
50.0	15.80	12.29
50.5	11.98	13.87
51.0	13.09	13.25
51.5	13.89	12.21
52.0	12.45	12.60
52.5	13.28	11.36
53.0	10.60	14.16
53.5	16.35	10.98
54.0	15.88	11.53

54.0	13.16	11.70
54.5	14.24	12.13
55.0	12.93	11.61
55.5	15.45	10.68
56.0	14.29	10.86
56.5	18.97	10.96
57.0	14.90	11.31
57.5	18.44	12.37
58.0	13.51	11.77
58.5	10.95	13.54
59.0	16.15	12.84
59.0	16.30	12.96
59.5	15.27	11.76
60.0	10.99	11.83
60.5	15.84	11.50

Table E2: Oxygen isotope composition (‰ VSMOW ± 0.3‰) of cellulose isolated from sediment core C2 from lake AC3.

Depth (cm)	Oxygen (%)	$\delta^{18}O$ (‰ VSMOW)
0.0	16.08	15.77
0.5	19.18	15.30
1.0	20.73	15.30
1.5	22.47	15.13
2.0	26.69	14.77
2.5	23.10	14.96
2.5	23.12	14.92
3.0	24.64	13.77
3.5	22.52	14.42
4.0	28.27	14.65
4.5	22.99	14.53
5.0	25.91	14.79
5.5	23.44	14.88
6.0	21.03	15.37
6.5	21.12	15.59
7.0	29.47	14.45
7.5	23.51	13.22
8.0	26.32	13.64
8.0	24.65	12.91
8.5	24.44	13.05
9.0	22.61	13.42
9.5	26.55	12.99
10.0	23.42	13.67
10.5	27.33	14.01
11.0	20.67	13.17
11.5	24.06	14.15
12.0	25.27	12.96
12.5	19.28	14.25
13.0	17.82	15.72
13.5	23.30	14.47
13.5	26.06	14.12
14.0	23.15	13.89
14.5	25.74	13.85
15.0	25.41	13.41
15.5	24.59	13.59
16.0	32.61	15.54
16.5	26.00	14.85
17.0	28.68	13.93
17.5	21.26	15.00
18.0	21.92	15.78
18.5	24.63	13.94

19.0	25.37	14.17
19.0	26.78	14.01
19.5	25.28	14.00
20.0	23.31	14.21
20.5	22.18	15.23
21.0	24.21	14.42
21.5	26.70	11.62
22.0	17.40	12.67
22.5	25.31	11.82
23.0	24.18	11.89
23.5	21.41	13.32
24.0	18.11	14.12
24.5	21.58	13.54
24.5	21.25	13.67
25.0	19.76	14.53
25.5	25.01	13.96
26.0	24.74	13.26
26.5	21.06	13.28
27.0	NA	NA
27.5	16.60	14.04
28.0	16.31	13.38
28.5	16.69	13.96
29.0	19.57	15.05
29.0	19.03	15.41
29.5	19.03	15.42
30.0	18.58	15.08
30.5	17.88	15.09
31.0	19.76	12.75
31.5	22.03	13.26
32.0	23.73	14.30
32.5	18.59	13.71
33.0	19.76	13.86
33.5	19.66	14.05
34.0	20.96	13.90
34.5	20.35	13.52
34.5	18.59	13.10
35.0	21.50	13.16
35.5	21.19	12.68
36.0	20.94	12.39
36.5	20.21	12.61
37.0	20.65	12.52
37.5	20.45	12.96
38.0	19.05	12.84
38.5	15.11	12.05
38.5	15.75	12.26

39.0	18.56	13.06
39.5	21.87	12.80
40.0	19.59	12.43
40.5	20.52	13.77
41.0	17.06	13.32
41.5	19.46	12.66
42.0	15.74	13.27
42.5	20.10	11.18
43.0	21.76	14.06
43.5	18.88	11.95
44.0	21.72	13.78
44.0	18.76	13.80
44.5	17.16	12.56
45.0	19.19	13.37
45.5	21.53	13.10
46.0	21.17	12.67
46.5	21.44	12.83
47.0	19.25	13.95
47.5	24.78	12.08
48.0	18.33	13.30
48.5	21.84	13.39
49.0	18.97	12.62
49.0	17.36	13.48
49.5	18.10	12.85
50.0	22.89	14.20
50.5	20.71	14.67
51.0	21.75	13.79
51.5	23.18	16.35
52.0	19.88	15.89
52.5	17.57	15.86
53.0	15.77	14.30
53.5	19.17	16.05
54.0	19.86	16.16
54.0	18.40	16.13
54.5	19.29	15.10
55.0	18.11	14.81
55.5	21.90	14.87
56.0	20.54	15.65
56.5	20.36	13.76
57.0	22.12	14.04
57.5	16.43	16.38
58.0	22.85	15.53
58.5	22.00	16.05
59.0	21.00	15.81
59.0	21.02	14.69

59.5	19.58	16.02
60.0	13.62	13.72
60.5	14.14	14.82
61.0	17.16	12.73
61.5	17.37	15.55
62.0	18.80	15.04
62.5	18.31	14.85
63.0	19.17	15.66
63.5	18.60	15.53
64.0	18.04	13.94
64.0	19.71	15.17
64.5	20.57	14.37
65.0	19.97	14.12
65.5	13.65	14.69
66.0	17.23	13.28
66.5	15.26	13.88
67.0	14.13	13.84
67.5	16.67	14.24
68.0	14.66	15.17
68.5	14.12	15.08
69.0	17.79	14.84
69.0	14.71	13.32
69.5	17.13	13.88
70.0	13.59	14.82
70.5	NA	NA
71.0	19.35	14.14
71.5	15.57	12.40
72.0	12.75	14.79
72.5	13.86	15.23
73.0	20.01	16.00
73.5	20.60	12.87
74.0	18.09	12.97
74.0	17.98	13.13
74.5	15.24	14.54
75.0	17.82	14.04
75.5	16.32	13.43
76.0	16.96	14.28
76.5	16.45	14.52
77.0	15.99	14.21
77.5	14.99	14.28
78.0	12.63	13.87
78.5	19.13	13.25
79.0	13.76	15.32
79.5	17.17	13.87
79.5	16.01	15.57

80.0	17.79	14.99
80.5	15.76	15.06
81.0	17.83	14.16
81.5	18.15	11.90
82.0	18.17	13.32
82.5	10.81	13.63
83.0	14.49	13.87
83.5	13.08	14.07
84.0	13.43	14.22
84.5	13.35	14.15
84.5	12.86	14.86
85.0	16.54	14.16
85.5	14.62	14.97
86.0	13.29	16.29
86.5	18.92	14.18
87.0	14.17	14.37
87.5	17.40	14.45
88.0	19.46	14.80
88.5	16.50	15.12
89.0	17.20	16.43
89.0	15.68	14.90
89.5	16.79	15.32
90.0	12.42	15.35
90.5	21.32	13.52
91.0	18.91	13.74

Table E3: Oxygen isotope composition (‰ VSMOW ± 0.3‰) of cellulose isolated from sediment core C2 from lake AC5.

Depth (cm)	Oxygen (%)	$\delta^{18}O$ (‰ VSMOW)
0.0	29.11	14.79
0.5	26.42	14.26
1.0	34.02	16.67
1.5	25.01	14.43
2.0	26.50	13.91
2.5	31.84	15.73
3.0	26.71	13.73
4.0	27.37	13.93
3.5	24.09	13.65
3.5	28.68	14.23
4.5	22.36	13.69
5.0	25.09	14.67
5.5	29.31	14.41
6.0	21.96	13.71
6.5	22.17	13.21
7.0	19.46	12.58
7.5	20.07	12.95
8.0	23.35	13.40
8.5	33.85	15.41
9.0	24.25	14.02
9.0	16.98	12.04
9.5	16.91	12.21
10.0	18.96	12.22
10.5	16.91	12.01
11.0	24.50	12.89
11.5	21.44	12.68
12.0	15.70	11.18
12.5	23.10	11.29
13.0	19.44	11.12
13.5	24.17	12.23
14.0	17.30	11.02
14.0	17.40	11.09
14.5	18.72	10.25
15.0	18.80	13.48
15.5	15.73	11.46
16.0	21.67	10.51
16.5	14.47	12.67
17.0	23.05	13.05

17.5	16.77	11.55
18.0	19.43	11.33
18.5	21.74	11.03
19.0	19.28	12.22
19.0	21.53	11.71
19.5	18.86	10.44
20.0	16.82	10.44
20.5	0.02	10.43
21.0	20.26	10.76
21.5	15.27	12.03
22.0	11.59	14.39
22.5	17.99	10.62
23.0	19.88	10.77
23.5	18.68	12.02
24.0	21.23	12.20
24.0	22.46	12.89
24.5	19.46	11.74
25.0	27.58	14.37
25.5	19.74	11.93
26.0	21.72	10.53
26.5	17.95	11.47
27.0	19.77	11.28
27.5	20.51	11.10
28.0	26.16	13.68
28.5	24.78	11.97
29.0	28.32	14.60
29.0	21.72	12.02
29.5	20.46	11.38
30.0	16.71	11.48
30.5	13.36	14.86
31.0	12.34	9.57
31.5	16.59	7.66
32.0	18.64	11.54
32.5	24.07	12.22
33.0	13.16	18.07
33.5	18.06	14.74
34.0	17.57	13.28
34.0	19.27	13.03
34.5	21.36	15.26
35.0	17.38	14.16
35.5	17.19	14.62

36.0	17.16	15.29
36.5	11.86	20.64
37.0	14.11	17.25
37.5	10.14	21.07
38.0	12.64	18.48
38.5	14.00	16.60
39.0	19.11	13.31
39.0	18.94	13.82
39.5	14.75	16.17
40.0	13.78	10.17
40.5	14.71	12.23
41.0	13.15	12.92
41.5	14.61	11.01
42.0	20.61	10.85
42.5	13.60	12.19
43.0	16.29	10.68
43.5	18.04	10.31
44.0	14.51	13.07
44.0	12.88	12.55
44.5	15.25	9.79
45.0	16.40	10.27
45.5	14.37	9.58
46.0	12.18	11.73
46.5	12.95	10.90
47.0	13.60	9.50
47.5	9.98	12.79
48.0	11.06	12.09
48.5	13.48	10.19
49.0	12.55	10.22
49.0	13.20	10.53
49.5	11.76	11.13

Table E4: Oxygen isotope composition (‰ VSMOW ± 0.3‰) of cellulose isolated from sediment core C2 from lake PC4.

Depth (cm)	Oxygen (%)	$\delta^{18}O$ (‰ VSMOW)
0.0	18.950	13.05
0.5	27.167	11.83
1.0	20.114	12.01
1.5	21.424	12.30
2.0	27.508	13.03
2.5	21.507	12.24
3.0	21.842	11.98
3.5	23.453	12.10
4.0	25.386	12.84
4.0	26.006	12.81
4.5	23.210	11.99
5.0	28.496	13.05
5.5	27.554	12.56
6.0	25.315	10.84
6.5	24.945	12.23
7.0	23.623	12.67
7.5	24.260	12.84
8.0	23.493	12.09
8.5	24.798	12.34
9.0	27.149	13.27
9.0	24.212	11.93
9.5	25.166	12.35
10.0	26.766	12.19
10.5	26.359	12.29
11.0	17.241	13.32
11.5	16.604	13.45
12.0	17.175	12.88
12.5	18.368	13.18
13.0	18.208	13.07
13.5	17.496	12.71
14.0	17.073	12.76
14.0	17.672	12.43
14.5	14.666	12.16
15.0	22.069	13.20
15.5	15.526	12.27
16.0	17.587	11.74
16.5	14.816	12.85
17.0	13.537	13.48
17.5	15.028	13.38
18.0	17.347	13.26
18.5	13.239	13.62
19.0	15.822	12.79

19.0	18.163	12.10
19.5	17.138	12.68
20.0	23.175	12.67
20.5	24.205	13.15
21.0	22.283	12.35
21.5	19.823	12.08
22.0	18.979	11.36
22.5	17.859	10.99
23.0	17.330	11.46
23.5	18.481	11.72
24.0	17.255	12.25
24.0	16.876	11.98
24.5	14.515	12.22
25.0	18.387	11.11
25.5	19.468	11.03
26.0	19.377	11.09
26.5	20.143	10.97
27.0	22.993	11.27
27.5	20.497	11.60
28.0	17.415	12.73
28.5	19.870	10.63
29.0	13.170	13.36
29.0	16.728	10.85
29.5	18.190	13.42
30.0	18.712	12.76
30.5	18.208	12.61
31.0	16.935	12.81
31.5	16.210	15.54
32.0	20.216	14.59
32.5	24.347	11.05
33.0	19.385	11.80
33.5	25.782	9.71
34.0	17.424	12.69
34.0	18.676	12.07
34.5	25.509	9.60
35.0	23.684	10.23
35.5	24.135	11.77
36.0	24.775	11.99
36.5	22.960	11.12
37.0	25.119	11.72
37.5	24.142	11.63
38.0	15.863	11.37
38.5	26.412	11.09
39.0	21.169	13.13
39.0	23.930	12.00

39.5	20.648	8.99
40.0	21.343	9.85
40.5	20.485	9.76
41.0	19.511	8.99
41.5	24.042	11.19
42.0	23.818	11.14
42.5	19.679	10.98
43.0	18.735	11.67
43.5	20.657	11.24
44.0	12.275	12.56
44.0	13.084	13.08
44.5	19.215	12.10
45.0	25.001	11.84
45.5	23.269	11.05
46.0	21.793	10.82
46.5	27.198	11.99
47.0	20.162	11.64
47.5	19.537	10.94
48.0	25.321	10.99
49.0	23.734	9.97
48.5	24.561	10.29
48.5	23.195	11.12
49.5	23.785	11.25

Appendix F: Stratigraphic records of carbon and nitrogen elemental and isotope data and cellulose oxygen isotope data

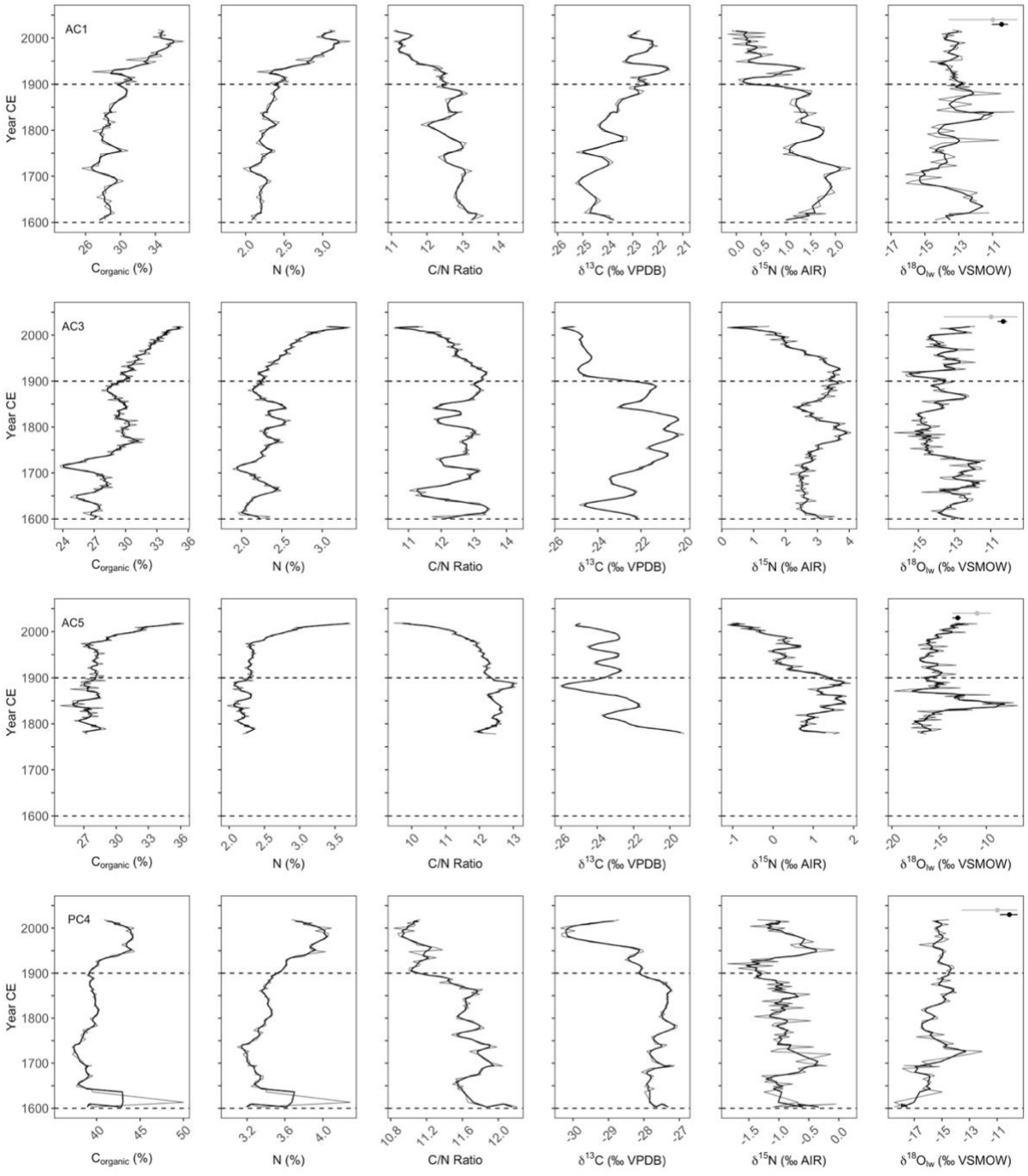

Figure F1. Organic carbon, nitrogen, carbon-to-nitrogen ratio (C/N Ratio), $\delta^{13}C_{org}$, $\delta^{15}N$, and cellulose-inferred $\delta^{18}O_{lw}$ at the study lakes from 1600 CE to present. Average and range of measured $\delta^{18}O_{lw}$ for each lake (black) and all four lakes (grey) are included in the $\delta^{18}O_{lw}$ graph. A three-point running mean is drawn through each variable. The beginning and termination of the LIA is distinguished by a horizontal dashed line at 1600 CE and 1900 CE, respectively.

Appendix G: Statistical analyses

Table G1. Mann-Kendall U rank trend test results performed to determine a significant increase in $\delta^{18}O_{lw}$ values at the study lakes during the 1900-1999 and 2000-present periods. Significant p-values (<0.05) are bolded.

Climate Period	Lake	tau	One-sided p-value
1900-1999	AC1	-0.982	>0.050
	AC3	-0.068	>0.050
	AC5	0.189	0.054
	PC4	-0.284	>0.050
Since 2000	AC1	-0.333	>0.050
	AC3	0.293	0.062
	AC5	0.293	**0.001**
	PC4	-0.067	>0.050